Development of a transient diesel exhaust emissions measurement system

by

Bennett Clark Murray

A Thesis Submitted to the
Graduate Faculty in Partial Fulfillment of the
Requirements for the Degree of
MASTER OF SCIENCE

Major: Mechanical Engineering

Iowa State University
Ames, Iowa

1989

TABLE OF CONTENTS

LIST OF TABLES

v

LIST OF FIGURES

NOMENCLATURE

A_{dt} cross-sectional area of dilution tunnel

$A_{orifice}$ cross-sectional area of calibrated orifice

BS   brake-specific

$BSCO_2$ brake-specific carbon dioxide

BSFC   brake-specific fuel consumption

BSHC   brake-specific hydrocarbons

$BSNO_x$ brake-specific oxides of nitrogen

CO_2 carbon dioxide

cfm   cubic feet per minute

dilution ratio   ratio of mass flow rate of dilution air to mass flow rate of exhaust

EPA   Environmental Protection Agency

HC   hydrocarbons

k   ratio of specific heats

M   Mach number

m_{partic} total mass of particulates emitted by engine during a measurement period

$m_{species}$ total mass of exhaust species of interest

m_{intake} total mass of intake air

$\dot{m}_{dil\ air}$ mass flow rate of dilution air

$\dot{m}_{dil\ tun}$ total dilution tunnel mass flow rate

$\dot{m}_{exhaust}$ mass flow rate of engine exhaust

$\dot{m}_{fuel}$ mass flow rate of fuel

$\dot{m}_{intake}$ mass flow rate of engine intake air

$\dot{m}_{sample}$ mass flow rate through particulate sampling system

$MW_{dil\ exh}$ molecular weight of diluted exhaust

$MW_{exhaust}$ molecular weight of exhaust species of interest

n number of data-acquisition sampling intervals during one measurement

NO_x oxides of nitrogen

P_{atm} atmospheric pressure

P_{dt} pressure in dilution tunnel

P_s static pressure

P_{sample} pressure at gas meter in particulate sampling system

P_{su} pressure upstream of calibrated orifice

R_{air} ideal gas constant for air

SF sampling fraction, ratio of mass flow rate of particulate sample to total
mass flow rate of diluted exhaust in tunnel

T_s static temperature

T_{amb} ambient temperature

T_{dt} temperature of dilution tunnel

T_{sample} temperature of particulate sample stream at gas meter

T_u temperature upstream of calibrated orifice

V velocity of dilution air in dilution tunnel

$V_{orifice}$ velocity of dilution air through calibrated orifice

$\dot{V}_{intake}$ volume flow rate of engine intake air

$\dot{V}_{sample}$ volume flow rate through gas meter in particulate sampling system

W_{total} total work done by engined during measurement

X molar concentration

Δm_{filter} change in mass of the particulate filter, particulate sample mass

Δm_{fuel} change in mass of fuel in fuel supply tank during measurement

Δt data acquisition sampling time interval

ϕ equivalence ratio

$\dot{\theta}$ engine speed

ρ density

τ torque

ABSTRACT

An exhaust emissions measurement system was designed, fabricated and tested for use in measuring particulate, unburned hydrocarbon and oxides of nitrogen production during steady-state and transient tests of a commercial diesel engine. The system includes a full-flow dilution tunnel of simpler design than specified by the Environmental Protection Agency (EPA). A series of steady-state and transient tests were conducted to characterize the repeatability of measurements made with the system. The consecutive-measurement and day-to-day repeatabilities of steady-state measurements and transient measurements were determined. The period of transient emissions production following a change in operating condition was determined as well as the measurement influence of previous operating condtions. The system was found to provided acceptable repeatability for use in comparing emissions at different engine operating conditions although it may not duplicate measurements taken with an EPA-type system.

CHAPTER I. INTRODUCTION

Diesel engines are the most widely used power plant for over-the-road trucks and buses in the United States. These engines are also responsible for a large fraction of vehicle-generated pollutants. The Environmental Protection Agency (EPA) has mandated significantly lower diesel exhaust emission levels to take effect in 1991 and 1994. Table 1.1 shows the current and future standards for heavy-duty diesel engines. A large amount of research is currently being done to design and modify engines to meet the new regulations. A critical component of experimental emissions research is the emissions measurement system. The EPA has mandated the measurement system to be used for validating an engine's conformance to the regulations. However, the size and expense of the EPA system limits the number that any one company can build and also limits the number of researchers who can do work in the field. Therefore, a smaller and less expensive design than that specified by the EPA is needed to increase the amount of research that can be done.

Table 1.1: Environmental Protection Agency Heavy-Duty Diesel Standards

	1989	1991	1994
Hydrocarbons (g/hp-hr)	1.3	1.3	1.3
Carbon Monoxide (g/hp-hr)	15.5	15.5	15.5
Oxides of Nitrogen (g/hp-hr)	10.7	6.0	5.0
Particulates (g/hp-hr)	0.6	0.25[a]	0.1

[a] Value is 0.1 for urban buses.

The objectives of this work were to develop a laboratory-scale exhaust-emissions measurement system for use with a commercial diesel engine, and to determine the repeatability of the measurements made with the system. Since the system is to be used for testing the engine in both steady-state and transient operating modes, the repeatability of measurements for both cases was to be determined. There are two types of

repeatability that were of interest. The first type is the repeatability of consecutive measurements, and the second is the repeatability of measurements made on different days. A number of possible influences on repeatability exist for measurements made within the same day. Following a speed and load change in a steady-state test, some amount of time will be required for the engine to produce a steady amount of emissions. The repeatability of measurements made during this period may be affected. Also, the engine's operation may be influenced by the operating condition prior to the change so that steady-state test repeatability may be influenced by the engine's previous schedule of speeds and loads. A moderate condition following a full-speed, full-load condition may produce different results than the same condition following a low-speed, light-load condition. Day-to-day repeatability is generally a function of a larger number of variables than consecutive-measurement repeatability. The condition of the engine and its surroundings are less likely to be the same after a day has passed than after only a few minutes or hours have passed. In this study, the repeatabilities and influences that were to be determined were:

- The repeatability of consecutive measurements for steady-state engine operation
- The amount of time following a speed and load change required for steady-state emission production to be reached.
- The influence of previous operating conditions on the engine's emissions
- The repeatability of measurements for steady-state engine operation from day to day
- The repeatability of consecutive measurements for transient-cycle engine operation
- The repeatability of measurements for transient-cycle engine operation from day to day

The Iowa State University engine laboratory needed an emissions measurement system for use in a study of the effects of alcohol fumigation on diesel emissions. An EPA-type system was not desirable from a laboratory-space and monetary standpoint. Also, the research was be comprised of comparative tests in which changes in the engine's emissions rather than the absolute magnitude of those emissions were of interest. It is important to distinguish this need from the need to use an EPA-type system to determine if a specific engine is meeting the EPA emission regulations.

The scope of this work included the design, fabrication and testing of the measurement system. Tests were conducted to characterize the six aspects of the system's repeatability listed above. The emissions that were measured were particulates, unburned hydrocarbons and oxides of nitrogen.

This thesis includes background information regarding diesel emissions, the EPA emissions measurement system and other smaller and simpler measurement systems that have been developed. The design of the system is then presented followed by the procedures followed to run the repeatability tests. The results of those tests are presented, and finally, conclusions are drawn on the repeatability and adequacy of the system, and recommendations are made with regard to future improvements.

CHAPTER II. BACKGROUND

This chapter provides the essential background information for understanding work in the area of diesel exhaust emissions measurement. An overview of diesel emissions is given in the first section followed by an explanation of transient dynamometer tests. The concepts of dilution tunnels and constant volume sampling (CVS) systems are then discussed, and finally, examples of simplified dilution tunnel systems are reviewed.

Diesel Emissions

The primary source of air pollution from a diesel engine is the products of combustion that are discharged through the exhaust pipe. While the crankcase breather and fuel tank breather are both contributors, the exhaust pipe emissions comprise from 65 to 85 percent of the engine's pollutants. The engine exhaust contains particulates, unburned hydrocarbons (HC), oxides of nitrogen (NO_x), carbon dioxide (CO_2), carbon monoxide (CO) and traces of alcohols, aldehydes, ketones, phenols, acids, esters, ethers, epoxides, peroxides and other oxygenates. This study focuses on the measurement of particulates, HC and NOx.

Particulates in diesel exhaust are made up of carbonaceous soot particles that have hydrocarbons adsorbed and condensed onto their surfaces. The hydrocarbon part of the particulates is referred to as the soluble organic fraction (SOF). This name comes from the fact that a solvent is used to remove the organic fraction from the carbonaceous core in the analysis of a particulate sample. The amount of SOF in a particulate sample can be influenced by the manner in which the sample is collected. The amount of hydrocarbons that adsorb and condense onto the surfaces of the particulate will depend on the length of time between formation and collection and the temperatures in the collection system. The sources of hydrocarbons that make up the SOF have been shown to be both unburned fuel and engine oil [1], while the insoluble fraction is a product primarily of the unburned paraffin, olefin and aromatic fuel components.

The amount of NO_x produced by diesel engines is comparable to the amount produced by spark-ignition engines. Typical concentrations range from 500 to 1000 parts per million or 20 grams per kilogram of fuel. Ten to thirty percent of the NO_x emissions are NO_2 while the remainder is NO. Although NO is the dominant species formed in the cylinder, most of the NO is converted to NO_2 in the atmosphere.

NO is formed by an endothermic reaction in the burned-gas regions of the cylinder. The formation of NO is very sensitive to temperature. The higher flame temperatures accompanying early or rapid combustion greatly increase NO formation. Thus, the amount of NO_x in diesel exhaust is sensitive to injection timing and rate of combustion. The cooling that takes place during the expansion stroke freezes the reaction such that the concentrations that leave the engine are much higher than the equilibrium concentrations would be for the exhaust temperature.

HC emission by diesel engines is large enough to be significant, but is about a factor of 5 lower than spark-ignition engines. The two primary sources of hydrocarbons in diesel exhaust are fuel mixed leaner than the lean combustion limit for ignition during the ignition delay period and undermixing of fuel which leaves the fuel injector nozzle at low velocity, late in the combustion process. High molecular weight hydrocarbons have very low vapor pressures and will condense on carbonaceous particulates and become the SOF of the exhaust particulates. These hydrocarbons may comprise 15 to 45 percent of the total particulate mass.

Transient Dynamometer Tests

In 1988 the Environmental Protection Agency (EPA) specified a new test procedure for heavy-duty diesel engine emissions measurement. The test requires the engine to be run through a transient operating cycle which simulates city and highway driving of a truck in both New York and Los Angeles.

The engine is prepared for the test by cold soaking, that is, remaining inoperative in a 68 to 86 degree Fahrenheit environment, for 12 hours or until the oil temperature reaches 75 °F. Then the engine is started and immediately controlled according to a twenty-minute schedule of speeds and torques that make up the simulation. This part is known as the cold-start or cold-cycle portion of the test. Once the schedule is complete, the engine is shut off and allowed to stand for twenty minutes. The engine is then restarted and immediately controlled according to the same schedule. Again, once the schedule is completed the engine is shut off. This part of the test is termed the hot-start or hot-cycle portion. The results of the test are normally reported as weighted averages of the emission measurements made in each of the two portions of the test. The hot-start results are weighted six times greater than the cold start results.

Dilution Tunnels and CVS Systems

The Code of Federal Regulations (CFR) [2] specifies an exhaust emissions measurement system design that is to be used for determining whether an engine's emissions meet the applicable EPA standards or not. A schematic diagram of this system is shown in Fig. 2.1. A positive displacement pump, located at the exit of the system, draws ambient air through a filter into a dilution tunnel where it mixes with the exhaust of the engine being tested. Since the entire exhaust flow of the engine is introduced into the tunnel, not just a fraction, the tunnel is termed a "full-flow" dilution tunnel.

The purpose of mixing the exhaust with dilution air in this manner is to simulate the mixing that the exhaust will undergo with the atmosphere when the engine is in actual use. Simulation of atmospheric mixing is considered necessary when measuring particulates because much of the dynamics of particulate formation occur after the exhaust leaves the engine. As the exhaust mixes with the atmosphere and cools, some of the unburned hydrocarbons will adsorb and condense onto the surface of the particulate. The total mass of adsorbed and condensed hydrocarbons is the SOF of the particulates.

In addition to the interest in the total amount of mass of the carbonaceous soot plus SOF, sometimes researchers are interested in the quantity, chemical characteristics and biological characteristics of the SOF alone. In cases where a researcher wishes to characterize the size and/or shape of the individual particulates, the simulation of atmospheric mixing that the dilution tunnel provides is again important. A large amount of agglomeration among particulates tends to occur both inside and outside the engine. The dynamics of atmospheric mixing will play a role in the extent to which this occurs. Referring back to Fig. 2.1, the second part of the system which includes the heat exchanger and positive displacement pump, is called a constant-volume sampling system or a CVS system. Despite the name, the purpose of a CVS system is to draw a constant mass flow rate of diluted exhaust through the dilution tunnel. When the test engine is running in a transient cycle, the flow rate and temperature of the exhaust entering the dilution tunnel will be highly variable. The positive displacement pump alone will draw a constant volume flow rate through the tunnel. The addition of the large heat exchanger brings the diluted exhaust to almost a constant temperature. Since the pressure in the tunnel does not significantly vary, the fact that the positive displacement pump is drawing a constant volume flow rate of constant-temperature diluted exhaust means that the mass

7
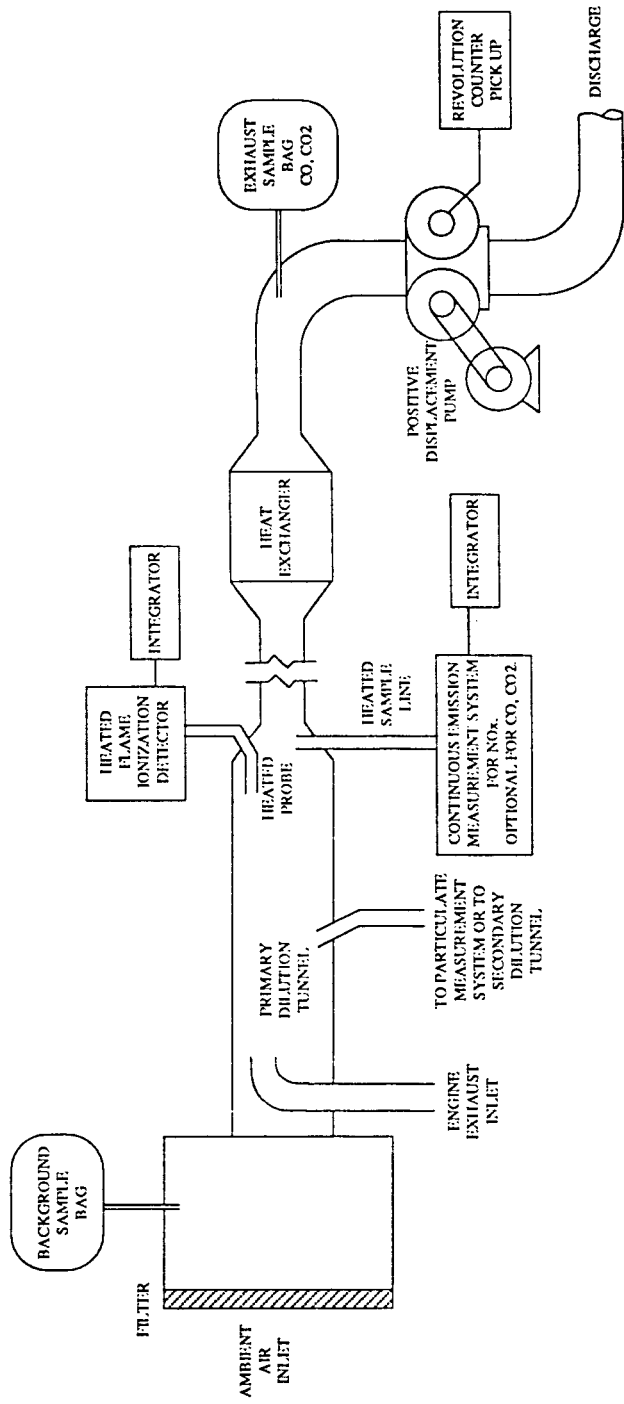
Fig. 2.1: Schematic diagram of the EPA-specified exhaust emissions measurement system

flow rate is also constant. It should be noted, however, that while the volume flow rate is constant downstream of the heat exchanger it is not constant upstream as the density of the mixture varies with its temperature.

A particulate sample is collected by passing a portion of the diluted exhaust through a filter. The best filters to use have been determined through experience and are Teflon-coated fiberglass [3,4]. It is important during a transient test that the flow rate of diluted exhaust passing through the filter is a constant mass fraction of the total diluted exhaust flow rate. If, for example, the flow rate of the engine exhaust increases momentarily and the sampling fraction changes, then the amount and type of particulate emitted by the engine during that period would not be accurately represented on the filter. Since the mass flow rate in the dilution tunnel is being held constant by the CVS system, drawing a constant mass flow rate through the particulate filter is required to maintain a constant mass sampling fraction. Because of the restriction of cooling the exhaust with dilution air only, and because a large amount of the particulate matter would be lost on the heat exchanger surfaces, the particulate sample must be taken upstream of the CVS heat exchanger.

The amount of dilution air required is indirectly specified by the EPA by saying that the temperature of the diluted exhaust at the filter must be maintained at 52 °C or less. Further, this cooling should be accomplished only through mixing with dilution air and not by heat transfer with the tunnel or sample line walls since such interaction can result in HC condensation and particulate deposition. Typical dilution ratios ($\dot{m}_{dilution\ air} / \dot{m}_{exhaust}$) range from 5 to 20.

Sometimes a secondary dilution tunnel is used to accomplish the temperature reduction. Such a design will be discussed later in this chapter. A sample of the diluted exhaust is transferred to a second, smaller tunnel and is diluted with more air such that the temperature is brought below 52 °C. Usage of a secondary dilution tunnel has the advantage that the total amount of dilution air required is less than if the temperature reduction were required for the entire exhaust stream. Also, generally, the length of the mixing process will be increased, thereby better simulating exhaust-atmosphere interactions.

Hydrocarbons also must be measured upstream of the heat exchanger since some might condense on the heat exchanger surfaces. A heated sample probe is used to transfer the sample from the tunnel to the HC analyzer in order to prevent condensation in the sample line. The analyzer is a heated flame ionization detector (HFID). As was the

case for the particulates, the mass flow rate through the HFID must be maintained constant in order to have a constant sampling fraction.

During a transient test, the HC concentration determined by the HFID is continuously integrated to give the total amount of HC for the whole cycle. For a gaseous emission like HC, there is another option besides maintaining a constant mass flow rate through the analyzer. The volume flow rate of the dilution tunnel can be continuously measured and multiplied by the concentration given by the HFID and integrated throughout the cycle.

Since the temperatures of the diluted exhaust should be well above the dew point when it enters the NO_x, CO or CO_2 analyzers, sampling for these gases is also done upstream of the heat exchanger before the mixture is cooled. As was the case for HC, either a constant mass flow can be maintained through these analyzers or measurements of the volume flow rate of the dilution tunnel can be used in integrating the concentrations over the transient cycle.

The EPA also allows the CO and CO_2 measurements to be made via bag sampling downstream of the heat exchanger. As mentioned before, both the volume flow rate and the mass flow rate of diluted exhaust are constant in this region. Therefore, all that is needed is a simple constant-speed pump to fill a Tedlar bag. Then, after the test is complete, the contents of the bag may be fed into CO and CO_2 analyzers. This is a desirable procedure when the response time of the analyzers is too slow for continuous measurement and integration upstream of the heat exchanger.

Simplified Dilution Tunnel Systems

The emissions measurement system specified in the Code of Federal Regulations is not always compatible with the needs, size and budget of a given engine laboratory. In some cases, although there is a need to measure particulates and gaseous emissions, there is not a need to determine if the engines being used meet any specific emission-level requirements. Thus a full-scale EPA-type system is not necessary.

Harrington and Yetter [5] have shown that a simplified dilution tunnel design can provide particulate mass measurements that agree to within 10% of those made with a full flow dilution tunnel. In their case, they required a particulate measurement system suitable for steady-state tests on small, single-cylinder laboratory engines. Their design, a schematic of which is shown in Fig. 2.2, uses a 1.4 meter-long stainless-steel tube which, being 29.5 millimeters in diameter, has a smaller cross-section than the 47

millimeters particulate filter that is placed in it. As the figure shows, the entire diluted-exhaust stream is passed through the filter. A common wet/dry vacuum cleaner is used as the pump to draw the dilution air and exhaust through the dilution tube. As the particulate filter becomes loaded, the pressure drop across it increases. To compensate for this increase in flow resistance, a variable transformer is used to increase the speed of the pump. In a typical application, the tunnel flow rate can be held constant for a five minute steady-state test.
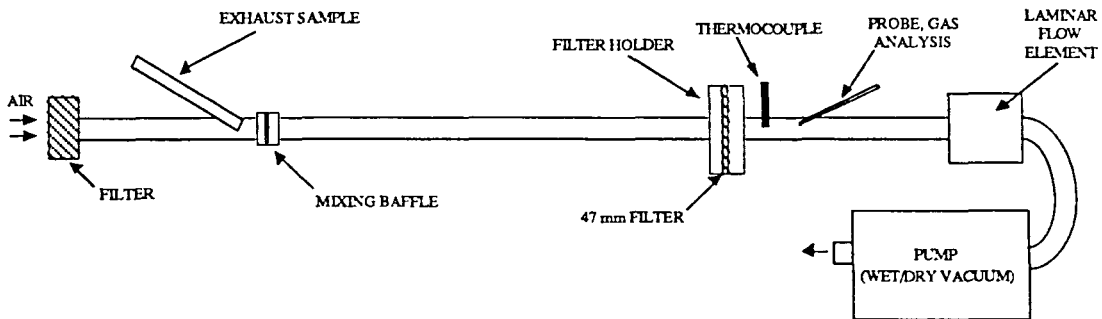
Fig. 2.2: Mini-dilution tunnel design of Harrington and Yetter [5]

The fraction of exhaust admitted into the tunnel is a function of the size of the exhaust sample tube and the difference between the pressure in the exhaust pipe and the pressure in the dilution tunnel. In a transient test, the exhaust pressure would change throughout the test and the exhaust sampling fraction would not be constant. Also, the temperature of the diluted exhaust in the tunnel will vary with exhaust gas temperature and therefore the pump, which will essentially draw a constant volume flow rate, will not be drawing a constant mass flow rate through the dilution-tube. Thus, this simplified dilution tunnel design meets the needs of its designers for much less money and space than a complete full-flow EPA-type system, but is not adequate for transient tests.

Heavy-duty diesel engines produce large volume flow rates of exhaust. The use of a full-flow dilution tunnel requires a volume flow rate of dilution air that is several times the flow rate of the exhaust. Thus, large air-supply systems and large dilution tunnels are needed as part of the emission measurement equipment. In some cases, researchers have cited lack of space for such large equipment as the motivation for developing smaller dilution tunnels that use only a fraction of the engine's exhaust .

Suzuki et al. [6] developed a mini-dilution tunnel for particulate measurements whose design differed from the EPA specifications by being smaller, but retained many of the features of the EPA system. Fig. 2.3 shows a schematic of the design. The length of the tunnel is only 1.7 meters, and the diameter is 84 millimeters. The CVS components are included but instead of introducing the entire exhaust stream into the tunnel, an air ejector is used to draw in only a portion. The key to the success of this system is that the air-ejector driving air can be adjusted to seven discrete flow rates using a group of parallel solenoid valves. The valves are opened and closed according to the flow rate of the exhaust. By doing so, the system is capable of drawing a roughly constant fraction of the total exhaust into the tunnel. Thus transient testing is feasible with this system. Transient tests were conducted using both the mini-tunnel and a full-flow dilution tunnel. In these tests, the mini-tunnel results were found to be directly proportional to the full-flow tunnel results with a correlation coefficient of 0.998. The mini-tunnel's particulate measurements were consistently about 10% lower than the full-flow tunnel's. In steady-state tests the measurements differed by only 6%.
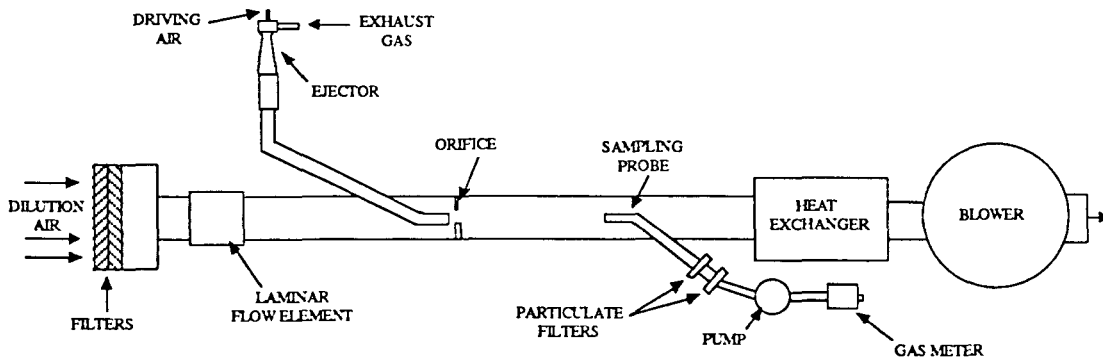
Fig. 2.3: Mini-dilution tunnel design of Suzuki et al. [6]

Hirakouchi, Fukano and Shoji [7], who also developed a mini-dilution tunnel, initially considered an air-ejector type of induction system. However, unlike Suzuki et al., they only considered a system in which the driving air flow rate would be constant. The researchers rejected the system because their experiments showed significantly lower particulate measurements than those made using a full-flow dilution tunnel. They noted that the basic problem with an air-ejector system is that a constant volume flow rate of

exhaust is drawn into the dilution tunnel from the total engine exhaust rather than a constant fraction.

Hirakouchi, Fukano and Shoji's final design is shown schematically in Fig 2.4. It is similar to the system of Fig. 2.3 except for the method used to draw a constant fraction of the total exhaust into the tunnel. The mini-tunnel draws a constant fraction of an engine's exhaust gas into the tunnel using a multi-tube exhaust gas induction system. After passing through a diffuser, the exhaust enters a group of parallel tubes of equal diameter. One of the tubes is the induction tube that directs its fraction of the exhaust into the dilution tunnel. The rest of the tubes send the remainder of the exhaust into a surge tank whose pressure can be monitored. When the pressure in the dilution tunnel is maintained at a value equal to that of the surge tank, the mass fraction of the total exhaust gas that enters the dilution tunnel is constant. Generally, however, the researchers merely recorded the pressures and applied a correction to the data.
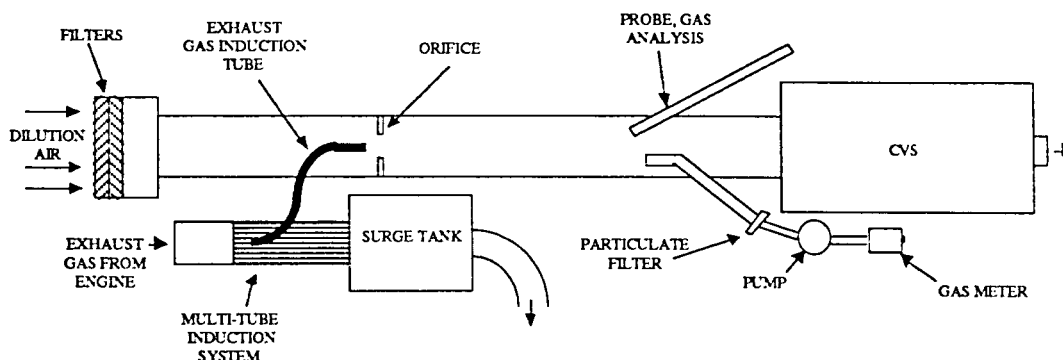
Fig. 2.4: Mini dilution tunnel design of Hirakouchi, Fukano and Shoji [7]

This design was capable of matching the measurements of a full-flow dilution tunnel quite closely in both steady-state and transient engine operating modes. In their work they measured mass emissions of NO_x, HC, CO, sulfate, particulates and the SOF of the particulates. Correlation coefficients of greater than 0.97 were obtained from the comparison of measurements taken with their mini-dilution tunnel to measurements taken with an EPA-type system. The differences between the measurements were generally 10% or less.

Heden, Eriksson and Gustavsson [8] developed a simplified full-flow dilution tunnel that did not use a CVS system. In their design, shown schematically in Fig. 2.5, the engine exhaust was drawn into the dilution tunnel, along with ambient air from the test cell, by a constant-speed radial fan located at the exit of the tunnel. There was no heat exchanger and thus, in transient testing, the mass flow rate in the tunnel varied with the exhaust temperature. However, since a flow sensor was used to track the tunnel mass flow rate throughout each transient test, the only compromise made in this design applies to the particulate measurements. The total masses of each of the gaseous emissions for a transient test could be accurately determined by multiplying the flow rate information by the emission concentration values provided by the analyzers after accounting for sample-line delays. However, the particulate measurements could not be as accurate since the sample was drawn from the tunnel into the secondary dilution tunnel at a constant mass flow rate. This resulted in a systematic error since the sampling fraction was not held constant during the tests. The quantity of diluted exhaust sampled for particulates was not proportional to the total quantity of diluted exhaust. It should be noted though, that a systematic error will not affect repeatability.
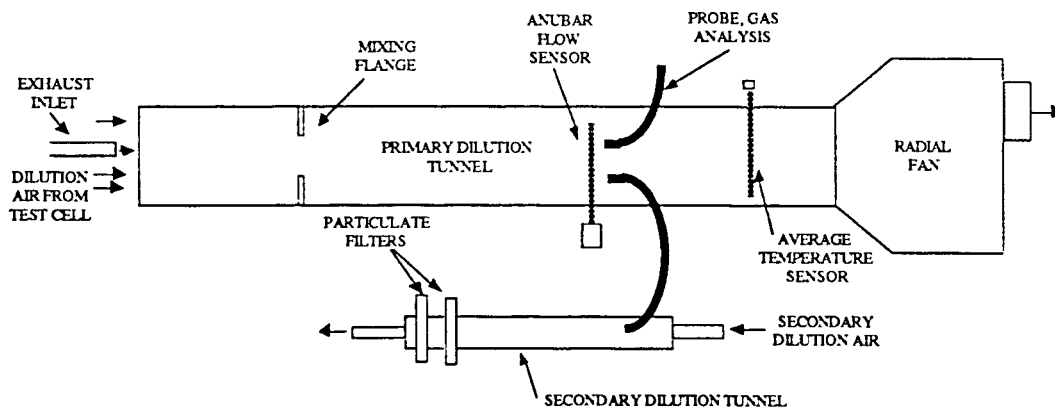
Fig. 2.5: Simplified dilution tunnel design of Heden, Eriksson and Gustavsson [8]

With this system, particulate measurement repeatability was within 14% of the mean values. HC measurement repeatability was within 10% and NO_x measurement repeatability was within 3%. The researchers concluded that the repeatability of the HC measurements could likely be improved by using a stable supply of clean, filtered dilution air instead of the test cell air which is subject to variations in HC levels due to oil and fuel

spills. Also, the systematic error in the particulate measurements could be eliminated by varying the secondary dilution tunnel flow rate and keeping it proportional to the primary tunnel flow rate.

These four examples of reduced-size and simplified dilution tunnels demonstrate that in some situations, adequate exhaust sampling systems can be developed when a full-flow, EPA-type system is not practical. In the first case, the engines being tested were small, non-production, laboratory engines and the interest was in fuel development, not in making the engines meet certain emission levels. In the last three cases, the engines being tested were heavy and light-duty diesel engines and although the interest was in meeting specific emission levels, most of the existing test cells did not have adequate space for a full-flow EPA type tunnel. Also, the cost of several such systems was prohibitive. Thus, smaller systems or simplified systems were designed for use until the engines were closer to the final stages of development. This approach reduces the number of EPA-type systems a company has to own.

In the case of the ISU engine laboratory, the situation is similar to all four examples. A heavy-duty diesel engine is being used for fuel additive research and the primary need is to compare diffent cases, not to try to make the engine meet specific emission levels. Thus, an EPA-type system is not essential. Also, similar to the last three examples, transient tests are to be performed but money and space are both constraining factors.

The examples illustrate that proportional sampling of the exhaust stream is possible through the use of either a controlled air ejector or special exhaust partitioning apparatus such as the multi-tube sampling system. Also, it is seen that a full-flow tunnel that does not use proportional sampling of the diluted exhaust can still achieve good repeatability since non-proportional sampling results in a systematic error. The last example demonstrates that a CVS system is not necessary for gaseous emission measurement if the dilution tunnel flow rate can be continuously monitored. The last example also brought out the importance of a clean, stable supply of dilution air.

The design that was chosen for the ISU laboratory was a full-flow tunnel that makes use of a clean, stable supply of dilution air from a high-capacity compressor. The tunnel flow rate is continuously monitored to facilitate gaseous emissions measurement and the systematic error of non-proportional sampling of the diluted exhaust for particulates is accepted. The details of the design appear in the following chapter.

CHAPTER III. EXPERIMENTAL APPARATUS

The emissions measurement system that was developed for this work is presented in this chapter. Aspects of the dilution tunnel and dilution-air supply are discussed first. Then the particulate sampling system that was used is presented. Finally, an overview of the engine test setup is given.

Dilution Tunnel

A diagram of the dilution tunnel appears in Fig. 3.1. The dilution tunnel is 0.305 meters (12 inches) in diameter. The distance between the introduction of the exhaust and the sample probes is 3.05 m (10 ft.) which corresponds to 10 tunnel diameters. Ten tunnel diameters is generally considered to be adequate for good mixing. In a dilution tunnel, it is desirable to maximize the volume-to-surface area ratio to reduce the opportunity for interactions between the diluted exhaust and the tunnel walls. Such interactions include heat transfer, hydrocarbon (HC) condensation and particulate deposition and re-entrainment. The volume-to-surface area ratio is maximized by making the diameter as large as practical.

The tunnel is made of standard galvanized spiral tubing. This material is not ideal since it does not have a perfectly smooth interior. A rough interior has the potential of catching some of the particulates that would otherwise have been part of the measurement, and further, causing problems with the particulates being reentrained into the stream at a later point in time within a transient test or perhaps during a different test altogether. The material was chosen based on its availability and low cost.

The exhaust is introduced into the tunnel through a 90° elbow of 6 cm exhaust pipe. The elbow faces downstream. The elbow was used to direct the exhaust into the center of the tunnel cross-sectional area to enhance even mixing of the exhaust with the dilution air.

A 20 cm diameter orifice was placed in the dilution tunnel at the point of entry of the exhaust. The increase in flow velocity and turbulence caused by the orifice is intended to enhance mixing. It should be noted that although the enhancement of mixing is desirable, any type of obstruction such as mixing vanes, could allow particulate deposition and re-entrainment. The orifice, when placed at the entrance of the exhaust, does not act as an obstruction to the mixture and consequently should not adversely effect particulate measurements.
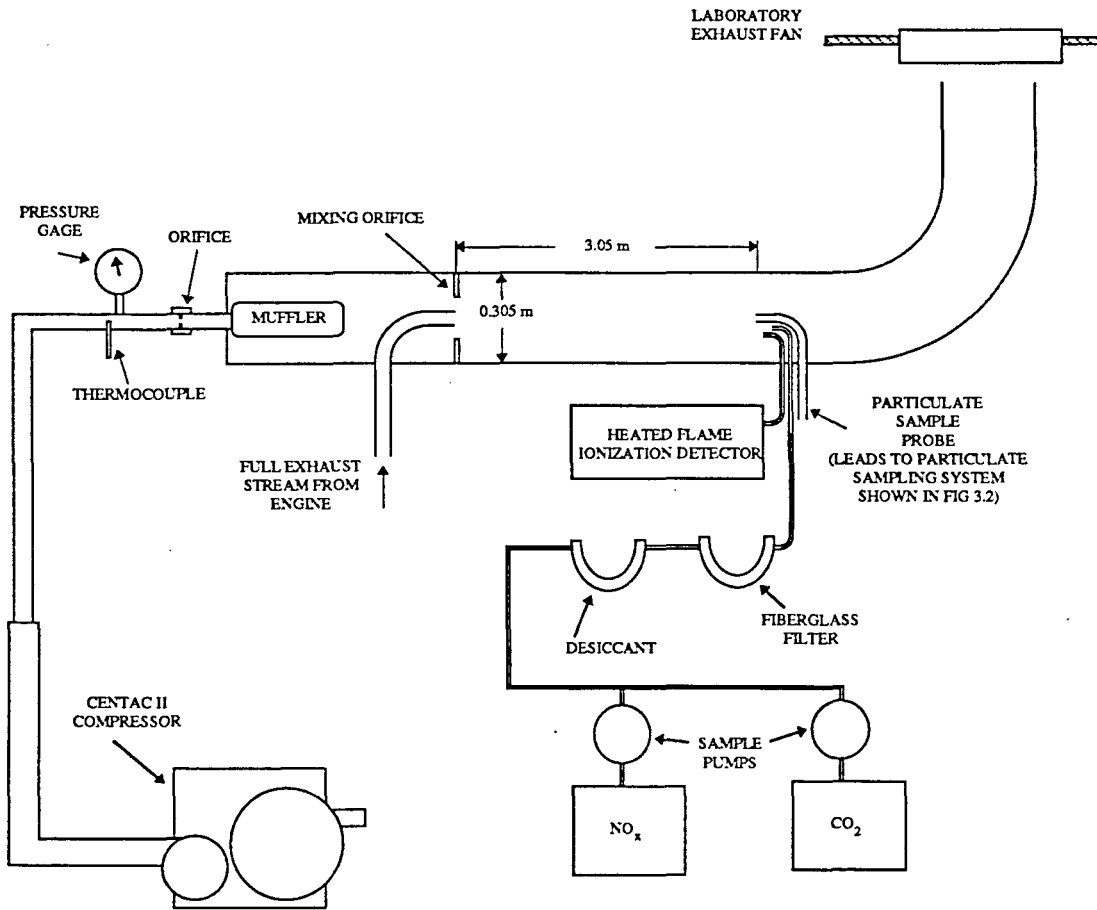
Fig. 3.1: Schematic diagram of emissions measurement system

The dilution tunnel exit is a few inches from a high-volume ceiling exhaust fan. The fan is in operation whenever the dilution tunnel is in operation and does an adequate job of keeping the laboratory ventilated.

Sample probes are located at a point 10 ft. downstream from the mixing orifice and exhaust inlet. Three stainless-steel probes have been installed into the tunnel. A 3/4-inch probe leads to the particulate sampling system, a 1/4-inch probe leads to the hydrocarbon analyzer and a 3/8-inch probe leads to the oxides of nitrogen (NO_x) and CO_2 analyzers.

Dilution Air System

Dilution air is provided by an Ingersoll-Rand Centac II two-stage air compressor located one floor below the engine laboratory. The compressor develops an outlet pressure of 620 kPa (90 psig). Between the compressor and the dilution tunnel is 9.8 meters of 15 centimeter (6 inch) diameter schedule 40 pipe followed by 14.44 meters 5 centimeter (2 inch) diameter schedule 40 pipe. The line loss for the maximum flow rate was measured to be 170 kPa (25 psi). The compressor's controller is able to hold the pressure within ± 7 kPa (1.0 psi) of the set value.

The dilution air supply system consists of a 5-centimeter (2-inch) pipe line with a ball valve followed by a standard in-line air filter and a smooth-edged orifice. Between the orifice and the pressure regulator is a static pressure probe with a manually readable gage and a thermocouple.

The flow rate of the dilution air in the tunnel is controlled by the dilution-air ball valve shown in Fig 3.1. The smooth-edged orifice downstream of it was calibrated as described in Appendix A to provide a means for determining the flow rate. Once calibrated, the flow rate could be determined from the pressure and temperature upstream of the orifice.

A considerable amount of noise is created by the uncontrolled expansion of the dilution air as it exits the 2 inch-diameter compressed air line to enter the dilution tunnel. An air-exhaust muffler was fitted to the end of the compressed air line and the noise was reduced to a tolerable level.

A fairly wide range of dilution ratios (ratio of dilution-air mass flow rate to exhaust mass flow rate) can be achieved with the dilution tunnel. The maximum dilution-air flow rate achievable in the tunnel is approximately 0.91 kg/s. The engine exhaust flow rate varies from about 0.05 kg/s for low-speed, light-load conditions to about 0.11

kg/s for the full-speed, full-load condition. Therefore, dilution ratios as large as 18 can be achieved for light loads while the maximum for the full-speed, full-load case is about 8.

During steady-state operation, the velocity of the diluted exhaust in the tunnel ranges from 7.4 m/s to 12.3 m/s. These high velocities enhance the mixing process by causing highly turbulent flow with Reynolds numbers of 1.3×10^5 to 2.1×10^5. The disadvantage of the high velocities, however, is that the time for the particulates to interact with the dilution air is less than 1 second. A secondary dilution tunnel could be used to increase the residence time of the diluted exhaust.

The ability of the dilution tunnel to thoroughly mix the exhaust and air was found to be quite good. Both horizontal and vertical sampling tranverses were made across the tunnel and uniform measurements were found. A discussion of the mixing tests that were performed is included in Appendix B. The EPA specifies the temperature of the diluted exhaust to be 52 °C or less. The dilution tunnel is capable of meeting this criteria for engine operating conditions of no more than 50% load.

Particulate Sampling System

A schematic diagram of the particulate sampling system appears in Fig. 3.2. The system consists of a ball valve to keep the diluted exhaust out of the system between tests, the particulate filter, a sample pump, and a gas meter with an electronic counter. The electronic counter is capable of displaying the total amount of gas that has passed though the system during a test as well as the instantaneous flow rate. The sample pump has a by-pass line with a valve. This by-pass valve provides a means for manually adjusting the flow rate though the particulate filter. This is necessary since the flow rate will tend to drop as the filter becomes loaded with particulates. An indication of the pressure drop across the particulate filter is given by the vacuum gage in the by-pass line. The vacuum pump shown in Fig. 3.2 is used to check the system leaks. A discussion of these leak tests is included in Appendix C.

As mentioned in the previous chapter, to accurately measure particulates during a transient test, the flow rate of the particulate sampling system must be a constant fraction of the total diluted exhaust flow rate. However, for this system, such proportional sampling is not possible. The problem is that the diluted exhaust flow rate varies in the dilution tunnel as the exhaust flow rate varies, and the volume flow rate of the particulate sampling system is held constant. This produces a variation in the sampling fraction. As
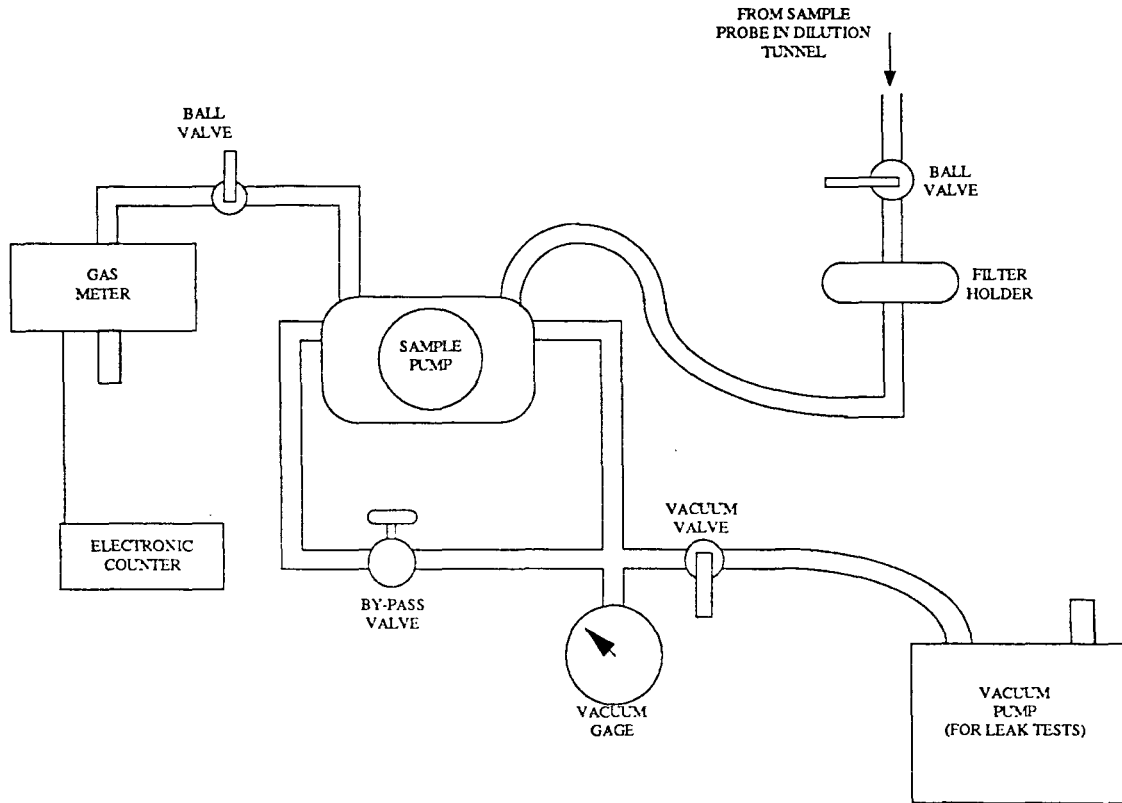
Fig. 3.2: Schematic diagram of particulate sampling system

was the case for Heden, Eriksson and Gustavsson [8], this results in a systematic error and therefore does not diminish the repeatability of the measurements.

While using higher dilution-air flow rates minimizes this non-proportional-sampling error, less particulate can be collected from the more highly diluted exhaust. Also, the concentrations of the gaseous emissions will be lower for more highly diluted exhaust. Thus, the random errors associated with measuring the emissions will become larger percentages of the measurements themselves.

Since the volume flow rate is held constant in the particulate sampling train, temperature fluctuations in the diluted exhaust during the transient test cause the mass flow rate in the sample train to vary. These variations are minimized since the sample volume flow rate is adjusted according to the flow rate measured by the gas meter at the end of the sample train. As the sample travels through the line, heat transfer with the surroundings brings the temperature of the sample closer to the ambient temperature, thereby eliminating some of the variation.

To minimize the impact of random errors in particulate filter weighing, it is desirable to obtain a large sample of particulate. Given a time constraint for each test, a large flow rate through the particulate filter must be used. The sample volume flow rate used for the tests in this study was 3.3 x 10^{-3} m^3/s (7 cfm). This rate was chosen because it was the largest flow that could be maintained through the filter for a 20-minute test with the engine operating in a high particulate-producing condition.

Engine Test Setup

The engine that was used in this study was a John Deere four-cylinder, four-stroke, model 4276T turbo-charged diesel engine. The basic engine specifications are presented in Table 3.1. The engine is connected to a General Electric DC dynamometer. A control program is run on a Digital Equipment Professional 380 computer which sends speed commands to the dynamometer controller and torque commands to a linear actuator attached to the fuel governor lever. This control program was used to set and maintain the engine's speed and load during steady-state tests and to control the engine during transient tests.

The volume flow rate of air into the engine was measured using a Meriam laminar flow element in conjunction with a Baratron pressure transducer to measure the pressure drop across it. The flow rate of diesel fuel was measured using a stopwatch and a Toledo electronic scale.

Table 3.1: Specifications for John Deere 4276T engine

Bore	106.5 mm
Displacement	4525.2 cm^3
Compression Ratio	16.8:1
Maximum Power	57.1 kW @ 2100 rpm
Peak Torque	305.0 Nm @ 1300 rpm

Dry bulb and wet bulb thermocouples were located at the inlet to the laminar flow element attached to the intake of the engine. Also, thermocouples were used to measure the engine oil and coolant temperatures. A thermocouple located at the fuel pump was used to measure the temperature of the fuel being supplied to the engine. Lastly, a thermocouple was located about four inches downstream of the turbocharger to measure the exhaust temperature. The barometric pressure was measured with a Datametrics Barocel pressure sensor.

Hydrocarbon measurements were made using a Beckman Model 402 Heated Flame Ionization Detector type hydrocarbon analyzer which includes a 3.5-meter long, electrically-heated sample line. A Beckman Model 955 chemiluminescent nitrogen oxides analyzer was used to measure the nitrogen oxides emissions. A Beckman Model 864 non-dispersive infrared radiation analyzer was used to make the carbon dioxide measurements.

A Digital Equipment ADM data acquisition module and a Digital Equipment Professional 380 computer were used to acquire the output of the three analyzers as well as the laminar flow element's pressure transducer. The voltage inputs were converted to units of ppm for the HC and NO_x and percent for the CO_2 and displayed on the screen at the sample rate of 0.5 Hz for the steady-state tests and 1.6 Hz for the transient tests. These readings were stored on the computer's hard disk for later use.

For the collection of particulates, 110 mm Pallflex T60A20 filters were used. The filters were weighed using a Christian Becker Model EA-1AP mechanical microbalance. The sensitivity of the balance was 0.0001 mg. A plexiglass desiccator

was used for drying the filters before weighing. The desiccator measures 35 cm x 94 cm x 71 cm and is subdivided into two chambers each with their own door and each housing about 5 lbs. of Drierite desiccant. A Scientific Glass Instruments four-inch, glass filter holder was used in the particulate sample train.

The next chapter describes the prodecures used to operate this equipment and perform the repeatability tests required to validate the dilution tunnel.

CHAPTER IV. EXPERIMENTAL PROCEDURE

In this study, both steady-state and transient tests of the dilution tunnel were conducted to investigate the repeatability of the measurement technique. The procedures used to conduct these tests are described in this chapter. The test data reduction is also discussed. Lastly, the schedules of tests for each day of testing are presented and discussed.

Steady-State Test Procedures

The steady-state tests were twenty minutes in length. This length was chosen so that the particulate filters could accumulate a sample of at least 10 mg. The measurement error of the microbalance used to weigh the filters was $\pm$ 0.3 mg. Thus, for samples of at least this size, the error in each weighing is no greater than $\pm$ 3 %. The gaseous emissions were also sampled for twenty minutes since it was desired to measure all of the emission species for the same period of time.

The procedure followed to conduct the steady-state tests in this study started with placing the particulate filters to be used into the desiccator. The purpose of the desiccator was to remove most of the moisture from the filters so the mass of the filter material alone could be determined. After 48 hours, the filters were removed from the desiccator and weighed with the Christian Becker microbalance. The approximate length of time between removing a filter from the desiccator and obtaining a reading on the microbalance was 45 seconds. It was assumed that in that amount of time, a negligible amount of moisture would be reabsorbed from the atmosphere. The relative humidity in the room containing the microbalance was consistently between 53% and 56%.

Once the tare weights of the filters were determined, the engine tests could be conducted. Before starting the engine, the gaseous emission analyzers were calibrated, a particulate filter was placed in the filter holder shown in Fig 3.1, and the data acquisition program was started. Regarding instrument calibration, on the first day the instruments were calibrated just prior to the tests, and the calibration was checked at the end of the nine-hour schedule. On all subsequent days, the instrument calibration was checked every three hours and recalibrations were done as necessary.

When the engine was started, the speed and load were immediately set at 1400 rpm and 50% rated load. The flow rate of the engine's intake air was viewed on the

screen of the data acquisition computer and used to set the dilution air-system orifice pressure needed for a dilution ratio of 10.

Five minutes after the engine was started, the first measurement began. The data acquisition system automatically recorded the emission analyzer readings and engine inlet-air flow rate. The particulate sampling system was started by opening the sample line valve shown in Fig 3.1 and then immediately starting the sample pump. The electronic counter shown in the same figure displayed the sample flow rate. During the test, the sample pump bypass valve was adjusted as necessary to maintain the flow rate within 3% of 7 cfm.

At the beginning of the test the weight of the diesel fuel-supply tank was recorded. Within five minutes after the beginning of the test, the ambient, wet bulb, fuel, oil and exhaust temperatures were recorded as well as the atmospheric pressure. At the end of the test, the particulate sample pump was turned off, the sample-line valve was immediately shut, and the weight of the diesel fuel-supply tank was recorded.

Ten minute intervals were allowed between each test to facilitate calibration checks, desiccant replacements and particulate filter changes. When the test schedule called for a speed and load change, the change was made in the middle of the ten minute interval such that the next test began five minutes after the change.

After the last test was finished, the particulate filters were replaced into the desiccator for 48 hours. At the end of that period, they were removed and weighed. The difference in the final weight and the tare weight was considered to be the mass of the particulate sample. These data were then combined with the sample flow rate and total tunnel flow rates to determine the total mass of particulates emitted by the engine during the twenty minute test. At all times the filters were handled using steel forceps.

The HC and NO_x data for each two-second data-acquisition sampling interval were combined with the total tunnel flow rate for the same interval and totaled over the twenty minute period to determine the total mass of each emission emitted during the test. The change in calibration of the analyzers was recorded prior to each calibration of the analyzers and after the completion of all of the tests each day. This information was then used to correct the data for errors due to calibration drift. To do so, a linear change was assumed between the initial and final calibrations. A typical calibration drift was 2% of the span-gas concentration.

While the particulate, HC and NO_x data are reported as the total masses emitted by the engine during the twenty-minute test, the CO_2 results were normalized to brake-

specific CO_2 (BSCO$_2$) values by dividing by the total engine work of the test. Brake-specific fuel consumption (BSFC) values were calculated from the change in the fuel supply-tank weight and the total engine work of the test. Finally, the average equivalence ratio of each test was calculated from the fuel consumption and average inlet-air flow rate. The details of these calculations are given in Appendix D. Graphical representations of these quantities appear in Chapter V and Appendix F while complete tables of the results appear in Appendix G.

Transient Test Procedures

For the transient tests, the procedure specified in the Code of Federal Regulations (CFR) [1] was followed as closely as possible. The procedure specified for the federal test procedure (FTP) transient test is to cold-soak the engine by shutting it off for a minimum of 12 hours or until the oil temperature reaches 75 °F. In this study, the cold-soak periods were at least 21 hours in length resulting in an oil temperature of 84 °F. Then the engine is started and immediately controlled according to the twenty-minute FTP schedule of speeds and loads. However, in this work, due to the nature of the control program, an extra one minute of idle (1200 rpm, 0% load) condition occurred between the starting of the engine and the beginning of the transient control.

Although as soon as the schedule is completed, the engine is to be shut off, there was another one minute of idle operation in the tests of this study. Then, as specified in the CFR, the engine remained off for twenty minutes. Following this period, known as the "hot-soak," the engine was restarted for the hot-start test, and following the one minute idle period, controlled according to the same schedule of speeds and loads. Once the schedule is completed and the extra idle period finished, the engine was shut off, and the official FTP test was complete. However, several hot-start tests were run consecutively thereafter. Between each of the tests a twenty minute hot-soak period was scheduled.

The sample valve was opened at the same time as the engine was started for each test, and the sample pump was turned on immediately thereafter. The sample flow rate was maintained within 3% of 7 cfm for the whole test via the sample pump by-pass valve. The pump was turned off at the completion of the transient schedule, before the one-minute idle period, and the sample line valve closed. The particulate filters were dried and weighed in the same manner as described above for the steady-state tests.

The total mass of the particulate emitted by the engine during each test was determined from the sample mass, the average sample flow rate and the average total dilution tunnel flow rate. The total masses were then normalized to brake-specific particulate values by dividing by the total engine work of the test. The details of this calculation are shown in Appendix D.

The gaseous emission analyzers were calibrated prior to the cold-start test and before each hot start test. A correction was applied to the gaseous emission data by using the average of the initial and final calibrations for each test. The gaseous emissions data were recorded from the beginning of the transient test schedule to the end, not including the two extra one-minute idle periods.

In order to properly determine the total amount of each emission produced during the test, the delay times between the exhaust leaving the engine and being measured by the analyzers was taken into account. The delay time for each analyzer was determined by introducing a calibration gas at the sample probe and measuring the length of time required for the analyzer to reach 90% of its final reading. Then assuming an typical exhaust flowrate and corresponding tunnel flowrate the length of time required for the exhaust to travel from the engine exit, through the exhaust pipe, and down the tunnel to the sample probes was calculated and added to the sample-line/instrument delay. The resulting values for delay times were 8.0 seconds, 3.7 seconds and 25.8 seconds for the CO_2, HC and NO_x analyzers respectively.

The total amount of each of the gaseous species for a given test was determined by multiplying the concentration data provided by the emission analyzers by the total tunnel flow rate for each data acquisition-sampling interval, taking into account the delay times. The results were then normalized to brake-specific values by dividing by the total engine work of the test. The details of these calculations are given in Appendix D.

Test Program

The types of repeatability and aspects of repeatability outlined in Chapter I were investigated though an eight-day series of steady-state tests followed by a three-day series of transient tests. Through this program, the consecutive-measurement and day-to-day repeatabilities of each type of test were to be determined. Also, during the steady-state tests, the influence of previous operating conditions on the engine's emissions and the length of time following a speed and load change required for steady-state emissions production to be acheived were to be determined.

Table 4.1 shows the test schedules for the eight days of steady-state tests. The first column in Table 4.1 shows the time at which each test began and ended relative to when the engine was started. Then in the second and fifth columns of the table, Roman numerals are assigned to each period of time between speed and load changes.

Days 1, 4 and 6 were days that engine or dynamometer problems occurred, thus ending the experiments for the day. Their partial schedules are identical to the the first test day immediately following them. The schedules for each day were designed to help determine the various types of repeatability of measurements made with the engine and dilution tunnel system. The first six measurements during each of the steady-state test days were made at the same speeds and loads so that the day-to-day reproducibility of the measurements could be determined. The schedule for day 2 was chosen to investigate reproducibility of consecutive measurements. The schedule for day 3 was set up to have that day's data act as control data in the determination of the effect of previous operating conditions on the emissions of the engine. The engine was set at 1400 rpm, 50% during period I and then changed to 1400 rpm 100% load for period II. This sequence of operating conditions was then repeated for periods III and IV and periods V and VI.

For days 5, 6 and 7, a variety of speed and load combinations were chosen for periods I, III and V to precede the 1400 rpm, 100% load condition of periods II, IV and VI. The test schedule for day 5 was identical to day 3, the control, with the exception that during period III, the engine was run at a different speed than during periods I and V. This was done to determine if the 1800 rpm, 50% load condition of period III would cause the emissions in period IV to differ from those of period II and if so, whether or not the state of the engine during period II could be restored during period VI by duplicating the speed and load of period I during period V.

On days 7 and 8, again the effect of previous operating conditions on repeatability was to be determined. During period III of day 7, the engine was run at a full-speed full-load condition, and during period V it was run at a low-speed, light-load condition. This was done to determine if the emissions of the 1400 rpm, 100% load conditions of periods IV and VI were significantly affected by these previous operating conditions. During day 8, the same speed and load settings were set during periods III and V as were in day 7. However, the engine was set at 1400 rpm and 25% load during periods IV and VI to determine if such a light-load condition is more sensitive to previous operating conditions than the 1400 rpm, 100% load condition of day 7. The data from all of the days was

Table 4.1. Test schedules for each day of steady-state reproducibility tests

Time (hr after start)	DAY 1 Test Period	Speed (rpm)	Load (% of rated)	DAY 2 Test Period	Speed (rpm)	Load (% of rated)
0:05 - 0:25	I	1400	50	I	1400	50
0:35 - 0:55	I	1400	50	I	1400	50
1:05 - 1:25				II	1400	100
1:35 - 1:55				II	1400	100
2:05 - 2:25				II	1400	100
2:35 - 2:55				II	1400	100
3:05 - 3:25				II	1400	100
3:35 - 3:55				II	1400	100
4:05 - 4:25				II	1400	100
4:35 - 4:55				II	1400	100
5:05 - 5:25				III	1800	100
5:35 - 5:55				III	1800	100
6:05 - 6:25				III	1800	100
6:35 - 6:55				III	1800	100
7:05 - 7:25				III	1800	100
7:35 - 7:55				III	1800	100
8:05 - 8:25				III	1800	100
8:35 - 8:55				III	1800	100

Time (hr after start)	DAY 3 Test Period	Speed (rpm)	Load (% of rated)	DAY 4 Test Period	Speed (rpm)	Load (% of rated)
0:05 - 0:25	I	1400	50	I	1400	50
0:35 - 0:55	I	1400	50	I	1400	50
1:05 - 1:25	II	1400	100	II	1400	100
1:35 - 1:55	II	1400	100	II	1400	100
2:05 - 2:25	II	1400	100	II	1400	100
2:35 - 2:55	II	1400	100	II	1400	100
3:05 - 3:25	III	1400	50	III	1800	50
3:35 - 3:55	III	1400	50	III	1800	50
4:05 - 4:25	IV	1400	100	IV	1400	100
4:35 - 4:55	IV	1400	100	IV	1400	100
5:05 - 5:25	IV	1400	100			
5:35 - 5:55	IV	1400	100			
6:05 - 6:25	V	1400	50			
6:35 - 6:55	V	1400	50			
7:05 - 7:25	VI	1400	100			
7:35 - 7:55	VI	1400	100			
8:05 - 8:25	VI	1400	100			
8:35 - 8:55	VI	1400	100			

Table 4.1 (continued)

Time (hr after start)	Test Period	DAY 5 Speed (rpm)	Load (% of rated)	Test Period	DAY 6 Speed (rpm)	Load (% of rated)
0:05 - 0:25	I	1400	50	I	1400	50
0:35 - 0:55	I	1400	50	I	1400	50
1:05 - 1:25	II	1400	100	II	1400	100
1:35 - 1:55	II	1400	100	II	1400	100
2:05 - 2:25	II	1400	100	II	1400	100
2:35 - 2:55	II	1400	100	II	1400	100
3:05 - 3:25	III	1800	50	III	2100	100
3:35 - 3:55	III	1800	50	III	2100	100
4:05 - 4:25	IV	1400	100	IV	1400	100
4:35 - 4:55	IV	1400	100	IV	1400	100
5:05 - 5:25	IV	1400	100	IV	1400	100
5:35 - 5:55	IV	1400	100	IV	1400	100
6:05 - 6:25	V	1400	50			
6:35 - 6:55	V	1400	50			
7:05 - 7:25	VI	1400	100			
7:35 - 7:55	VI	1400	100			
8:05 - 8:25	VI	1400	100			
8:35 - 8:55	VI	1400	100			

Time (hr after start)	Test Period	DAY 7 Speed (rpm)	Load (% of rated)	Test Period	DAY 8 Speed (rpm)	Load (% of rated)
0:05 - 0:25	I	1400	50	I	1400	50
0:35 - 0:55	I	1400	50	I	1400	50
1:05 - 1:25	II	1400	100	II	1400	100
1:35 - 1:55	II	1400	100	II	1400	100
2:05 - 2:25	II	1400	100	II	1400	100
2:35 - 2:55	II	1400	100	II	1400	100
3:05 - 3:25	III	2100	100	III	2100	100
3:35 - 3:55	III	2100	100	III	2100	100
4:05 - 4:25	IV	1400	100	IV	1400	25
4:35 - 4:55	IV	1400	100	IV	1400	25
5:05 - 5:25	IV	1400	100	IV	1400	25
5:35 - 5:55	IV	1400	100	IV	1400	25
6:05 - 6:25	V	1250	25	V	1250	25
6:35 - 6:55	V	1250	25	V	1250	25
7:05 - 7:25	VI	1400	100	VI	1400	25
7:35 - 7:55	VI	1400	100	VI	1400	25
8:05 - 8:25	VI	1400	100	VI	1400	25
8:35 - 8:55	VI	1400	100	VI	1400	25

used to determine the length of time following a speed and load change that is required for steady-state emission production to be resumed.

Table 4.2 shows the schedules that were followed during the transient tests. The objective of the transient tests was to establish the repeatability of measurements made during consecutive hot-start tests, and to determine the day-to-day repeatability of the cold-start and hot-start portions of the test. The Code of Federal Regulations [2] specifies a transient test to consist of the cold start test followed by a twenty-minute hot-soak period and then one hot-start test. This was done on each of the three days, but in addition, several more hot-start tests were conducted spaced each time by a twenty-minute hot-soak period.

The results from these tests are examined in the next chapter. The repeatabilities of the measurements are determined and the influence of transient periods following speed and load changes and the influence of previous operating conditions of the data are assessed.

Table 4.2. Test schedules for each day of transient tests

	DAY 1	DAY 2	DAY 3
Time (hr after start)	Transient Test	Transient Test	Transient Test
0:00 - 0:20	cold	cold	cold
0:40 - 1:00	hot 1	hot 1	hot 1
1:20 - 1:40	hot 2	hot 2	hot 2
2:00 - 2:20	hot 3	hot 3	hot 3
2:40 - 3:00	hot 4	hot 4	
3:20 - 3:40	hot 5	hot 5	
4:00 - 4:20		hot 6	
4:40 - 5:00		hot 7	
5:20 - 5:40		hot 8	

CHAPTER V. RESULTS AND DISCUSSION

In order to determine whether the emissions measurements taken using the dilution tunnel described in this thesis are valid, it would be desirable to compare the measurements with an EPA-type system. Such a comparison would insure that the system indicated the same level of emissions and that the repeatability was similar. However, an EPA-type system was not available for comparison so such a test was not conducted. Moreover, the repeatability can still be assessed without such a direct comparison. Since the system's intended use was for comparison of alcohol fumigation with standard diesel fuel operation, repeatability was more important than having the data correspond to an EPA system.

The results of the repeatability tests are discussed in this chapter. The eight days of steady-state tests and three days of transient tests discussed in Chapter IV comprise the data. In the first section, the steady-state test results are examined to determine the repeatability of consecutive measurements. Next, the length of time following a speed and load change required for the steady production of emissions to be resumed is discussed in light of the same data. Also, the influence of previous operating conditions on the engine's emissions is discussed. The day-to-day repeatability of the steady-state test measurements is then determined. The transient-test data are then examined to determine the repeatability of consecutive hot-start test measurements and the day-to-day repeatability of the measurements.

There is a limited amount of repeatability data available for comparison with the results of this study. The Coordinating Research Council (CRC)[3] has reported that between laboratories, high-speed steady-state particulate measurement tests are repeatable to within ± 6 - 17% of the mean. For low-speed steady-state tests the measurements are only repeatable to within ± 20 - 45% of the mean. These figures are based on inter-laboratory comparisons of the same engine and therefore reflect consecutive-measurement repeatability, day-to-day repeatability, and inter-laboratory repeatability. In this study, the consecutive measurement repeatability was determined separately from the day-to-day repeatability. In the case of the federal test procedure (FTP) transient test, the CRC reports particulate measurements within a test site typically do not deviate more than 6% from the mean.

Barsic [9] has compiled the results of a study in which six engines were sent to seven laboratories and tested on both the federal test procedure transient cycle and the

now-obsolete 13-mode test cycle. Since 13-mode test cycle data consist of a weighted average of 13 steady-state tests, the repeatability data from these tests is used, in this chapter, to compare with the steady-state repeatabilities of this study. Barsic reported 2s standard deviations of the emissions data which was normalized to brake-specific values. The term "2s standard deviation" simply means the standard deviation multiplied by two. The data were normalized by dividing the total mass of an emission species produced by the engine during a test by the total engine work of the test. This gives rise to the units of grams per kilowatt-hour (g/kW-hr).

The values of within-laboratory data variability reported by Barsic for the 13-mode tests are 2s standard deviations of 0.12 g/kW-hr for particulates, 0.06 g/kW-hr for unburned hydrocarbons (HC) and 0.76 g/kW-hr for oxides of nitrogen (NO_x). For the cold-start portion of the transient tests, the within-laboratory variations are reported as 2s standard deviations of 0.42 g/kW-hr for particulates, 0.50 g/kW-hr for HC and 0.57 g/kW-hr for NO_x. Finally, for the hot-start portion of transient tests, the within-laboratory variations are reported as 2s standard deviations of 0.11 g/kW-hr for particulates, 0.15 g/kW-hr for HC and 0.51 g/kW-hr for NO_x. When these variations are compared to the current EPA emissions standards, the 2s standard deviations for the hot-start transient test represent 18.3% of the standard for particulates, 11.5% for HC and 4.8% for NO_x.

In addition to the figures included in this chapter, graphs of the variation of test variables during each test day and from one day to the next are presented in Appendix E. A complete table of the results is located in Appendix F.

Consecutive Measurement Repeatability of Steady-State Tests

The repeatability of consecutive measurements was determined for steady-state tests from the data taken on the second day of tests. During that day, the engine was run at two different speed and load combinations for four hours each. For each of these periods, eight consecutive twenty-minute measurements were made. The average values of the measurements for each period were calculated along with the standard deviations. 2s coefficients of variation (2 x standard deviation / mean) were calculated as measures of repeatability. If the samples were collected from a large population, it would be expected that 95% of the measurements would fall within the range indicated by this parameter.

The results from day 2 are shown in Fig. 5.1. The quantities plotted are the total masses of particulates, HC and NO_x produced by the engine during consecutive twenty-

minute periods. Since the values are indicative of the engine's operation for a twenty-minute period, the width of each of the data points in the figure corresponds to twenty minutes on the x axis. The information at the top of the figure shows divisions at the times when the speed and load were changed, the values of the speed and load for each period and the roman numerals that were used in Table 4.1 to designate each period.

Fig. 5.1 indicates that the repeatability of the measurements of all three emissions is fairly good for both periods II and III with one exception. The HC measurements during period III dropped continuously for the entire four-hour period.

Table 5.1 summarizes the repeatability exhibited in Fig. 5.1. The average values of each group of eight measurements are given along with the maximum deviations from the mean of the data points, the standard deviation and the 2s coefficient of variation. Also included, for comparison with the results reported by Barsic and mentioned earlier in this chapter, are the 2s standard deviations normalized by the total engine work done during each test.

While the 2s coefficients of variation indicate that the best repeatability was seen in the NO_x measurements, comparison with Barsic's results show that the particulate repeatability compares the most favorably with other laboratories. The 2s coefficients of variation in five of the six cases indicate that data variability for consecutive measurements is no greater than 8.2%.

The cause of the continual downward drift in the HC measurements of period III is not clear. The resulting deviations from the mean were 32.8% above and 26.1% below and the 2s coefficient of variation was 42.0%. As Fig. 5.1 shows, these deviations appear to be a function of time rather than random. It is possible that some variation in one of the test variables could have caused this variation in HC emissions. Figs. 5.2 and 5.3 show the variation of several test variables throughout the day. In these two figures, the data points connected with lines are located with respect to the x axis at the times when the measurement of the respective quantity was made. The width of the data points for the dilution ratio, brake specific fuel consumption (BSFC) and equivalence ratio correspond to 20 minutes on the x axis. The dilution ratio data are represented in this way because they corresponds to manual settings that did not vary significantly during the test. The BSFC and equivalence ratio values are averages for the full length of each test and thus are also represented with the wide data points.
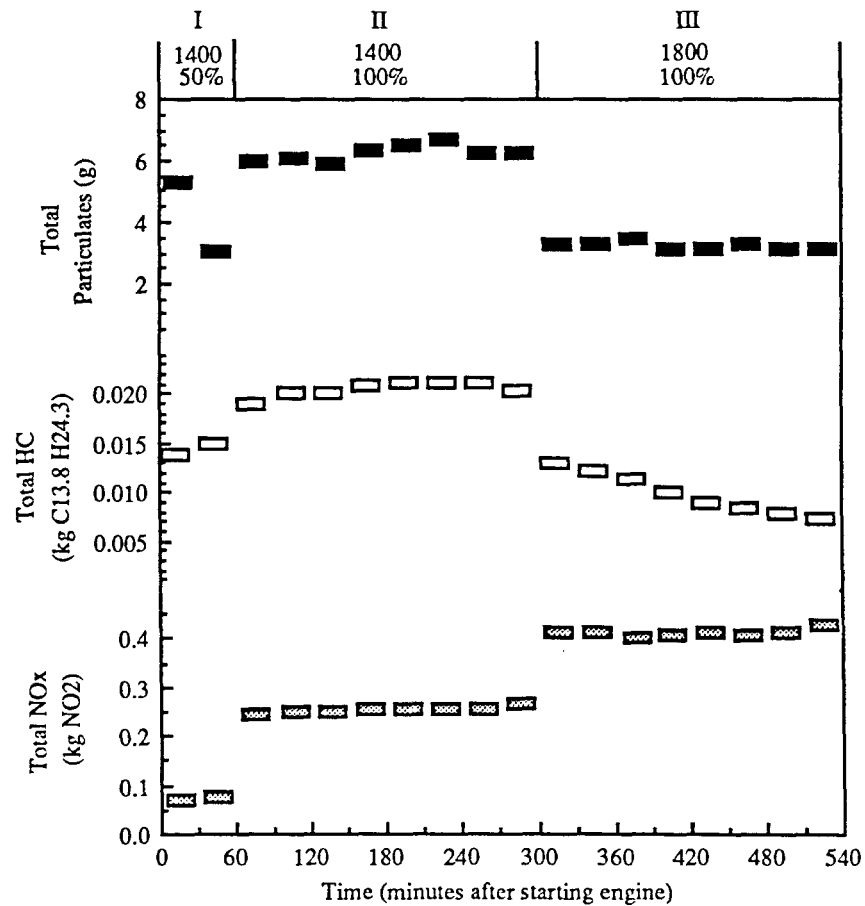
Fig. 5.1: Emission measurements from day 2

Of these variables, only the ambient temperature and humidity had significant trends during the last four hours of testing. However, Krause, Merrion and Green [10] were unable to find any correlation between humidity and HC emissions in their work. They did find an effect of intake temperature on HC emissions for some of the engines that they tested. However, similar HC drifts occurred in four of the other test days studied in this thesis, and in three of the cases, there was no corresponding temperature change. Further, during day 6, there was a substantial rise in temperature that was not accompanied by a change in the HC measurements.

The continuous decline in hydrocarbons is probably not due to instrument calibration drift since the calibration check at the end of the nine-hour test day showed the heated flame ionization detector calibration to have drifted only 0.2% from the span gas

concentration. This is a small drift and would cause the HC readings to appear higher than actuality instead of lower. Further, a correction for this slight drift was used in the calculations by assuming a linear drift throughout the entire day. A possible explanation is that a substantial amount of HC had built up in the deposits in the exhaust system during period II when the HC production was higher. This excess HC then may have slowly depleted during period III.

Overall, the data from day 2 indicate that consecutive measurements for steady-state tests are repeatable within 9% for particulates. This figure compares favorably with the 6-17% maximum deviations reported by the CRC[3]. The data also indicate that for HC the repeatability is within 8% of the mean and for NO_x the repeatability is within 5% of the mean. The 2s standard deviations for particulates were 0.037 and 0.017 g/kW-hr. These values are considerably lower than the value of 0.12 g/kW-hr reported by Barsic[9]. However, the HC 2s standard deviation of 0.12 g/kW-hr is twice as high as the 0.06 g/kW-hr value from the same reference. Likewise, the 2s standard deviations of 0.87 and 1.18 g/kW-hr for the NO_x measurements are high compared to the value of 0.76 g/kW-hr reported by Barsic.

Table 5.1: Summary of consecutive measurement repeatability for day 2

	Particulates		HC		NO_x	
Period	II	III	II	III	II	III
Average (g)	6.264	3.278	20.5	9.9	254	412
Maximum Deviation Above Mean (%)	6.4	6.6	3.4	32.8	4.5	4.1
Maximum Deviation Below Mean (%)	5.2	3.7	6.6	26.1	3.1	3.1
Standard Deviation (g)	0.258	0.121	0.8	2.1	6.0	8.2
2s Coefficient of Variation (%)	8.2	7.4	7.8	42.0	4.7	4.0
2s Standard Deviation (g/kW-hr)	0.037	0.017	0.12	0.30	0.87	1.18
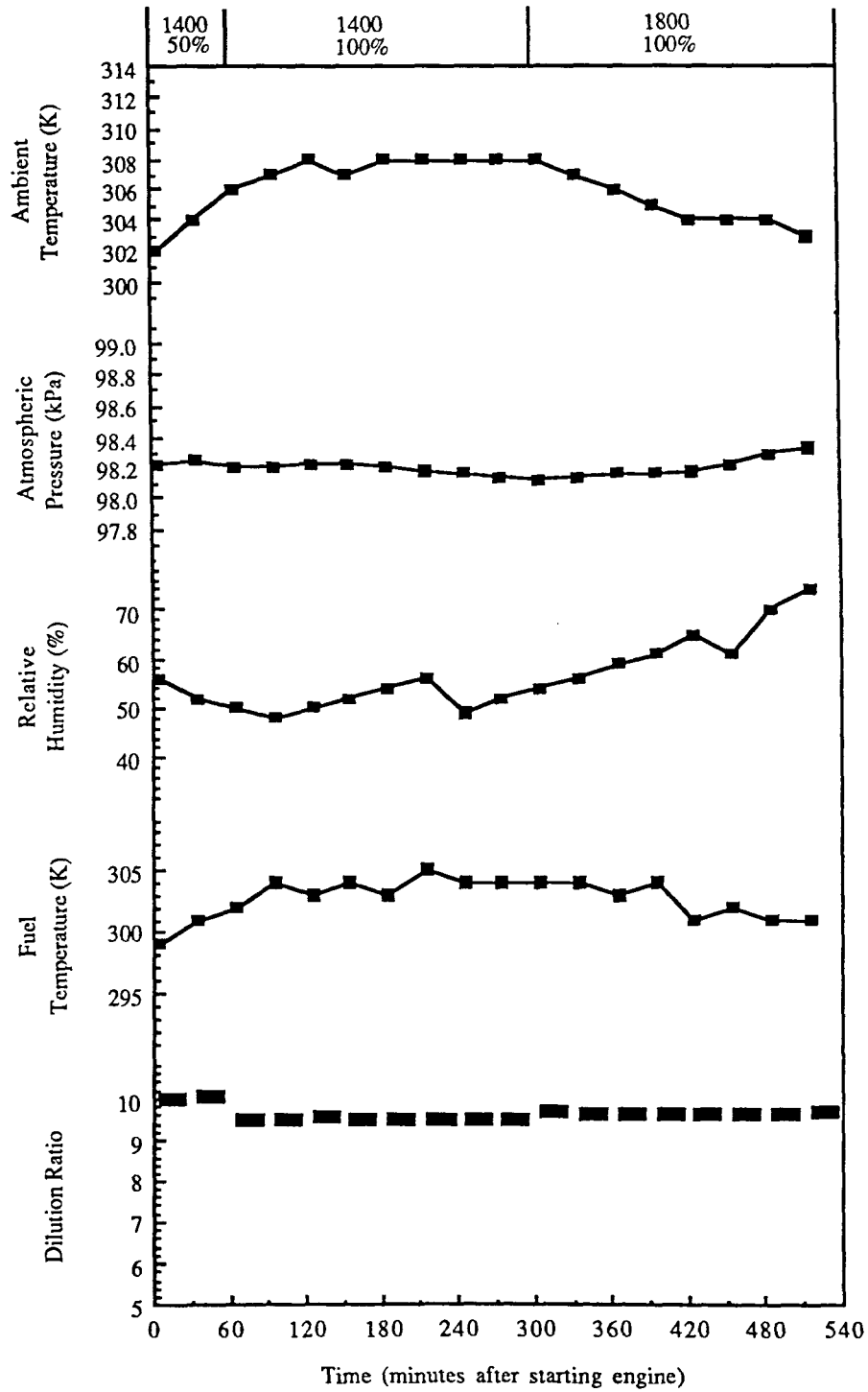
Fig. 5.2: Ambient conditions, fuel temperature and dilution ratio variations during day 2
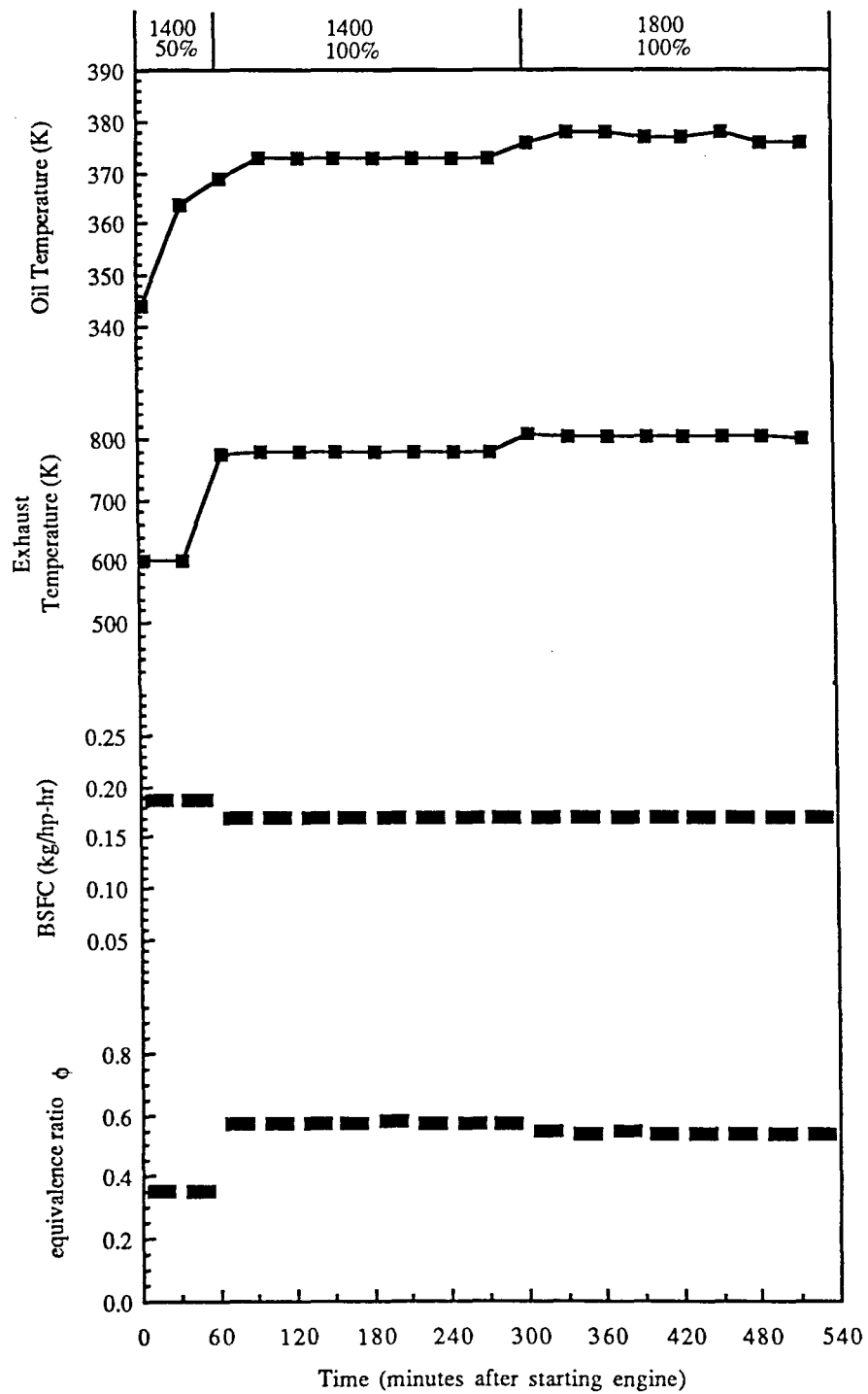
Fig. 5.3: Engine parameter variations during day 2

Transient Period Following a Change in Speed and Load

Following a speed and load change, there will be some period of time for which the production of emissions will not be steady. The length of that period of time was to be determined from the steady-state test data. On each of the days 3 through 8, the speed and load of the engine was changed from one setting to another and then held constant while four twenty-minute measurements were made. The first of these measurements started five minutes after the change was made. Upon initial inspection the data indicated that the transient period in question would affect at most the first of the four measurements. A criteria was chosen to determine if the first of four data points was significantly different than the rest of the group. If the data point differed from the mean by more than 1.645 standard deviations, which corresponds to 90% confidence limits, the point was considered different. There were instances in the HC data where the measurement changed continuously for one to four hours. These were also considered as possible indicators of a significant transient period.

There are two possible indications of a transient period following a speed and load change in the data from day 2 shown in Fig. 5.1. The first data point in the HC measurements of period II lies outside of the 90% confidence limits of the group. This deviation indicates a possible transient period in the range of five to twenty minutes in duration. The decreasing levels of the HC measurements made during period III, however, indicate a transient period of at least four hours in duration. Neither the particulate nor the NO_x data show any signs of being affected by a transient period.

The particulate, HC and NO_x data from the rest of the steady-state test days, with the exception of day 1 which consisted of only two measurements, appears in Fig. 5.4 through 5.9. Although the same speed and load combinations were used each day for periods I and II, the short transient period indicated by the period II HC data of Fig. 5.1 is not seen in any of the data from the rest of the test days. There is a drift in the period II HC data of day 4 as shown in Fig. 5.5, however values were decreasing instead of increasing as was the case in period II of Fig. 5.1. Thus, neither of these two changes in HC levels are indicative of a transient period of HC production resulting from the load change from period I to period II.

Again referring to the day 2 data of Fig. 5.1, after the engine was initially started the first particulate measurement of period I was substantially larger than the second. There was also a small difference between the two HC measurements of period I. This
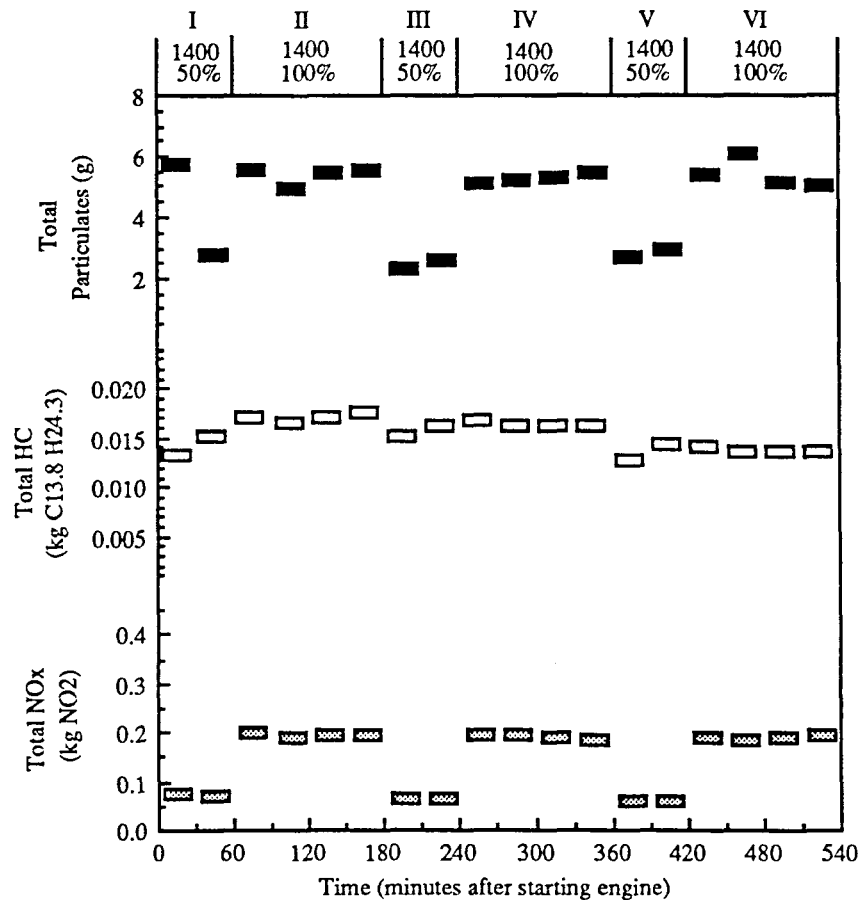
Fig 5.4: Emission measurements of day 3

indicates that there may be a period of time required after the engine is initially started for steady amounts of these two emissions to be produced and this period is long enough to effect a measurement made in the first five to 25 minutes of engine operation. The NOx measurements, however, were not affected in this way.

Particulate, HC and NO_x data from day 3 appear in Fig. 5.4. The groups of four measurements in periods II, IV and VI do not show any trends in the data following the load changes from the previous period. Although a slight trend appears in the particulate data of period IV, the variations of the period II and period VI particulate data indicate that it is probably just due to the random error of the measurement. As is the case for the data from days 4 through 8, none of the first data points for particulate, HC or NOx in periods II, IV or VI lie outside the 90% confidence limits of the data in the respective periods.
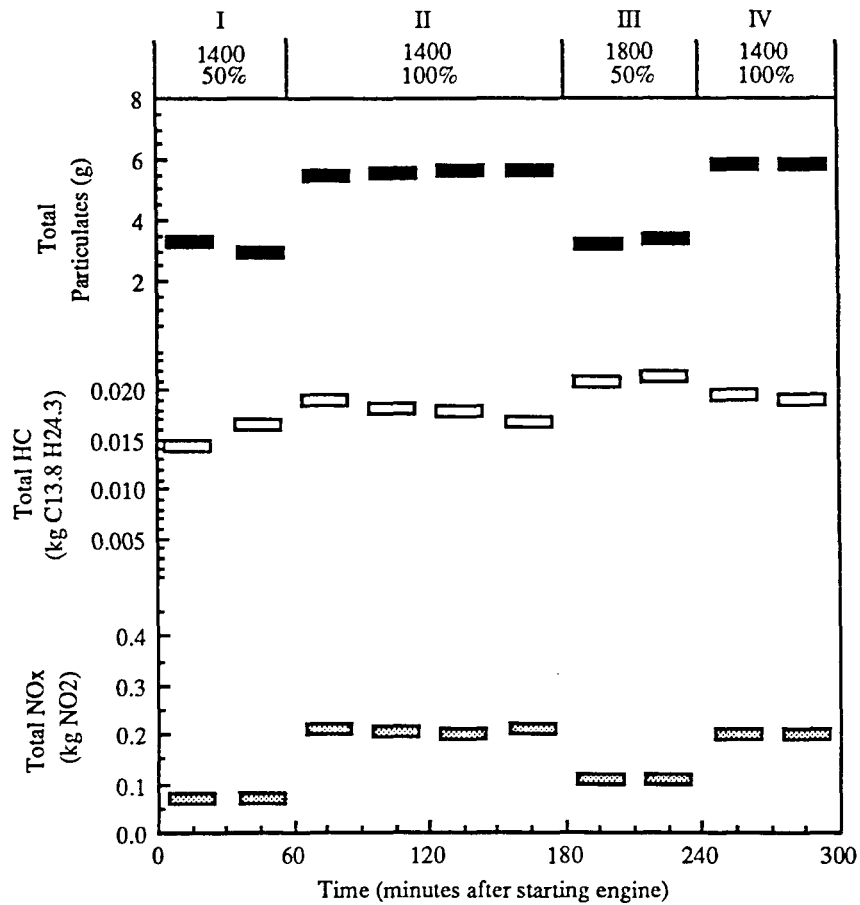
Fig. 5.5: Emission measurements of day 4

As was the case for day 2, the two period-I particulate measurements in Fig. 5.4 were substantially different indicating a possible period of transient particulate production following the start-up of the engine. There was also a substantial difference in the two period-I HC measurements. However, a similar difference is seen in the HC measurements from periods III and V. Thus, the 1400 rpm, 50% load condition exhibits either a period of transient HC production following start-up and speed and load changes or simply higher variations in HC levels. Which of these possibilities is correct cannot be determined because there are only two data points in each period. The measurements of NO_x in period I of Fig. 5.4 are nearly identical indicating that the measurements were not subject to any transient NO_x production period following the start-up of the engine.

41
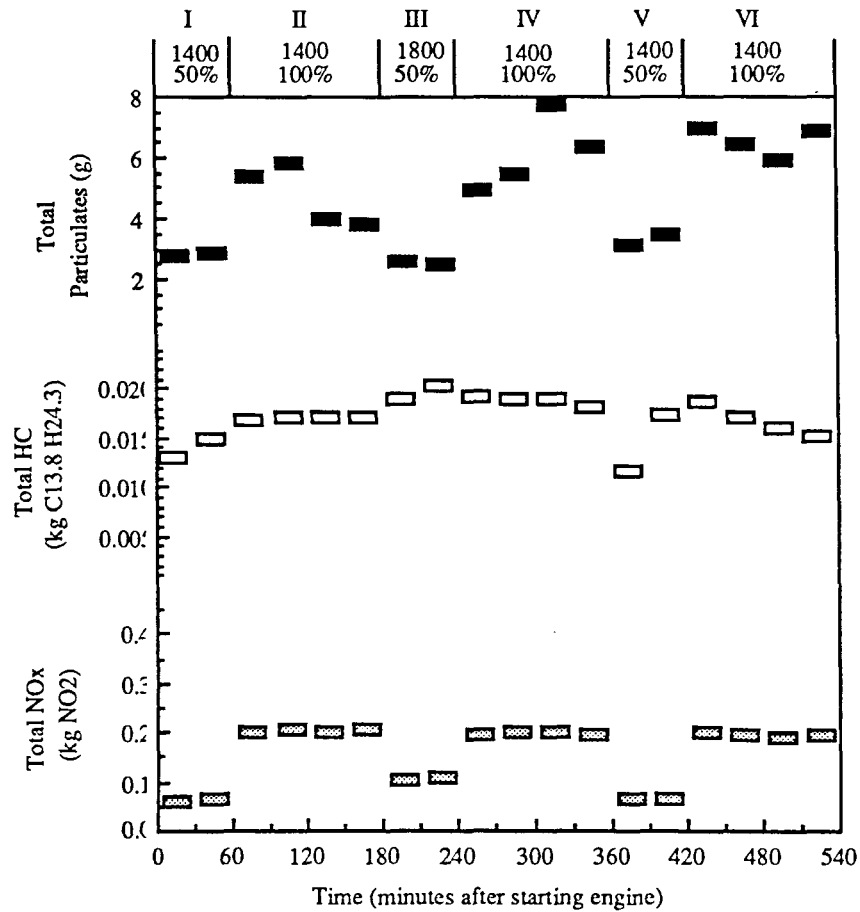
Fig. 5.6: Emission results of day 5

The results from day 4 appear in Fig. 5.5. The particulate and NO_x measurements of period II do not exhibit any trends to indicate a period of transient emission production following the load change from period I. There is, however, a slight downward trend in the HC measurements of period II. On this day the large difference between the first and second particulate measurements in period I that was seen in days 2 and 3 was not present. The first HC measurement in period I is still low compared to the second, and the NO_x measurements of period I had close to the same values.

The particulate, HC and NO_x results from day 5 are shown in Fig. 5.6. The only part of the data from this day that showed signs of a period of transient emission production was the period VI HC data which declined over the course of two-hours.
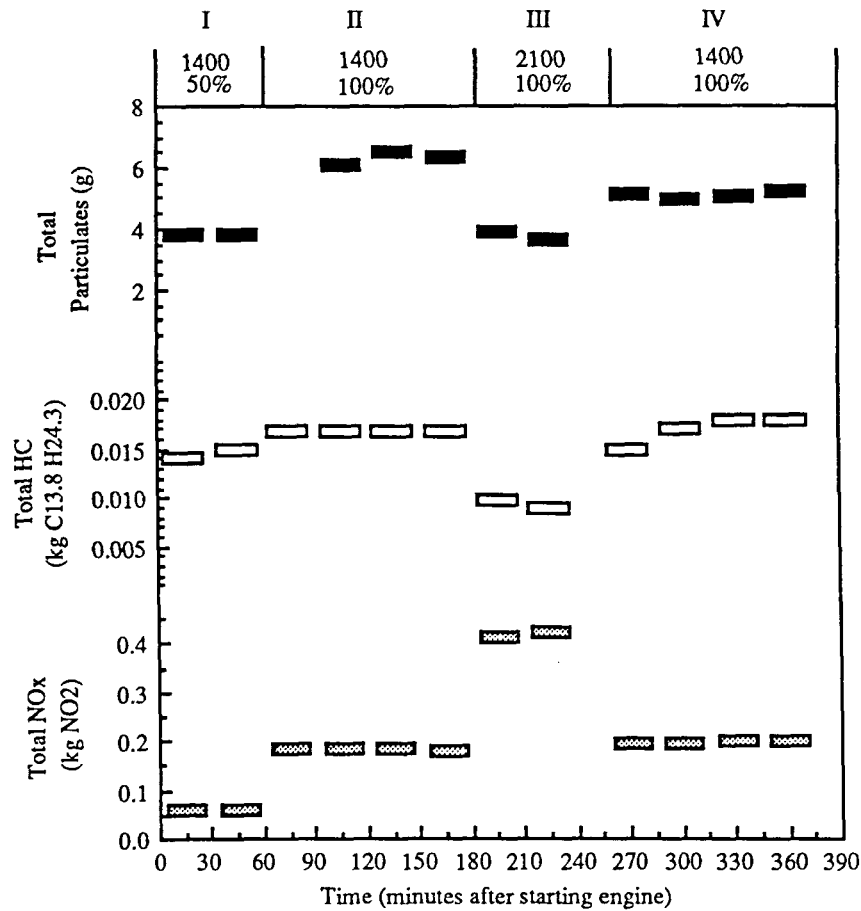
Fig. 5.7: Emission measurements of day 6

This decline was similar to the decline of HC in period III of day 2 shown in Fig. 5.1. The high deviations in the particulate measurements of periods II, IV and VI make it difficult to identify any possibletransient periods for the particulates. No large differences in the pairs of particulate, HC or NO_x measurements in periods I are seen in Fig. 5.6.

The day-6 results appear in Fig. 5.7. The first particulate measurement of period II is missing due to a problem with the filter. The only indication of a period of transient emission production is in HC data of period IV. During that period the HC level increased over the course of one hour. None of the pairs of measurements in period I of Fig. 5.7 show any large differences between the first and the second measurements. Thus, there does not appear to be a significant period of transient particulate, HC or NO_x production following the start-up of the engine for day 6.
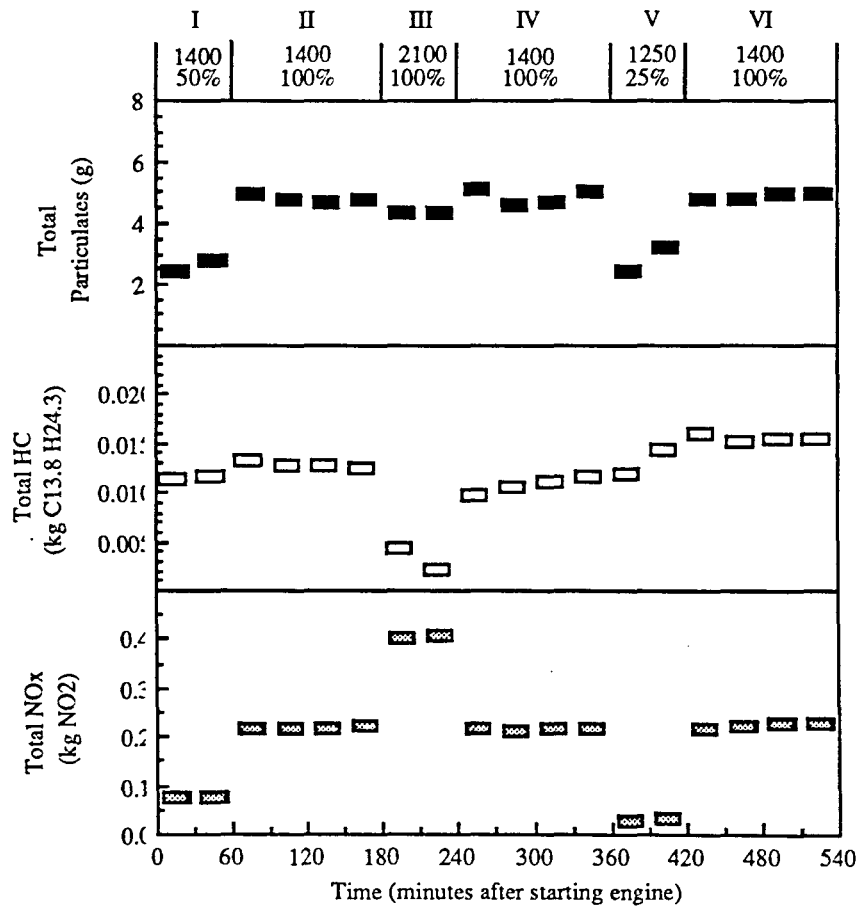
Fig. 5.8: Emission measurements of day 7

As shown in Fig. 5.8, there was upward HC data trend in period IV of day 7. Also, for that day, The measurements during period I did not change greatly from the first one to the second for any of the three emissions, and like day 6, there does not appear to be a significant period of transient particulate, HC or NO_x production following the start-up of the engine.

Finally, on day 8, as shown in Fig. 5.9, there was another upward HC trend in period IV. Also, there was no evidence in the period-I measurements of a period of transient emission production following the start-up of the engine.

Most of the data indicate that the transient period of emissions production is short enough so as not to affect even the first measurement after a speed and load change. Other data suggest that this period is occasionally quite lengthy, perhaps several hours in duration. None of the data clearly indicate a transient period of a length
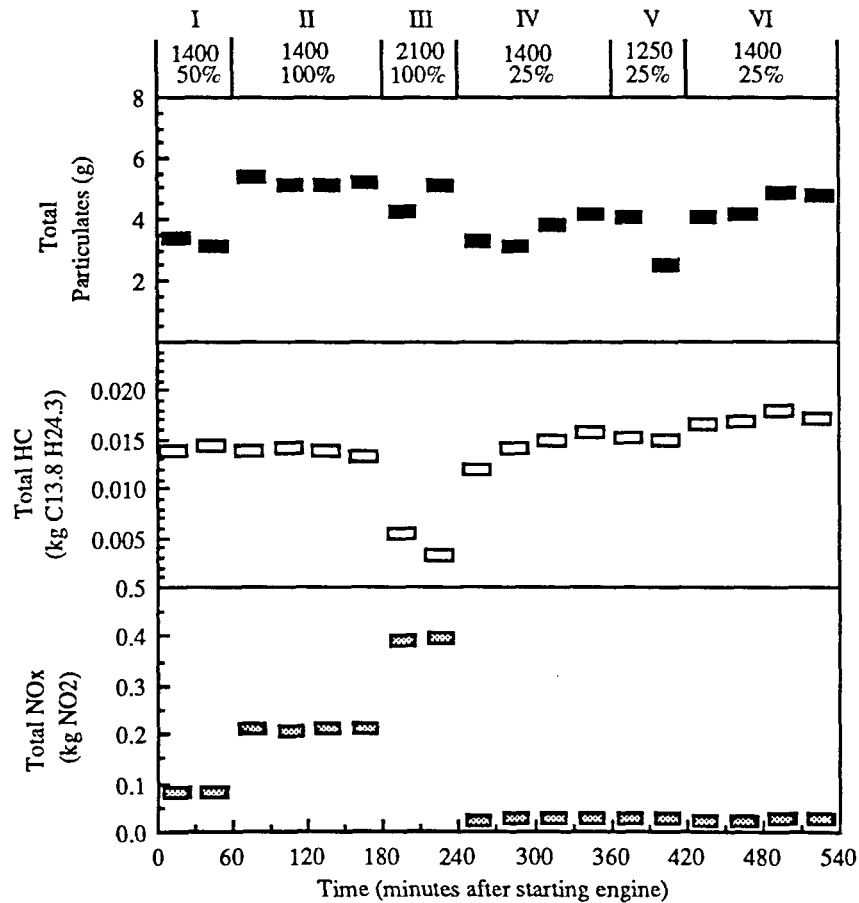
Fig. 5.9: Emission measurements of day 8

that is between these two extremes. Where there is a transient period in the data, it is in the HC measurements and lasts at least one hour. In only one case was it found that the first measurement following a speed and load change fell outside the 90% confidence limits of the rest of the data in the group. Thus, the transient period never appeared to be significant in the range of 5 minutes to 25 minutes after the speed and load change. In light of this conclusion, and the fact that all of the indications of transient emission production were in the HC data, the transient period following a speed and load change does not appear to have a significant influence on particulate or NO_x measurements made at least five minutes after the change. Since particulate and NOx measurements are steady, it is likely that the engine's production of all three emissions is steady and that the occasional drifts seen in the HC measurements are perhaps due to non-engine effects such as HC adsorption and re-entrainment from the exhaust system, dilution tunnel and

HC sample probe, significant background HC variations in the dilution air, or a substantial non-linear calibration drift problem with the heated flame ionization detector that was not recognized and corrected for.

Influence of Previous Operating Conditions on Measurements

It is possible that setting the same speed and load combination following two different operating conditions will not result in the same level of emissions production. In the previous section it was established that there does not seem to be a period of transient emission production following a speed and load change of sufficient length to affect the measurements. However, there is still a possibility that some long-term shift in the data might occur due to the operating condition prior to the change. The data from days 3, 5, 6 and 7 of steady-state testing were examined to determine the significant differences in the particulate, HC and NO_x measurements of the 1400 rpm, 100% load condition of periods II, IV and VI. The dependence of these differences on the previous operating conditions was then established.

By selecting the same speed and load combination of 1400 rpm, 50% load for periods I, III and V of day 3, whose schedule is shown in Table 4.1, the uncertainty associated with making speed and load changes from this same previous operating condition could be characterized. On day 8, a 1400 rpm, 25% load condition was chosen for periods IV and VI to determine if such a light-load condition is more sensitive to previous operating conditions than a heavy-load condition such as 1400 rpm and 100% load.

Table 5.2 lists the means and the standard deviations of the particulate, HC and NO_x measurements of periods II, IV and VI for days 3 though 8. The same information from periods II and III of day 2 is included, while day 1 is omitted since only the two measurements of period I were made on that day. Statistical F tests were used to determine the significant differences in standard deviations, and t tests with a significance level of 5% were used to determine the significant differences in average measurements discussed below.

The results from day 3, shown in Fig. 5.4 and Table 5.2, showed that there was not a significant difference between the averages of the particulate measurements made in periods II, IV and VI. That is, each time after returning from the 50% load condition, the engine produced the same amount of particulates. However, the standard deviation of particulate data from period VI was 0.490 which is significantly higher

than that of the first two groups. This indicates that perhaps the operation of the engine was not as steady in the last period as before. However, the notion of non-steady engine operation during period VI is not supported by the HC or NO_x data. In the case of the HC there was no significant difference observed in the standard deviations between the three periods. Period VI did, however, have a significantly lower average. The NO_x results for day 3 showed no significant difference in either the averages of periods II, IV and VI or their standard deviations. Thus, the data from day 3 show that perhaps some increase in particulate measurement standard deviation and some change in HC level may occur independent of the speed and load of the previous operating condition.

Table 5.2: Means and standard deviations of steady-state measurements

Day/Period	Speed/Load (rpm/%)	Total Partic. Average (g)	Total Partic. Standard Dev. (g)	Total HC Average (g)	Total HC Standard Dev. (g)	Total NOx Average (g)	Total NOx Standard Dev. (g)
3/II	1400/100	5.386	0.271	17.1	0.7	198	4.7
3/IV	1400/100	5.298	0.146	16.5	0.5	192	3.5
3/VI	1400/100	5.434	0.490	13.8	0.3	190	4.2
5/II	1400/100	4.758	0.987	17.1	0.2	203	1.3
5/IV	1400/100	6.125	1.207	18.9	0.5	199	2.9
5/VI	1400/100	6.535	0.447	16.8	1.5	195	3.5
6/II	1400/100	6.322	0.218	16.9	0.1	183	2.8
6/IV	1400/100	5.103	0.126	16.9	1.4	199	4.4
7/II	1400/100	4.810	0.124	12.9	0.3	220	3.3
7/IV	1400/100	4.861	0.253	10.8	0.8	216	2.1
7/VI	1400/100	4.864	0.009	15.6	0.4	224	5.3
8/IV	1400/25	3.609	0.458	14.2	1.7	25	1.9
8/VI	1400/25	4.466	0.379	17.2	0.6	25	2.1

During day 5, the engine speed and load were changed to 1400 rpm, 100% load three times. The first time the previous condition was 1400 rpm, 50% load, the second time it was 1800 rpm, 50% load and the last time it was 1400 rpm, 50% load again. Because of the high standard deviations in the particulate data of day 5, the effect of previous operating conditions on particulate production is difficult to ascertain. If the particulates are affected by previous operating conditions, a difference in the means of

periods II and IV should be seen. Any changes in the standard deviation should be ignored since the control data of day 3 determined that such a change can occur independent of previous operating conditions. The average of the particulate measurements in period IV was higher than that of period II. However, the high standard deviations prevented the t-test from concluding that the means were significantly different.

Since the same operating condition preceded period VI as preceded period I, it is expected that the means of the particulate measurements of the two periods should be statistically similar. However, the t-test indicated that there is a significant difference between the means of the two periods. This discrepancy raises the possibility that the unique operating condition of period III caused the particulates to be affected not only during period IV but much later in the day during period VI. However, this conclusion cannot be justified since the means of periods II and IV were statistically similar, meaning that the particulates in periods IV were not affected by the previous operating conditions. Instead, the conclusion that should be drawn is that, although the control data of day 3 does not indicate that changes in the mean value of the particulate measurements can occur independent of the previous operating condition, the data of day 4 shows that in fact, they can. The particulate data from day 5 has therefore effectively become part of the control data and in doing so, has established that both the particulate mean values and standard deviations may change independent of previous operating conditions. The data from days 6, 7 and 8 can still be examined for effects of previous operating conditions on particulates. However, the above conclusion dictates that only changes in the standard deviations and mean values of magnitudes substantially larger than the changes seen in the control data of days 3 and 5 should be considered. The data from those remaining days do not indicate any such large changes. The effect of previous operating conditions on particulate production can not be determined because another influencing variable dominates changes in the standard deviations and mean values of the measurements. It is not clear from the present experiments what this variable might be.

In the case of the HC results from day 5 shown in Fig. 5.6, the averages of periods II, IV and VI were all statistically different. However, the control data of day 3 indicates that such discrepancies may occur independently of the previous operating conditions. F tests showed the standard deviations to be statistically similar for periods II and IV. This indicates that the HC measurements of periods II and VI were not

dependent on the previous operating conditions. Further, the standard deviations of periods II and VI were significantly different. Since there was no significant difference between periods II and IV, the change in the standard deviation for period VI cannot be attributed to the unique operating condition that was chosen for period III. It would appear that, as was the case with the particulate measurements, both the mean values and standard deviations of the HC data vary independently of previous operating conditions. However, the variation in the period VI data does not appear to be random but rather is a consistent downward trend. Two observations can be made with regard to this distinction. First, since such a trend did not appear in period IV, it cannot be attributed to the unique operating condition of period III. It follows that such a trend can occur independently of previous operating conditions. The second observation is that the notion that a change in standard deviation may depend upon previous operating conditions cannot be dismissed. A substantial increase in the random variation of the data would be different from an increase in standard deviation due to a continuous decline or increase in the magnitude of the measurements. In fact, the statistical F test does not apply to period VI since the data is not normally distributed.

The HC data from day 6 which appear in Fig. 5.7 also show no indication of a dependence of HC measurements on previous operating conditions. The control data of day 3 and the observations made above about day 4 indicate that neither changes in mean values or the existence of trends in the data are indicative of an influence of previous operating conditions. Only comparisons of the standard deviations can be made. However, the trend in the HC measurements of period IV of day 6 indicate that the data are not normally distributed and consequently a comparison cannot be made of the standard deviations of periods II and IV.

During day 7, the engine speed and load were again changed to 1400 rpm and 100% load three times. The first time, the previous condition was 1400 rpm, 50% load, the second time it was 2100 rpm, 100% load and the last time is was 1250 rpm, 25% load.

The HC results of day 7 appear in Fig. 5.8. There was an upward trend in the data of period IV indicating that the data were not normally distributed. Thus, only the standard deviations of periods II and VI can be compared. For that comparison, the F test indicates that there is no significant difference in the standard deviations of the two periods. The data from day 7 give no indication that the standard deviation of HC measurements is dependent upon previous operating conditions.

During the last two-thirds of day 8, the engine speed and load were changed to 1400 rpm and 25% load twice. The first time, the previous condition was 2100 rpm, 100% load and the second time it was 1250 rpm, 25% load. The HC results of day 8 appear in Fig. 5.9. A comparison of the standard deviations of only periods IV and VI is desirable since in both cases the load was 25% whereas in period II it was 100%. However, the upward trend in the data during period IV indicate that the data are not normally distributed and thus comparison of standard deviations with an F test is not possible.

There are three conclusions that can be drawn about the HC data. First, as the data from day 3 show, the mean of the HC measurements varies independently of previous operating conditions. The second conclusion is that the data from day 4 show that trends in the HC data can also occur independently of previous operating conditions. Lastly, the data from days 5,7 and 8 indicate that the standard deviation of HC measurements is not significantly influenced by previous operating conditions.

It is immediately obvious upon inspection of Figs 5.6 through 5.9 that the means and standard deviations of the NO_x data were very consistent. An analysis of the NO_x data similar to that of the particulate and HC data could be made at this point. However, visual inspection of the NO_x data in Figs. 5.6 through 5.9 does not raise the concern that there may be some significant effect of previous operating conditions of the NO_x measurements. The investigation for particulates and HC was justified because of the existence of upward and downward trends and changes in the means and standard deviations of the particulate measurements. These discrepancies are immediately obvious upon inspection of Figs. 5.6 through 5.9., but if there is a dependance of the NO_x data upon previous operating conditions it is a negligible one.

In summary, no change in particulate measurement means and standard deviations due to previous operating conditions can be ascertained from the data. The data indicate that the standard deviations of HC measurements are not influenced by previous operating conditions. The mean values of HC measurements vary independently of the previous operating conditions to the extent that any dependence that may exist cannot be ascertained. Likewise, the upward and downward trends in some of the HC data occur independently of previous operating conditions and any dependence that may exist cannot be ascertained. Any dependence of the means or standard deviations of the NO_x data on previous operating conditions that may exist has a negligible impact on the data.
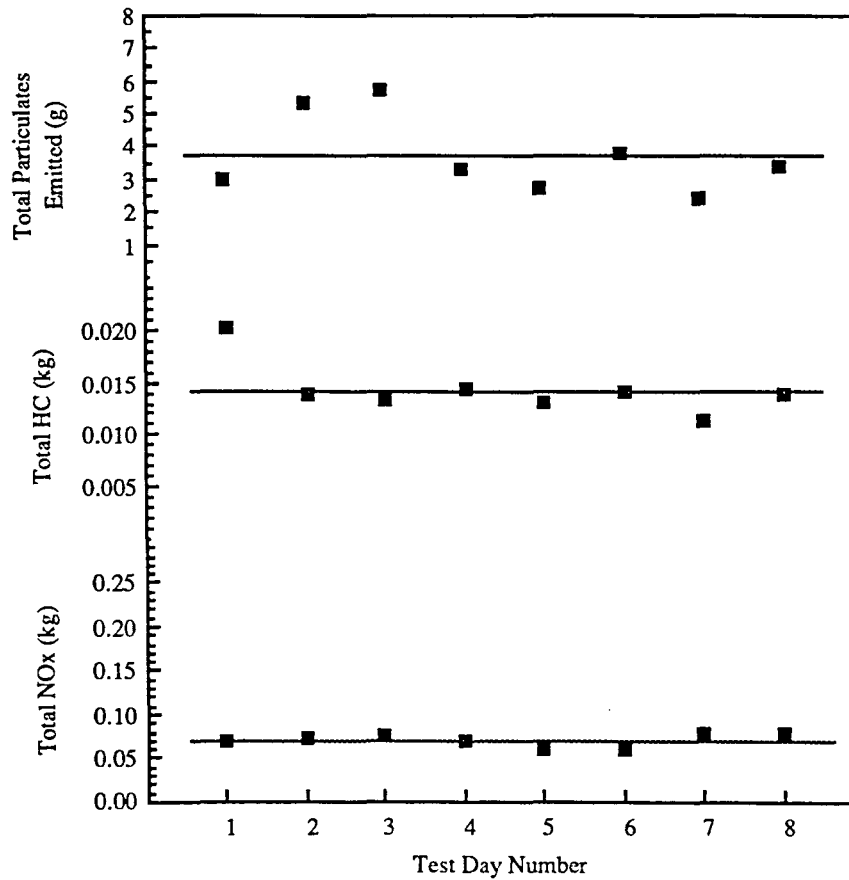
Fig. 5.10: Day-to-day repeatability of measurement 1

Day-to-Day Repeatability of Steady-State Tests

Variations in ambient laboratory conditions can cause the repeatability of particulate, HC and NOx measurements made on different days to differ from the consecutive-measurement repeatability. Since the day-to-day repeatability is influenced by the same random errors that influence consecutive-measurement repeatability, plus the additional ambient variations, it is expected that day-to-day repeatability will not be as good as consecutive-measurement repeatability. The first six measurements of each of the eight steady-state test days were taken at the same conditions on each day. In this section, their means are compared and 2s coefficients of variation are calculated to characterize the day-to-day repeatability. The results are then compared with published values.

Fig. 5.10 shows the particulate, HC and NOx measurement variations over the eight test days for the first measurement of the day. In the figure, the horizontal line through each set of data points represents the average value for the data. The variation in the particulates is noticeably large. The 2s coefficient of variation is 64%. The major reason for this poor repeatability is the measurements made on days 2 and 3. On these days there was a significant period of transient particulate production following the start-up of the engine. This transient period was not seen on any of the other days, and as indicated by the results of the rest of the measurements shown in Figs. 5.11 through 5.15, the repeatability of the particulates was the poorest for the first measurement of the day. period of transient particulate production following the start-up of the engine. This transient period was not seen on any of the other days, and as indicated by the results of the rest of the measurements shown in Figs. 5.11 through 5.15, the repeatability of the particulates was the poorest for the first measurement of the day. The HC results from measurement 1, again shown in Fig. 5.10, show that the measurement made during day 1 was significantly higher than for the rest of the days. Also, Fig. 5.11 shows that the second HC measurement made on day 1 was significantly lower than day 1 or that there is an unpredictable transient period of HC production following the start-up of the engine. The NOx measurements of Fig. 5.10 do not indicate a transient period of NOx production following the start-up of the engine.

Measurements 3 through 6, which appear in Figs. 5.12 through 5.15, are the four measurements corresponding to period II of each day. Since the data from day 1 included of only the two measurements of period I, there are no day-1 data shown in these figures. The four figures look similar to each other. For example, in each figure the last two HC measurements are lower than the rest of the HC measurements. The similarity of the figures suggests that the consecutive-measurement repeatability within each of the days was considerably better than the day-to-day repeatability. If the two types of repeatability had been of the same magnitude, the figures would not appear similar. For example, there would be no consistency in the positions of each of the two HC measurements mentioned relative to the rest of the measurements.

The reason for the low HC measurements could be related to the ambient temperature being about 5 °C lower during the last two days of tests. Krause, Merrion and Green [10] have reported significant, but variable temperature effects on the HC production of some engines.
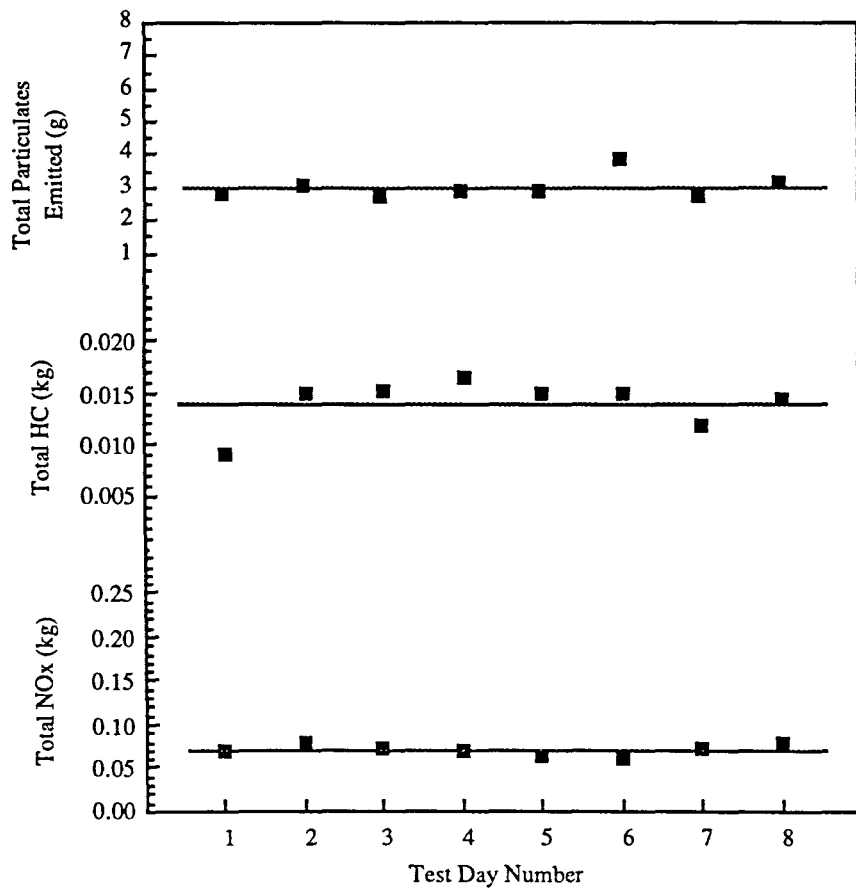
Fig. 5.11: Day-to-day repeatability of measurement 2

A noticeable feature of the particulate data in Figs. 5.12 through 5.15 is the large deviations in the measurements from days 5 and 6 that occur in measurement 5 and 6 but not in measurements 3 and 4. No significant changes in the ambient conditions or engine parameters of oil temperature, exhaust temperature and fuel consumption could be correlated to these deviations. Thus, the deviations may have been caused by filter handling and weighing errors.

Tables 5.3 through 5.5 summarize the day-to-day repeatability exhibited by the data. The last column in each table is a summary of the repeatability of the averages of the period II measurements, i.e., measurements 3 through 6. Included as the last row of each table are the 2s standard deviations normalized by the total engine work for each test. These values are for comparison with the those reported by Barsic [9].
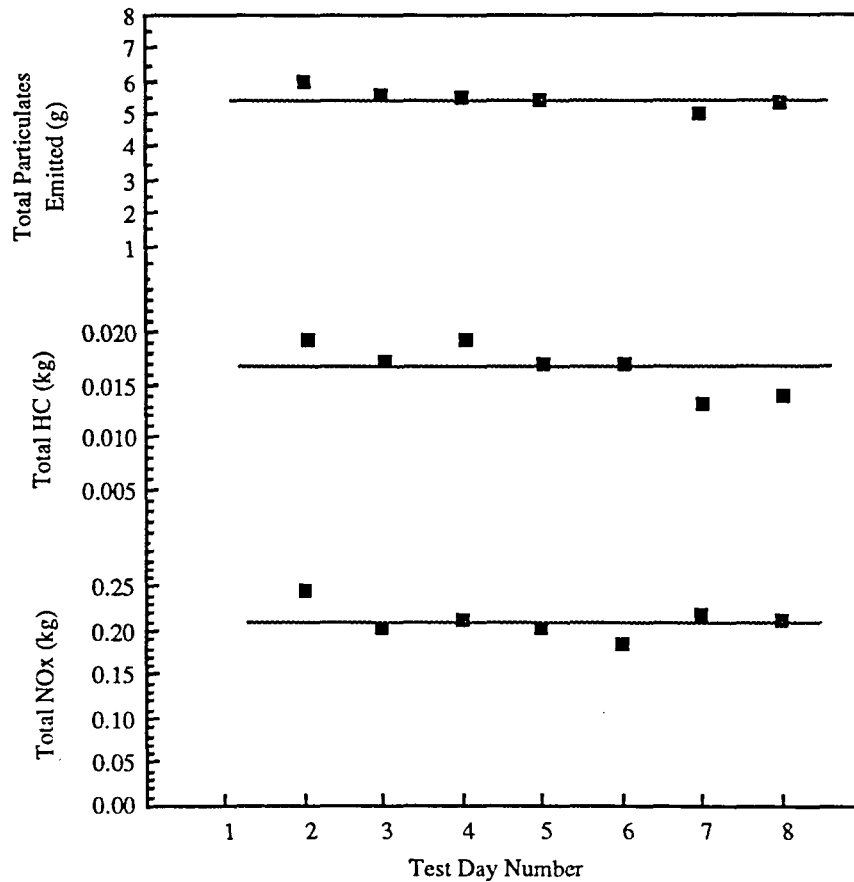
Fig. 5.12: Day-to-day repeatability of measurement 3

Overall, the day-to-day repeatability of particulate measurements for steady-state tests is ± 22% as measured by the 2s coefficient of variation. This figure is considerably higher than the consecutive measurement repeatability of 7.4 - 8.2% reported earlier in this chapter. It also does not compare well with the 6 - 17% maximum deviations in within-laboratory particulate measurements reported by the CRC [3]. The 2s standard deviations for the period-II particulate measurements were 0.087 g/kW-hr, whereas Barsic [9] reported larger within-laboratory 2s standard deviations of 0.12 g/kW-hr for 13-mode tests done within a given laboratory.

The HC measurements were repeatable to within 30% of the mean, while the consecutive-measurement repeatability reported earlier in this chapter was substantially better at ± 8%. The 2s standard deviation of the period-II data was 0.35 g/kW-hr.
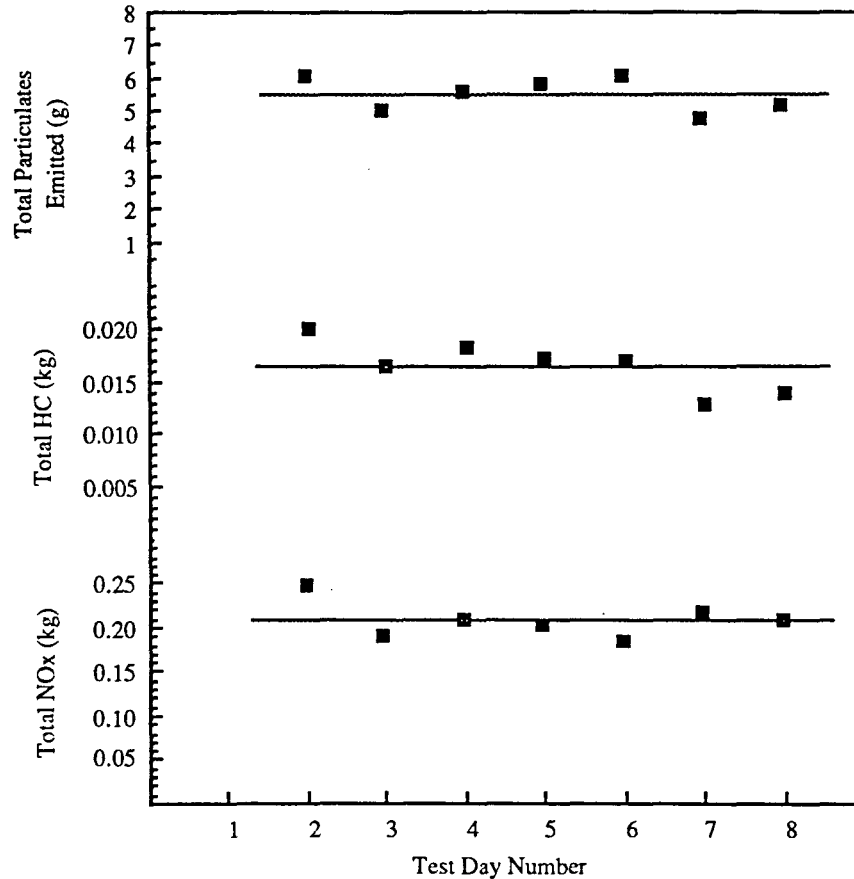
Fig. 5.13: Day-to-day repeatability of measurement 4

Barsic [9] reported 2s standard deviations of 0.06 g/kW-hr for within-laboratory, 13-mode test, HC measurements.

Finally, the period-II NOx measurements were repeatable to within about 20% of the mean. This repeatability is much poorer than the consecutive-measurement repeatability reported earlier in this chapter of ± 5%. The 2s standard deviation of the period-II data was 3.03 g/kW-hr which was high compared to the value of 0.76 g/kW-hr reported by Barsic [9].

In summary, the day-to-day repeatabilities of the particulate, HC and NOx measurements are ± 22%, ± 30% and ± 20% respectively. These values are substantially larger than the consecutive-measurement repeatabilities. The HC and NOx standard deviations do not compare favorably with published values, while the particulate standard
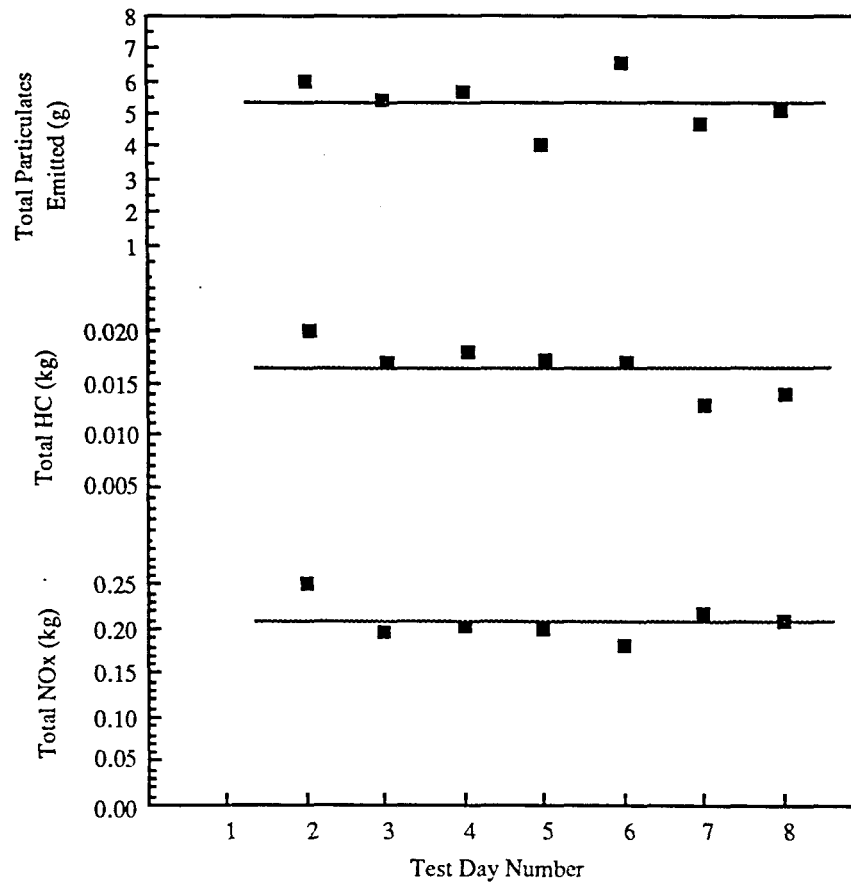
Fig. 5.14: Day-to-day repeatability of measurement 5

deviation of the particulate measurements compare well with the values reported by the CRC [3] but were not as good as those reported by Barsic [9]. These high day-to-day variations indicate that the ambient conditions need to be monitored and, if possible, controlled to consistent values. If improvements cannot be made, then comparison tests requiring higher sensitivities should be run within one day.

Repeatability of Transient Tests

The consecutive-measurement repeatability and day-to-day repeatability of particulate, HC and NOx measurements during transient tests was determined through a three-day series of tests. An FTP transient test consists of a cold-start test and a hot-start test. Only one cold-start test can be run per day. In order to collect data at a higher rate, often the hot-start portion of the test is conducted several times in succession after the initial cold-start test. Therefore, in this study, consecutive repeatability applies to consecutive hot-start tests, not
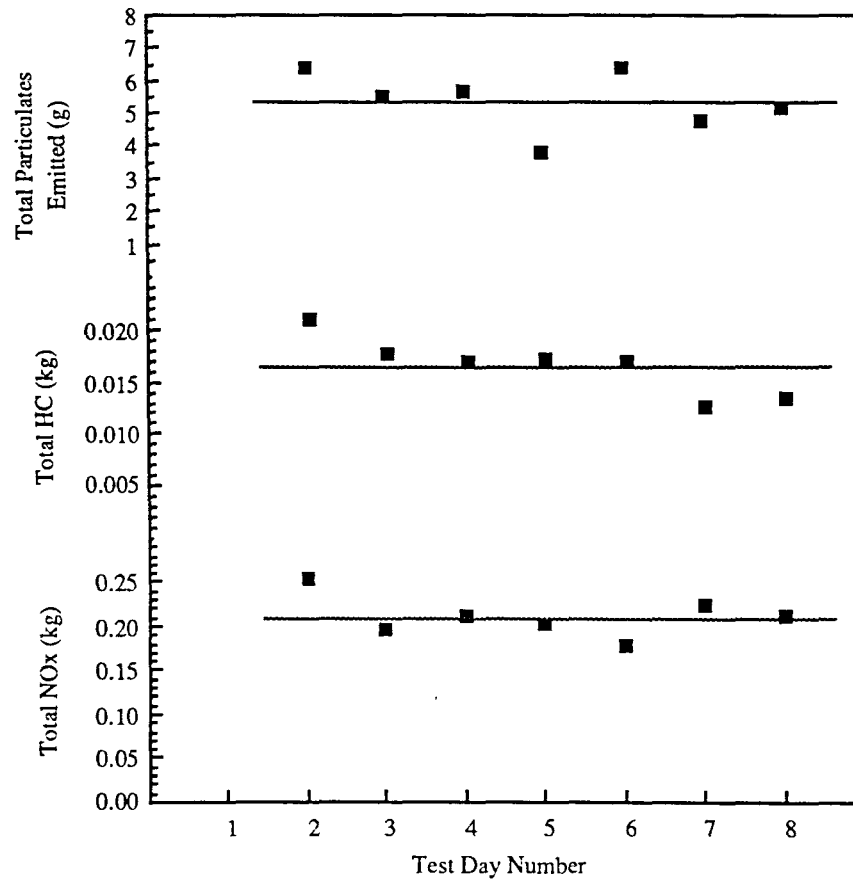
Fig. 5.15: Day-to-day repeatability of measurement 6

the entire FTP transient test. An important issue in running consecutive hot-start tests is the similarity of the data with the first hot-start test data. In this section the data are examined to determine if the results of the first hot start test are similar to that of the following hot-start tests. Then, 2s coefficients of variation of the hot-start data are determined to characterize their consecutive-measurement repeatability. Also, the means of the hot-start test results of each of the three days are compared and 2s coefficients of variation are calculated. The 2s coefficients of variation are calculated for the cold start results to characterize their day-to-day repeatability. Finally, comparisons of the repeatabilities are made with published values.

The results from the three days of transient tests are shown in Figs. 5.16 through 5.18. The values of brake-specific particulate (BS particulate), brake-specific hydrocarbons (BSHC) and brake-specific oxides of nitrogen (BSNO$_x$) measurements are

Table 5.3: Summary of day-to-day repeatability for steady-state-test particulate
measurements

Measurement #	1	2	3	4	5	6	Period II
Average (g)	3.721	3.028	5.473	5.496	5.345	5.390	5.456
Maximum Deviation Above Mean (%)	53	27	9.8	10.9	22	18	16
Maximum Deviation Below Mean (%)	35	8.8	9.1	12.7	25	29	28
Standard Deviation (g)	1.19	0.36	0.33	0.52	0.85	0.92	0.60
2s Coefficient of Variation (%)	64.0	23.8	12.2	19.0	32.1	33.9	22.0
2s Standard Deviation (g/kW-hr)	0.330	0.010	0.048	0.075	0.123	0.132	0.087

shown for the cold-start portion of the FTP test, which is designated on the x axis by the letter "C," the hot-start portion designated by "H1" and subsequent hot starts designated "H2, H3," etc. No NOx data was taken during the first hot-start test of the first day and thus the data point is missing.

During the first day, there was no significant difference in the particulate and HC measurements of the first hot-start test and the subsequent ones. However, as Fig. 5.17 shows, during the second day, there was a significant difference between the first particulate measurement and the subsequent ones. The HC and NOx measurements of the first hot-start test were not significantly different from the measurements of the subsequent tests. Finally, during the third day there were no significant differences seen. Thus, in seven of eight cases, there is no significant difference between the first hot-start test measurement and subsequent ones.

A summary of the consecutive-measurement repeatability of the hot-start tests is given in Table 5.6. Listed for each emission is the average, maximum deviations, standard deviation and 2s coefficients of variation for each of the three transient test days. Also included in the last row are the 2s standard deviations for comparison with the values reported by Barsic [9].

Table 5.4: Summary of day-to-day repeatability of steady-state-test HC measurements

Measurement #	1	2	3	4	5	6	Period II
Average (kg)	0.0143	0.0140	0.0166	0.0165	0.0165	0.0165	0.0165
Maximum Deviation Above Mean (%)	42	17.9	15	21	21	27	21
Maximum Deviation Below Mean (%)	20	36	20	22	22	24	22
Standard Deviation (kg)	0.0026	0.0024	0.0021	0.0024	0.0024	0.0028	0.0024
2s Coefficient of Variation (%)	36.2	34.0	24.9	30.1	30.1	33.9	30.0
2s Standard Deviation (g/kW-hr)	0.72	0.66	0.30	0.35	0.35	0.40	0.35

included in the last row are the 2s standard deviations for comparison with the values reported by Barsic [9].

Using the 2s coefficient of variation as a measure, the repeatability of the particulate measurements for the consecutive hot-start tests is about ± 6.8%. This is a slight improvement over the consecutive-measurement repeatability of steady-state tests of ± 8.2%. The CRC [3] reports that within laboratory transient-test particulate measurements usually deviate no more than 6% from the mean. The figure of 6.8% for this test is therefore comparable. However, the 2s standard deviation of 0.0422 g/kW-hr compares quite favorably against the value of 0.11 g/kW-hr reported by Barsic [9].

In the case of BSHC measurements, the consecutive hot-start repeatability as a 2s coefficient of variation is about ± 7.8%. This is the same repeatability as was determined for consecutive measurements during steady-state tests. Table 5.6 indicates the 2s standard deviation of the BSHC measurements is perhaps as much as 0.478 g/kW-hr. This figure higher than the value of 0.15 g/kW-hr reported by Barsic [9].

Finally, the consecutive hot-start test repeatability of the NOx measurements was found to be about ± 7.2%. This value does not compare well to the ± 4.7% figure for

Table 5.5: Summary of day-to-day repeatability of steady-state-test NOx measurements

Period	1	2	3	4	5	6	Period II
Average (kg)	0.0711	0.0713	0.2114	0.2092	0.2089	0.2119	0.2104
Maximum Deviation Above Mean (%)	11	12	16	19	20	20	18
Maximum Deviation Below Mean (%)	14	15	12	17	12	15	13
Standard Deviation (kg)	0.0070	0.0065	0.0180	0.0209	0.0209	0.0233	0.0210
2s Coefficient of Variation (%)	19.6	18.2	17.2	20.0	20.0	22.0	20.0
2s Standard Deviation (g/kW-hr)	1.94	1.80	2.60	3.02	3.02	3.36	3.03

steady-state tests. The 2s standard deviation of 1.098 g/kW-hr also does not compare well with the value of 0.51 g/kW-hr reported by Barsic [9] for within laboratory hot-start test repeatability.

The day-to-day repeatabilities of the cold-start and hot-start test are difficult to determine accurately from the data since only three days are available for comparison. With this in mind, Table 5.7 has been included as a summary of the day-to-day repeatability of the BS particulate, BSHC and BSNOx transient-test measurements. For both the hot-start and cold-start tests, the measurements of each emission had much better repeatabilities than the steady-state day-to-day repeatabilities. In fact, the repeatabilities of hot-start BS particulates and BSHC were better than their respective consecutive-measurement repeatabilities. As mentioned before, day-to-day repeatabilities are expected to be larger than consecutive-measurement repeatabilities due to the larger number of variables that change over the course of one or more days. Thus the values in Table 5.7 are somewhat suspicious but at the same time they indicate that the day-to-day repeatability is probably not substantially larger than the consecutive-measurement repeatability as was the case for the steady-state tests.
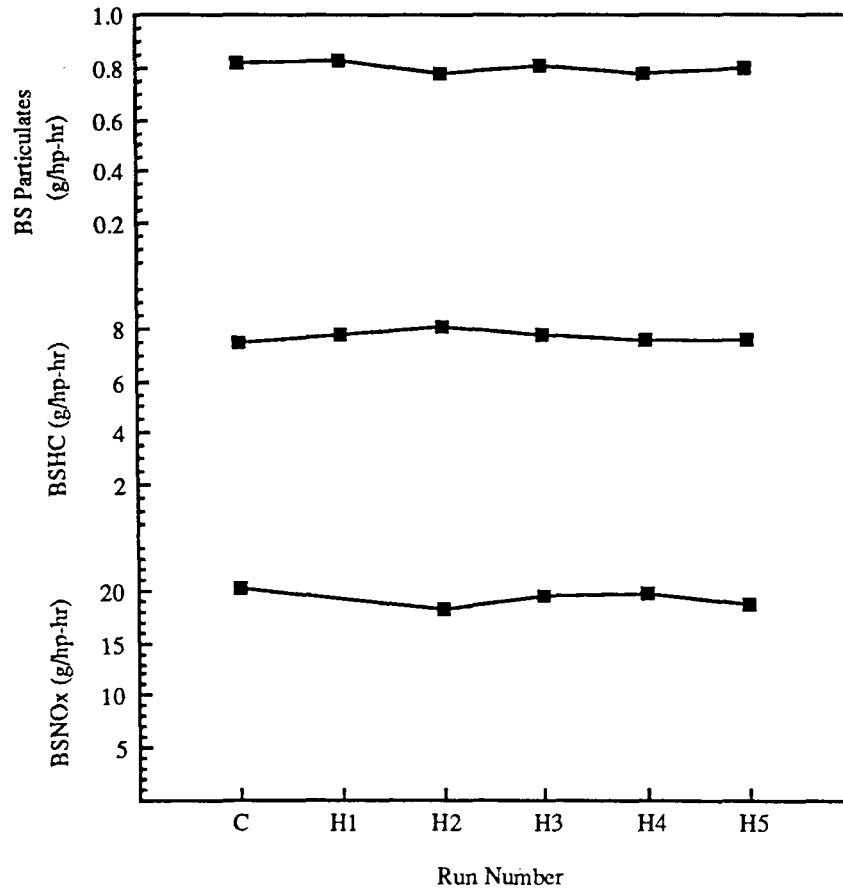
Fig. 5.16: Emission measurements from first day of transient tests

In summary, in 7 of 8 instances in the data, the first hot-start data point did not differ significantly from the subsequent hot-start data points, indicating that it is valid to run repeated hot-start tests and to consider the data equivalent to a first hot-start test result. The consecutive-measurement repeatabilities as 2s coefficients of variation of such subsequent hot-start tests are $\pm$ 6.8% , $\pm$ 7.8% and $\pm$ 7.2% for BS particulates, BSHC and $BSNO_x$ respectively. The BS particulate repeatability compares well with the value given by Barsic [9] but is somewhat higher than the CRC report [3]. The BSHC and $BSNO_x$ repeatabilities show more variation than was reported by Barsic [9]. However, all three repeatabilities are substantially within 10%. Day-to-day repeatabilities as 2s coefficients of variation were calculated from the limited sample of three test days. The values range from

61
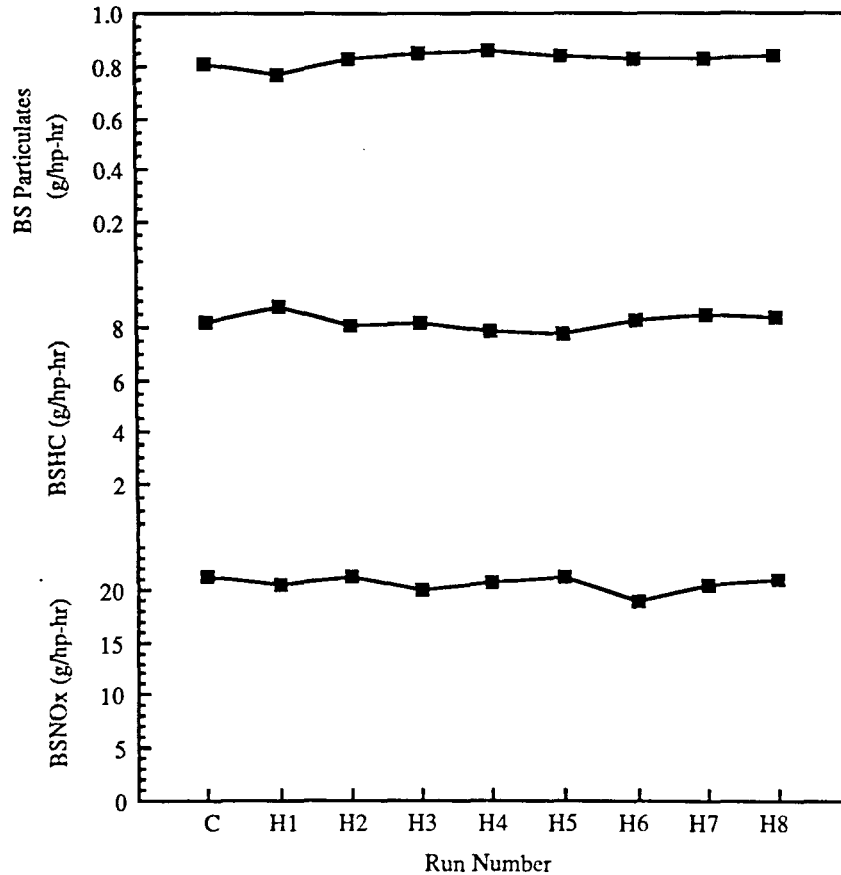
Fig. 5.17: Emission measurements from second day of transient tests

± 1.6% for cold-start particulate measurements to ± 12.4% for hot-start NOx measurements. Since the sample size was small, these values are not likely to be accurate. However, they do give an indication that the day-to-day repeatability is not substantially different than the consecutive measurement repeatability as was the case for the steady-state tests.

In the next chapter, the conclusions reached in this chapter about the repeatability influences of particulate, HC and NOx measurements made with the emissions measurement system of this study are reviewed. Also, some recommendations are made as to improvements that could be made in the system and measurement procedures.
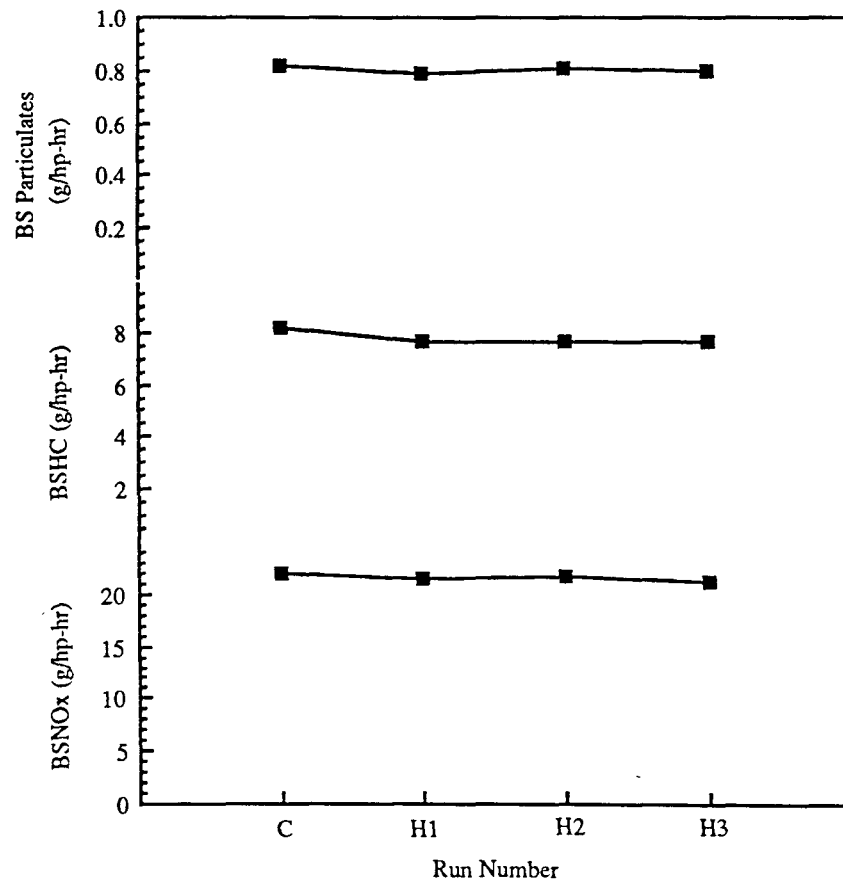
Fig. 5.18: Emission measurements from third day of transient tests

Table 5.6: Summary of consecutive hot-start transient test repeatability

Test Day Number	BS Particulates			BSHC			BSNOx		
	9	10	11	9	10	11	9	10	11
Average (g/kW-hr)	0.596	0.620	0.596	5.78	6.13	5.72	14.15	15.25	16.01
Maximum Deviation Above Mean (%)	4.2	3.8	1.1	6.4	6.4	4.2	3.4	3.9	1.1
Maximum Deviation Below Mean (%)	2.2	7.6	1.4	5.8	5.8	0.3	4.5	7.4	0.6
Standard Deviation (g/kW-hr)	0.0167	0.0211	0.0077	0.161	0.239	0.217	0.509	0.549	0.144
2s Coefficient of Variation (%)	5.6	6.8	2.6	5.6	7.8	7.6	7.2	7.2	1.8
2s Standard Deviation (g/kW-hr)	0.033	0.0422	0.0155	0.322	0.478	0.435	1.018	1.098	0.288

Table 5.7: Summary of the day-to-day repeatability of transient-test
emissions measurements

Measurement	Cold Start			Hot Start		
	BS Part.	BSHC	BSNOx	BS Part.	BSHC	BSNOx
Average (g/kW-hr)	0.605	5.924	15.77	0.604	5.88	15.14
2s Coefficient of Variation (%)	1.6	10.4	7.8	4.4	7.6	12.4
2s Standard Deviation (g/kW-hr)	0.010	0.62	1.24	0.027	12.4	1.86

CHAPTER VI. CONCLUSIONS

Summary of Conclusions from Test Program

Although improvements are needed in the hydrocarbon measurements and the day-to-day repeatability of steady-state measurements, the emissions measurements system should satisfy the needs of the ISU engine laboratory with regard to doing experimental alcohol fumigation work. It should be noted that some of the random errors that degrade the repeatability are probably due to inconsistant engine operation and would be seen in measurements made with any type of system. The following are the major conclusions drawn from the results of the test program.

1. The repeatabilities of particulate, hydrocarbon and oxides of nitrogen measurements for consecutive steady-state tests are 8.2%, 7.8% and 4.7% respectively. The value for particulates was comparable or better than the values in the literature while the hydrocarbons and oxides of nitrogen variations were somewhat larger than the values in the literature.

2. The period of transient emissions production that follows a speed and load change is short enough not to affect a twenty-minute measurement that begins five minutes after the change.

3. A dependence upon previous operating conditions of the means or standard deviations of particulate and hydrocarbon measurements could not be ascertained from the data. It was also not possible to show that the existence of drifts in the hydrocarbon data were dependent on previous operating conditions.

4. The day-to-day repeatabilities of the particulate, hydrocarbon and oxides of nitrogen measurements for steady-state tests were 22%, 30% and 20% respectively. The hydrocarbon variation is highest and indicates that further work may be required to obtain consistent hydrocarbon data. Some recommendations are provided at the end of this chapter. The somewhat high variations in the particulate and oxides of nitrogen measurements indicate that comparison tests that require high sensitivity should be conducted within one day.

5. It is a valid procedure to run several consecutive hot-start tests in one day to increase the amount of data that can be generated between cold-soak periods. The repeatabilities of the brake-specific particulate, hydrocarbon

and nitrogen oxides measurement for consecutive hot-start tests is 6.8%, 7.8% and 7.2% respectively. Although these figures are within 10%, they are not as low as the published values.

6. The rough indication of the day-to-day repeatability of measurements made during cold-start and hot-start transient tests is that it is not substantially larger than the consecutive hot-start measurement repeatability.

7. With the exception of the day-to-day repeatability of steady-state measurements, the repeatabilities are comparable to those reported for another simplified full-flow dilution tunnel of Heden, Eriksson and Gustavsson [8]. For that system the particulate, hydrocarbon and oxides of nitrogen repeatabilities were within 14%, 10% and 3% of the mean values respectively.

Recommendations

During most of the steady-state test days, there was a period of at least one hour in which the hydrocarbon measurements continually increased or decreased. During future measurements, recording the background hydrocarbon level in the dilution air is advised. It is possible some of the abnormal hydrocarbon data behavior is the result of fluctuating background hydrocarbon levels. The level of hydrocarbon measured in the dilution tunnel is so small (6 to 8 parts per million) that small amounts of lubricating oil from the air compressor could be interfering with the measurements. An inspection of the dilution air orifice did indicate the presence of oil in the dilution air. Also, in future measurements of oxides of nitrogen, a humidity correction factor such as the one developed by Krause, Merrion and Green [10] could be applied to try to improve the day-to-day repeatability of the oxides of nitrogen measurements. Finally, a microbalance with greater sensitivity would be quite helpful in improving the measurement repeatability of the particulate measurements as there is a measurement uncertainty of as much as 3% in the sample weighings with the current balance.

REFERENCES

1. Heywood, John B. *Internal Combustion Engine Fundamentals*. New York: McGraw-Hill, 1988.

2. Code of Federal Regulations 40. Chapter I, subpart N-1988 Heavy-Duty Federal Test Procedure, 1988.

3. Gross, G. P., MacDonald, J. S. and Shahed, S. M. "Informational Report on the Measurement of Diesel Particulate Emissions." Coordinating Research Council Report No. 522, 1982.

4. Perez, J. M., Jass, R. E. and Leddy, D. G. "Chemical Methods for the Measurement of Unregulated Diesel Emissions." Coordinating Research Council Report No. 551, 1987.

5. Harrington, J. A. and Yetter, R. A. "Application of a Mini-Dilution Tube in the Study of Fuel Effects on Stratified Charge Engine Emissions and Combustion." Society of Automotive Engineers Technical Paper No. 811198, 1981.

6. Suzuki, J. et al. "Development of Dilution Mini-Tunnel and Its Availability for Measuring Diesel Exhaust Particulate Matter." Society of Automotive Engineers Technical Paper No. 851547, 1985.

7. Hirakouchi, N., Fukano, I and Shoji, T. "Measurement of Diesel Exhaust Emissions with Mini-Dilution Tunnel." Society of Automotive Engineers Technical Paper No. 890181, 1989.

8. Heden, P, Eriksson, C. and Gustavsson, L. "A Simplified Dilution Tunnel System Intended for Heavy Duty Diesel Development." Society of Automotive Engineers Technical Paper No. 861279, 1986.

9. Barsic, N. "Variability of Heavy-Duty Diesel Engine Emissions for Transient and 13-Mode Steady-State Test Methods." Society of Automotive Engineers Technical Paper No. 840346, 1984.

10. Krause S., Merrion, D. and Green, G. "Effect of Inlet Air Humidity and Temperature on Diesel Exhaust Emissions." Society of Automotive Engineers Technical Paper No. 730213, 1973.

ACKNOWLEDGMENTS

APPENDIX A: DILUTION AIR SYSTEM CALIBRATION

A 3.68 cm diameter smooth-edged orifice, whose location is indicated in Fig. 3.1, was used as the flow measurement device for the dilution air. The calibration procedure and the validity of the calibration curve is discussed in this appendix.

The calibration curve of the orifice appears in Fig. A.1. Fourteen measurements were taken, and a quadratic expression was fit to the data to generate the curve. Using the graph or the quadratic expression, the mass flow rate of dilution air, $\dot{m}_{dil\ air}$, can be determined from the static pressure, P_{su}, and temperature, T_u, upstream of the orifice. For the calibration curve, the units of $\dot{m}_{dil\ air}$, P_{su} and T_u are kg/s, kPa and K respectively.

$$\dot{m}_{dil\ air} = -0.195 + 0.0705\left(\frac{P_{su}}{\sqrt{T_u}}\right) - 8.806 \times 10^{-4}\left(\frac{P_{su}}{\sqrt{T_u}}\right)^2$$
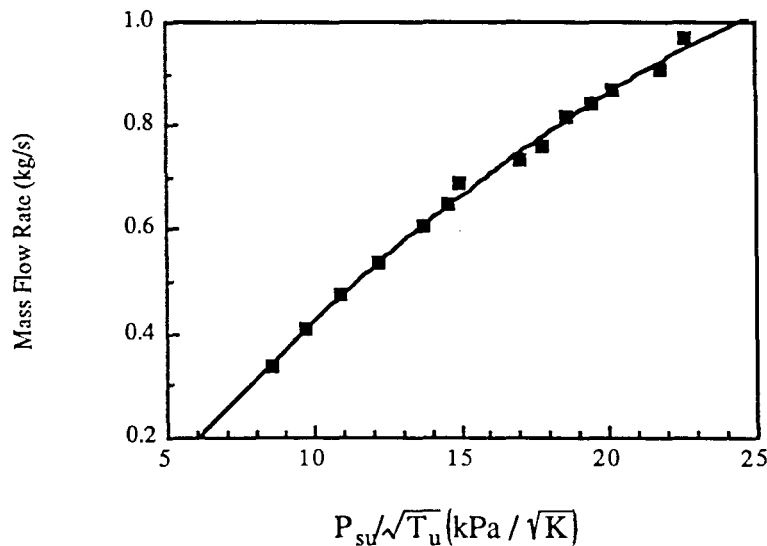
Fig. A.1: Calibration curve for dilution air system

The calibration data were obtained by adjusting the dilution-air ball valve, which is shown in Fig. 3.1, to fourteen different flow rates. At each setting, the static pressure

and temperature upstream of the orifice were recorded. The mass flow rate was determined using pitot tubes in the dilution tunnel.

To determine the mass flow rate, pitot tubes were traversed across the cross-sectional of the dilution tunnel both horizontally and vertically. The average velocity of the dilution air was determined from four pitot tube measurements in each of six equal-area annuluses. The mass flow rate was then calculated from the following form of the ideal gas equation:

$$\dot{m}_{dil\ air} = \frac{P_{dt}\ V\ A_{dt}}{R_{air}\ T_{dt}} \tag{1}$$

where $\dot{m}_{dil\ air}$ is the mass flow rate of the dilution air, P_{dt} is the pressure in the dilution tunnel which was assumed to be atmospheric, V is the average dilution air velocity as determined by the pitot tubes, A_{dt} is the cross-sectional area of the dilution tunnel, R_{air} is the ideal gas constant for air and T_{dt} is the temperature of the dilution air in the tunnel.

A point of concern is whether or not the calibration of the orifice can change, that is, whether Fig. A.1 is always valid. In constructing the calibration curve of Fig A.1 it was assumed that $\dot{m}_{dil\ air}$ was a function of $P_{su}/\sqrt{T_u}$ only. Indeed this is the case for a choked orifice as shown by the following derivation.

The mass flow rate of the dilution air can be expressed as:

$$\dot{m}_{dil\ air} = \rho\ A_{orifice}\ V_{orifice} \tag{2}$$

where ρ is the density of the dilution air as it passes through the orifice, $A_{orifice}$ is the cross-sectional area of the orifice and $V_{orifice}$ is the velocity of the dilution air through the orifice. The ideal gas relation and definition of Mach number can be expressed as follows:

$$\rho = P_s\ /\ (R_{air}\ T_s) \qquad\qquad V_{orifice} = M\sqrt{k\ R_{air}\ T_s} \tag{3}$$

where P_s is the static pressure in the orifice, T_s is the static temperature in the orifice, M is the mach number in the orifice, and k is the ratio of specific heats for air. Substituting equations (3) into (2) and rearranging gives:

$$\dot{m}_{dil\ air} = \left[\frac{A_{orifice}\ \sqrt{k}}{\sqrt{R_{air}}}\right]\frac{P_s}{\sqrt{T_s}}M \qquad (4)$$

where the bracketed quantity is constant. For choked flow, $M = 1$ and consequently, $\dot{m}_{dil\ air}$ depends only on the quantity $P_{su}/\sqrt{T_u}$.

With regard to the validity of the calibration curve, if the flow is not choked, $\dot{m}_{dil\ air}$ also depends on the Mach number. The Mach number will be a function of the local temperature and velocity, both of which are dependent on the upstream conditions and the downstream conditions when the flow is not choked. It was experimentally determined by comparing upstream and downstream pressures, that when the absolute static pressure reaches about 290 kPa, the flow through the orifice becomes choked. Therefore, the calibration curve is valid for P_{su} values of 290 kPa and larger.

For low dilution air flow rates, where the orifice is not choked, the calibration curve may shift if the downstream pressure or temperature shift. The only cause of such shifts would be changes in the atmospheric pressure and large ambient temperature changes. Changes in atmospheric pressure are small compared to the downstream pressure whose magnitude ranges from atmospheric pressure to about 1.5 times atmospheric pressure when the orifice becomes choked. Heat transfer effects in the vicinity of the orifice are likely to be small since the mass flow rate of dilution air is usually quite large. Thus the effect of changes in ambient temperature on the downstream temperature of the orifice are probably minimal. From these observations, the non-choked region of the calibration curve is not expected to shift much, and the entire curve can be considered valid.

APPENDIX B: MIXING TESTS

Tests were conducted to determine the effectiveness of the dilution tunnel in mixing the exhaust with air. The procedure is discussed in this appendix followed by graphs of typical results.

The mixing tests were conducted without the use of the engine's emissions. Instead, tanks of compressed CO_2 were used to feed a constant flow rate of CO_2 into the tunnel through the exhaust entry port. The engine was not used because the inherent difficulty in maintaining a true steady-state engine operating condition could cause the emissions to vary with time. Since checking the mixture at various transverse locations in the tunnel takes time, variations in the emissions would cause the mixing to appear poorer than it is in reality.

A single emission, CO_2, was used. There is no reason to expect the other gaseous emissions to behave significantly different than CO_2. Furthermore, diesel particulates are small enough (0.01 μm- 1.0 μm) to behave essentially as gaseous emissions. Therefore, the results for CO_2 mixing should accurately apply to all components of the exhaust gas from the engine.

The mixing test was conducted for several flow rates. The CO_2 regulator was set so that the flow of CO_2 comprised approximately 0.5% of the total flow in the tunnel as determined by the CO_2 analyzer. A probe was traversed horizontally and vertically across the cross-section of the tunnel and the concentration at each point recorded.

Fig. B.1 shows a typical example of the results of these tests. Inspection of these figures shows that the concentrations were even across the diameter of the tunnel. Therefore, the mixing is quite adequate.
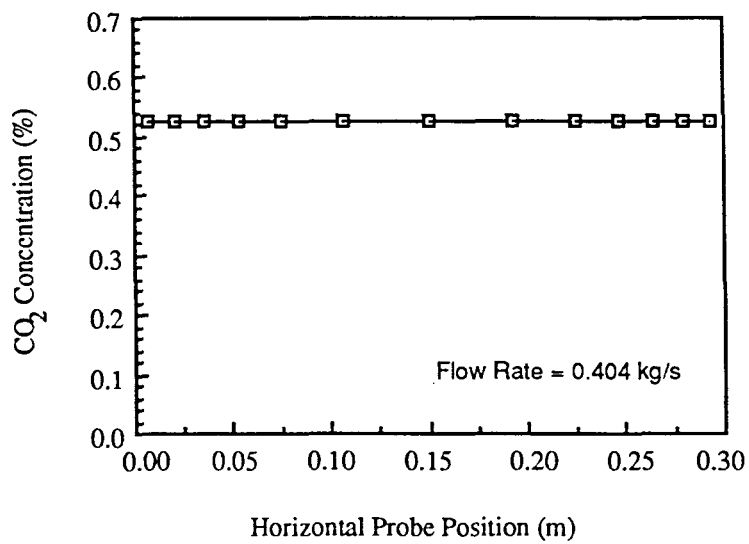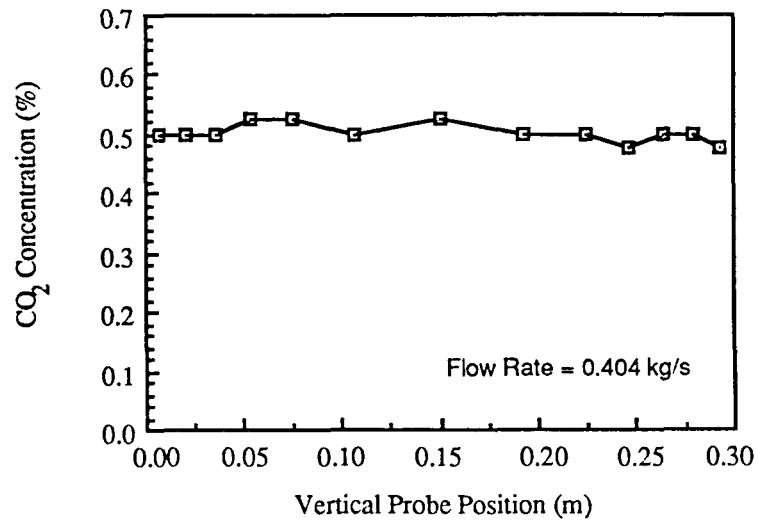
Fig. B.1: Mixing test results for 0.404 kg/s flow rate

APPENDIX C: SAMPLING SYSTEM LEAK TESTS

Periodic leak tests were performed on the particulate sampling system to determine if it was adequately sealed. Leakage of atmospheric air into the system reduces the amount of diluted exhaust that passes through the particulate filter, but at the same time does not affect the gas meter readings. The result is that the gas meter indicates more diluted exhaust has passed through the filter than actually has. This is a systematic error unless the leakage rate is intermittent in nature in which case it becomes a random error that affects repeatability, although it will always shift the data in one direction. The procedure for conducting the leak tests is outlined in this appendix and the two different leak-down behaviors that were observed throughout the test program are discussed.

To conduct a leak test, the ball valve between the sample pump and gas meter, as shown in Fig. 3.2, was shut and the inlet to the filter holder capped. The vacuum valve was opened and the vacuum pump used to draw the system down to a vacuum of 16 inches of mercury. A stopwatch was used with the system's vacuum gage to monitor the leak-down of the system. The vacuum valve was closed during leak-down so that the vacuum pump and connecting hose would not be a part of the leak test

Throughout the test program the system exhibited two types of leak-down behavior. Examples of each appear in Fig. C.1. For steady-state test days 1 through 4 and all three transient test days the leak-downs were similar to the curve labeled "normal leak-down." The system would lose most of the vacuum in just over three minutes. A much faster leakage rate was present in the system during steady-state test days 5 through 8. The leak-down behavior for those days was similar to the curve labeled "abnormal leak-down" in Fig. C.1. The cause for the abnormally high leakage was discovered to be a poorly-sealing filter-holder apparatus. A rubber edge of the filter backing was held in place by high vacuums but would lose the seal at vacuums of 4 inches of mercury or less. This leakage would have the greatest effect on measurements at light particulate loading conditions since the vacuum downstream of the filter in those cases never exceeds 3 inches of mercury.

The normal leak-down rate is acceptable. The rate of leakage in the 7 to 15 inches of mercury range corresponds to only about 0.3% of the mass flow rate of the particulate sample. The abnormal leak-down rate is only of concern when the vacuum is less than 4 inches of mercury. The light particulate loading measurements made before and after the abnormal leakage began do not show any effect of the leakage. Thus, the conditions of

the leak-down test may not accurately simulate the leakage that occurs during actual operation. The sample flow through the filter may force the rubber edge of the filter backing to seal more tightly as do higher vacuums during the leak test.
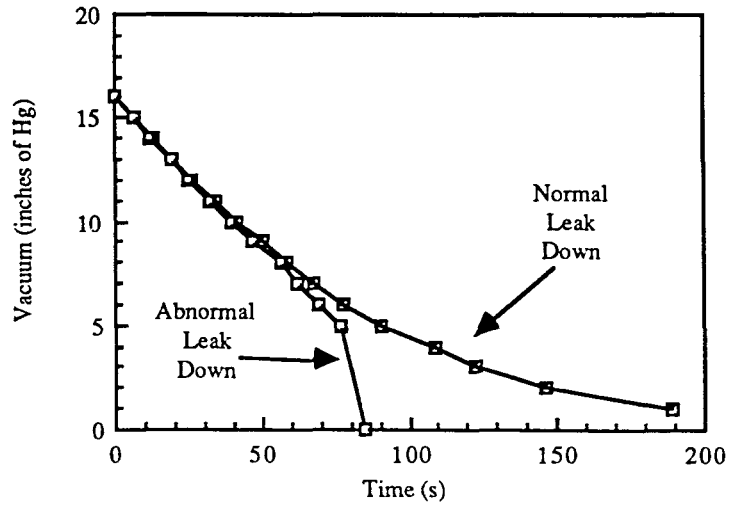
Fig. C.1: Comparison of normal and abnormal leak test results

APPENDIX D: CALCULATIONS

The details of the data-reduction calculations are given in this appendix. The calculation of the total amount of an exhaust species produced by the engine during a measurement period is given first. Also, the conversion of these values to brake-specific values is explained. The calculation of brake-specific fuel consumption is explained as well as the equivalence ratio. These calculations apply to both steady-state and transient tests.

The total mass of particulates produced by the engine during a 20-minute measurement period, m_{partic}, is found from the following equation:

$$m_{partic} = \Delta m_{filter} / SF \tag{D1}$$

where Δm_{filter} is the change in mass of the particulate filter as determined using the microbalance, and SF is the sampling fraction of the diluted exhaust. SF is given by:

$$SF = \frac{\dot{m}_{sample}}{\dot{m}_{dil\ tun}} \tag{D2}$$

where $\dot{m}_{sample}$ is the mass flow rate through the particulate sampling system and $\dot{m}_{dil\ tun}$ is the mass flow rate of the diluted exhaust in the dilution tunnel. $\dot{m}_{sample}$ is calculated from the ideal gas equation:

$$\dot{m}_{sample} = \frac{P_{sample}\dot{V}_{sample}}{R_{air}T_{sample}} \tag{D3}$$

where P_{sample} is the pressure in the gas meter and is assumed to be atmospheric, $\dot{V}_{sample}$ is the volume flow rate through the gas meter, R_{air} is the ideal gas constant for air and T_{sample} is the temperature in the gas meter. T_{sample} was not measured but estimated as the average of the sample-zone temperature in the dilution tunnel and the ambient temperature.

The mass flow of diluted exhaust in the tunnel, $\dot{m}_{dil\ tun}$ is calculated as the sum:

$$\dot{m}_{dil\ tun} = \dot{m}_{dil\ air} + \dot{m}_{exhaust} \tag{D4}$$

where $\dot{m}_{dil\ air}$ is the mass flow rate of dilution air as determined by the dilution air system calibration curve of Appendix A, and $\dot{m}_{exhaust}$ is the mass flow rate of exhaust which is given by:

$$\dot{m}_{exhaust} = \frac{P_{atm}\ \dot{V}_{intake}}{R_{air}\ T_{amb}} + \dot{m}_{fuel} \tag{D5}$$

where P_{atm} is the atmospheric pressure, $\dot{V}_{intake}$ is the volume flow rate of engine intake air, T_{amb} is the ambient temperature and $\dot{m}_{fuel}$ is the average mass flow rate of fuel as determined by the change in the weight of the supply tank during the test.

The total mass, $m_{species}$, of a gaseous species such as hydrocarbon (HC), oxides of nitrogen (NOx) and carbon dioxide (CO_2) is calculated by the equation:

$$m_{species} = \sum_{i=1}^{n} X_i\ MW_{species}\ \frac{\left(\dot{m}_{dil\ tun}\right)_i}{MW_{dil\ exh}} \tag{D6}$$

where n is the total number of data acquisition intervals during the test, X_i is the concentration of the species during data acquisition interval i as determined by the analyzer, $MW_{emission}$ is the molecular weight of the species, $\left(\dot{m}_{dil\ tun}\right)_i$ is the mass flow rate in the dilution tunnel during the data acquisition period as determined by equation (4), and $MW_{dil\ exh}$ is the molecular weight of the diluted exhaust which is assumed to be equal to the molecular weight of air.

The molecular weight of the unburned hydrocarbons is assumed to be equal to the molecular weight of typical number 2 diesel fuel. The representative molecule used was $C_{13.8}H_{24.3}$ whose molecular weight is 190 g/mole. For the oxides of nitrogen, since eventually the NO molecules become NO_2 molecules in the atmosphere, the molecular weight of NO_2 (46 g/mole) was used in equation 6. This procedure is in accord with standard Environmental Protection Agency procedure.

The values of m_{partic} and $m_{emission}$ can be normalized by dividing by the total work done by the engine during the measurement. The resultant values are termed brake-specific (BS) quantities. The work done by the engine is calculated as:

$$W_{total} = \tau \dot{\theta} \, t_{test} \qquad (D7)$$

where W_{total} is the total work done by the engine, τ is the torque, $\dot{\theta}$ is the speed of the engine and t_{test} is the length of the test. For a transient test in which the speed and torque change, the expression becomes:

$$W_{total} = \sum_{i=1}^{n} T_i \dot{\theta}_i \, \Delta t \qquad (D8)$$

where T_i and $\dot{\theta}_i$ are the torque and speed for one data acquisition interval, and Δt is the length of the interval.

The brake-specific fuel consumption (BSFC) is calculated as:

$$BSFC = \Delta m_{fuel} / W_{total} \qquad (D9)$$

where Δm_{fuel} is the change in fuel mass in the supply tank during the test.

Finally, the equivalence ratio is calculated as:

$$\phi = \frac{\Delta m_{fuel} / m_{intake}}{\left(\dot{m}_{fuel} / \dot{m}_{intake} \right)_{stoichiometric}} \qquad (D10)$$

where m_{intake} is the total mass of air the engine used during the test, and $\left(\dot{m}_{fuel} / \dot{m}_{intake} \right)_{stoichiometric}$ is the stoichiometric fuel / air ratio.

APPENDIX E: TEST VARIABLE FIGURES

This appendix contains graphs of the variations in testing conditions and engine parameters for each of the steady-state and transient test days. Graphs are also include showing the variation of testing conditions and engine parameters on a day-to-day basis for each of the first six measurements of the steady-state test days.
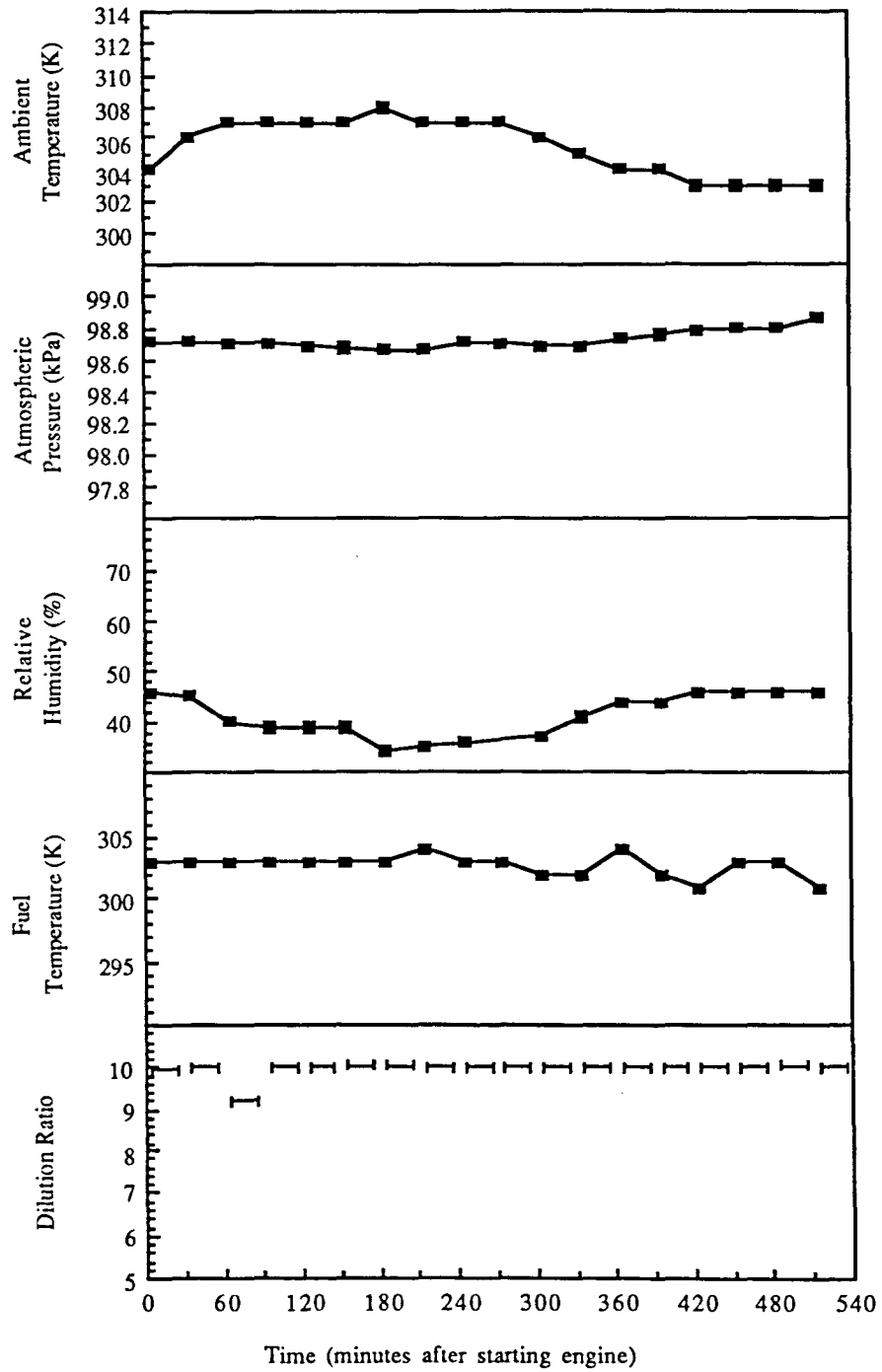
Fig. E1: Ambient conditions, fuel temperature and dilution ratio variations during day 3
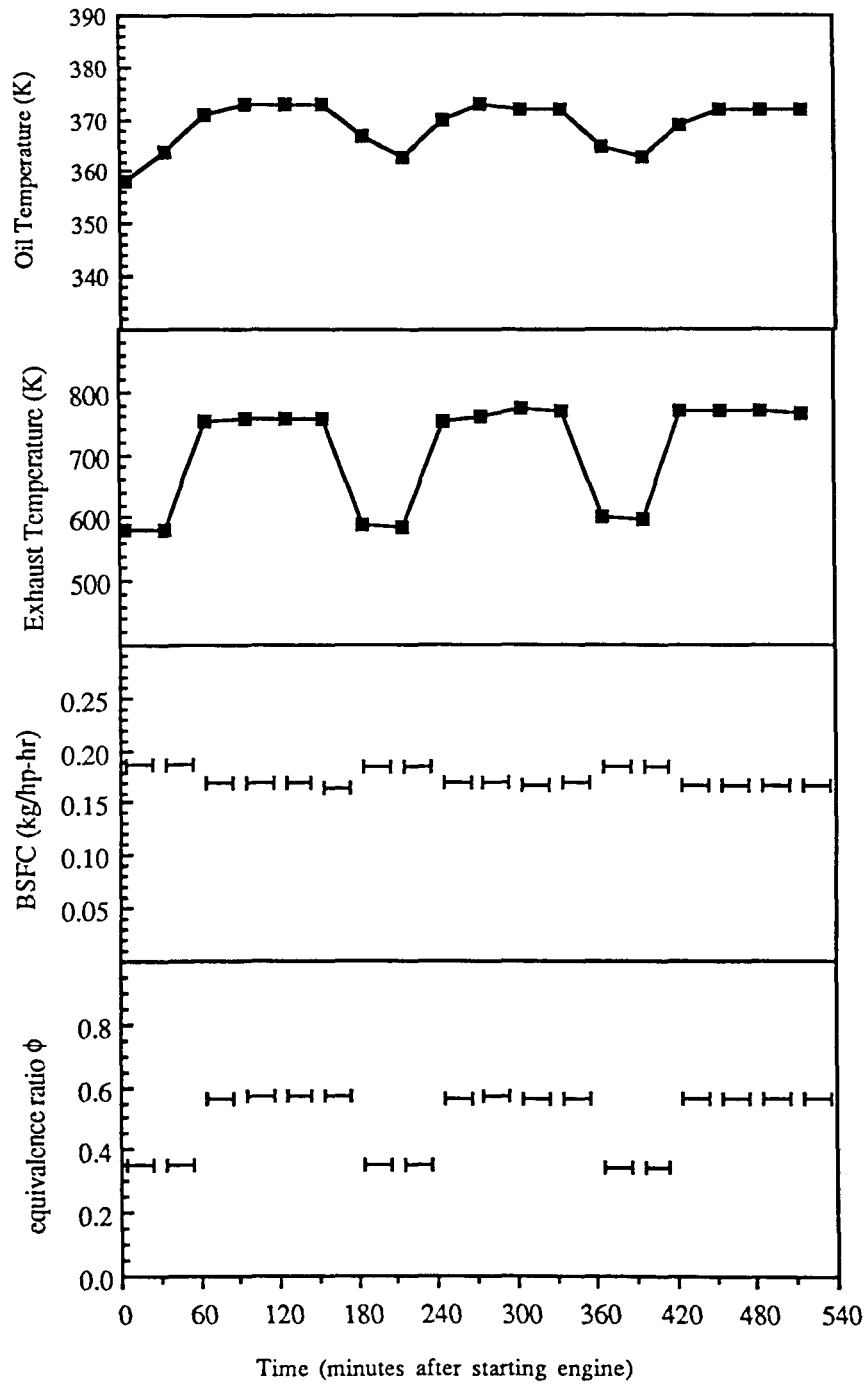
Fig. E2: Engine parameter variations during day 3
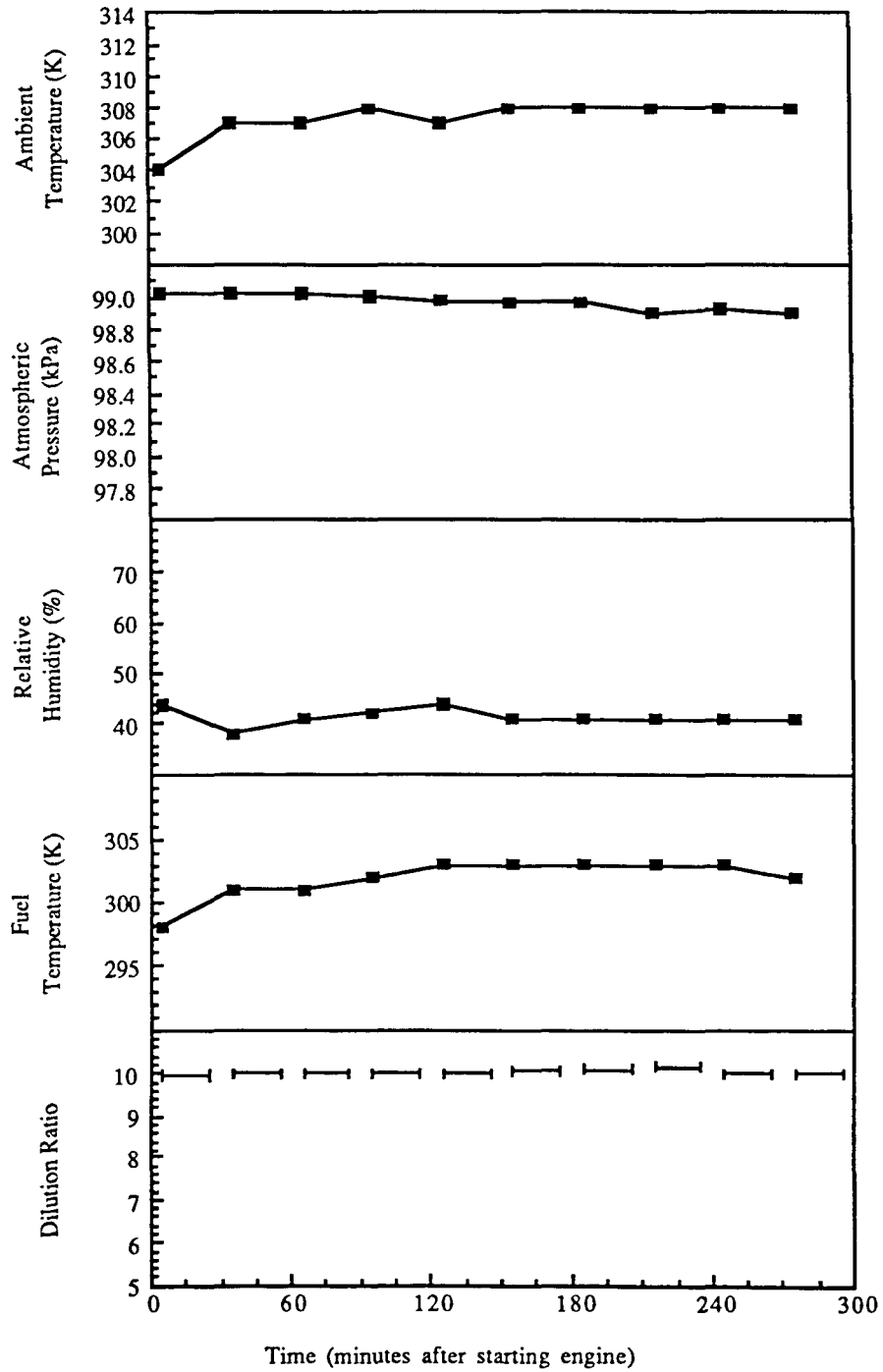
Fig. E3: Ambient conditions, fuel temperature and dilution ratio variations during day 4
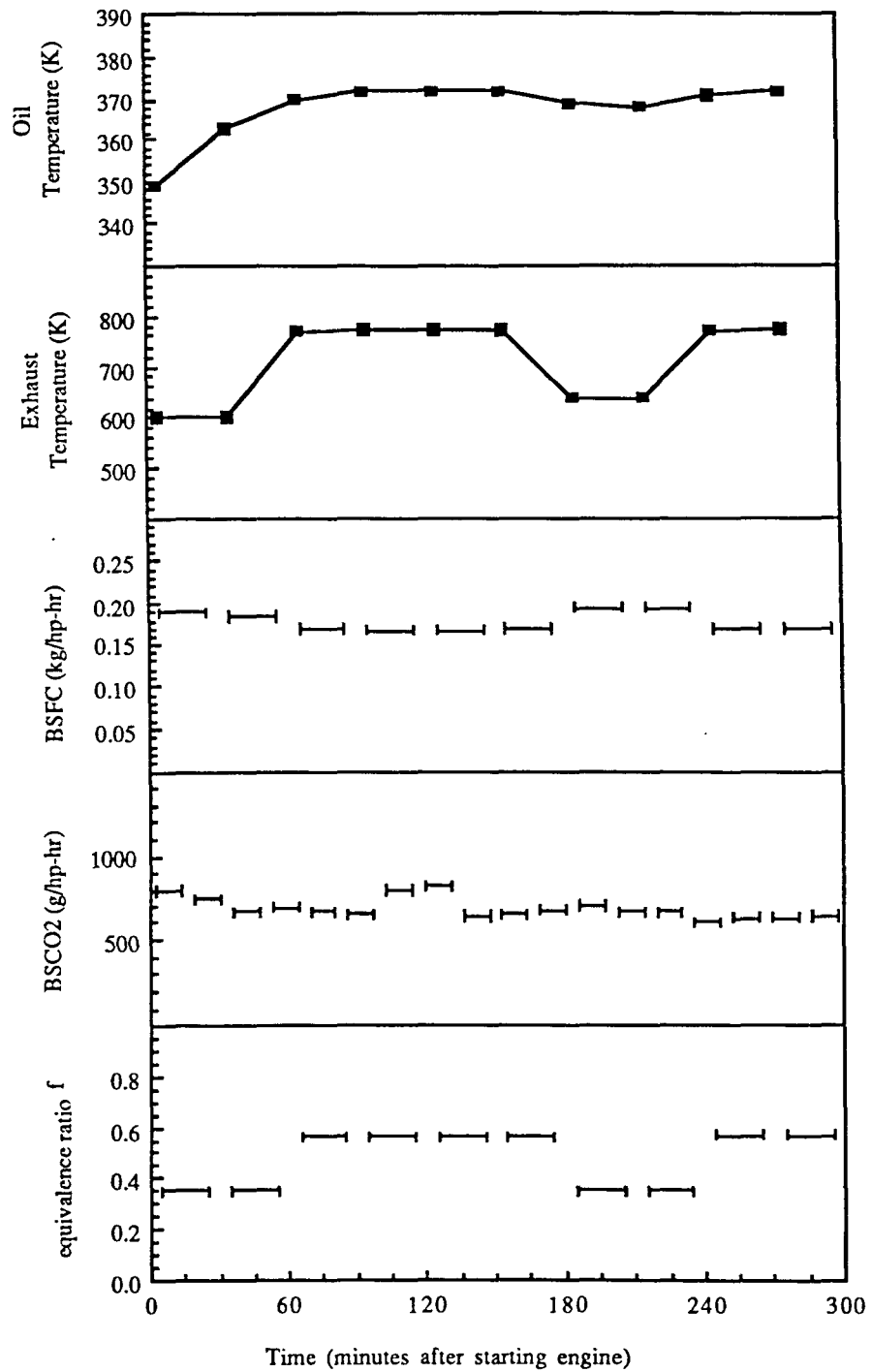
Fig. E4: Engine parameter variations during day 4
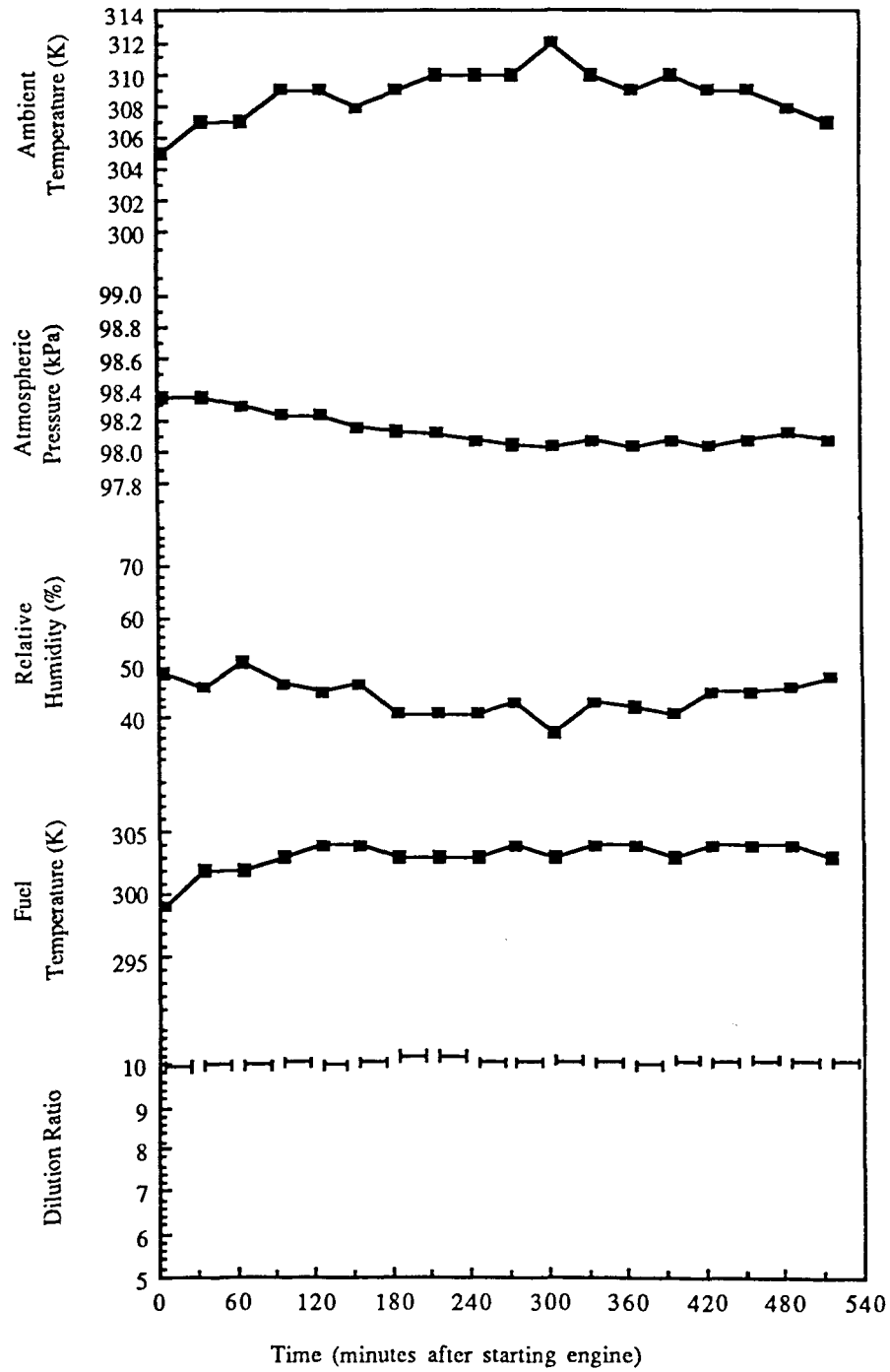
Fig. E5: Ambient conditions, fuel temperature and dilution ratio variations during day 5
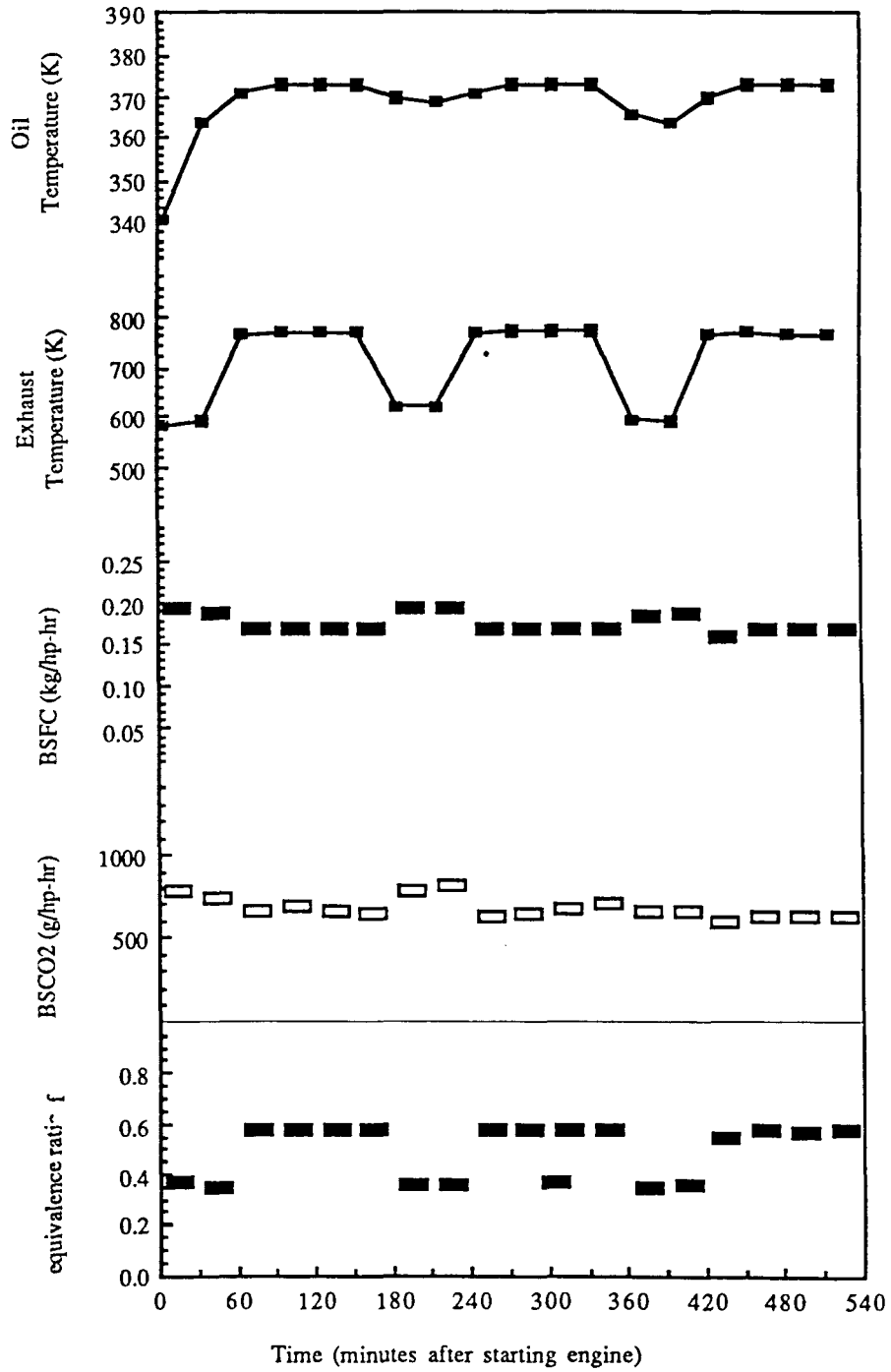
Fig. E6: Engine parameter variations during day 5
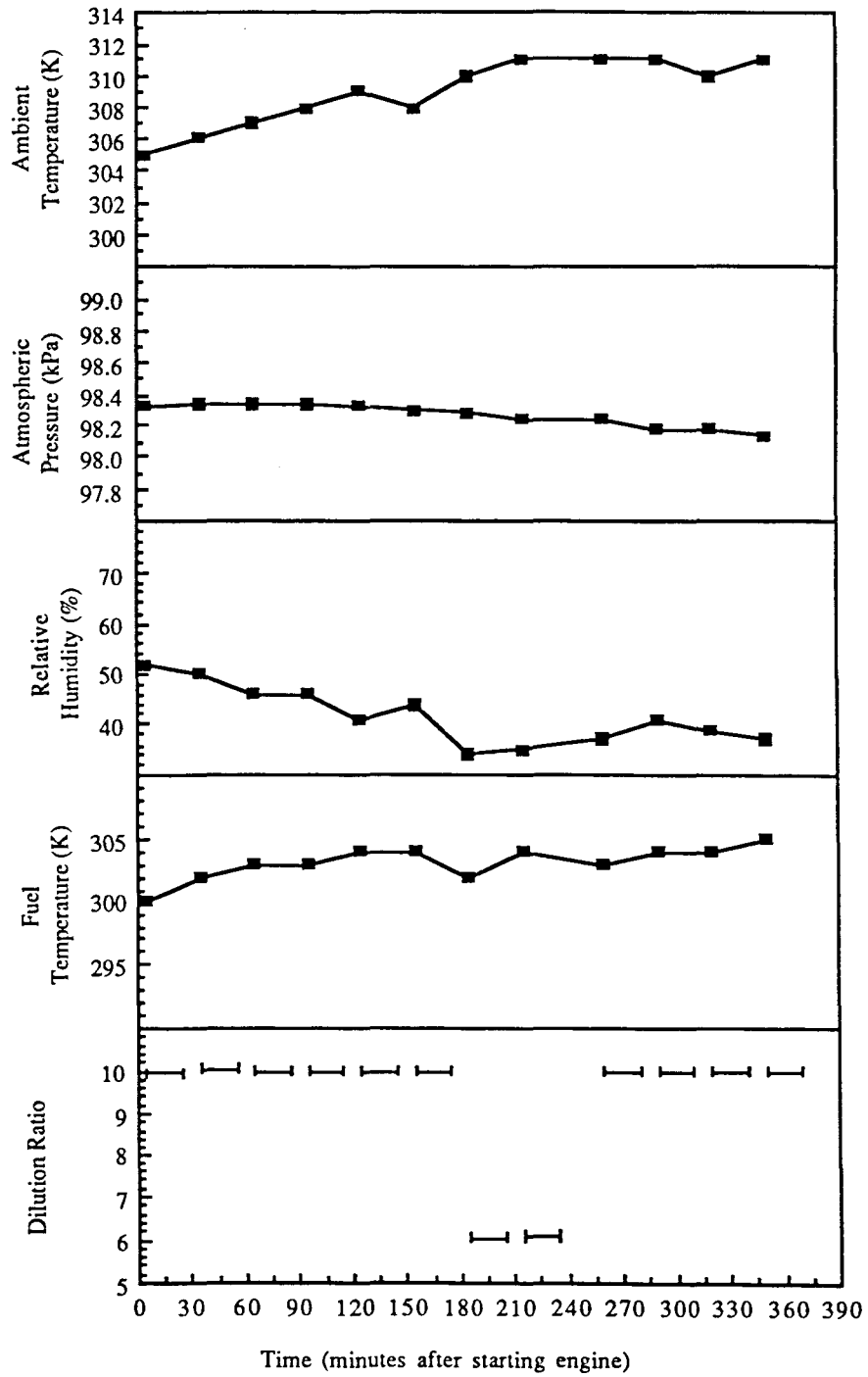
Fig. E7: Ambient conditions, fuel temperature and dilution ratio variations during day 6
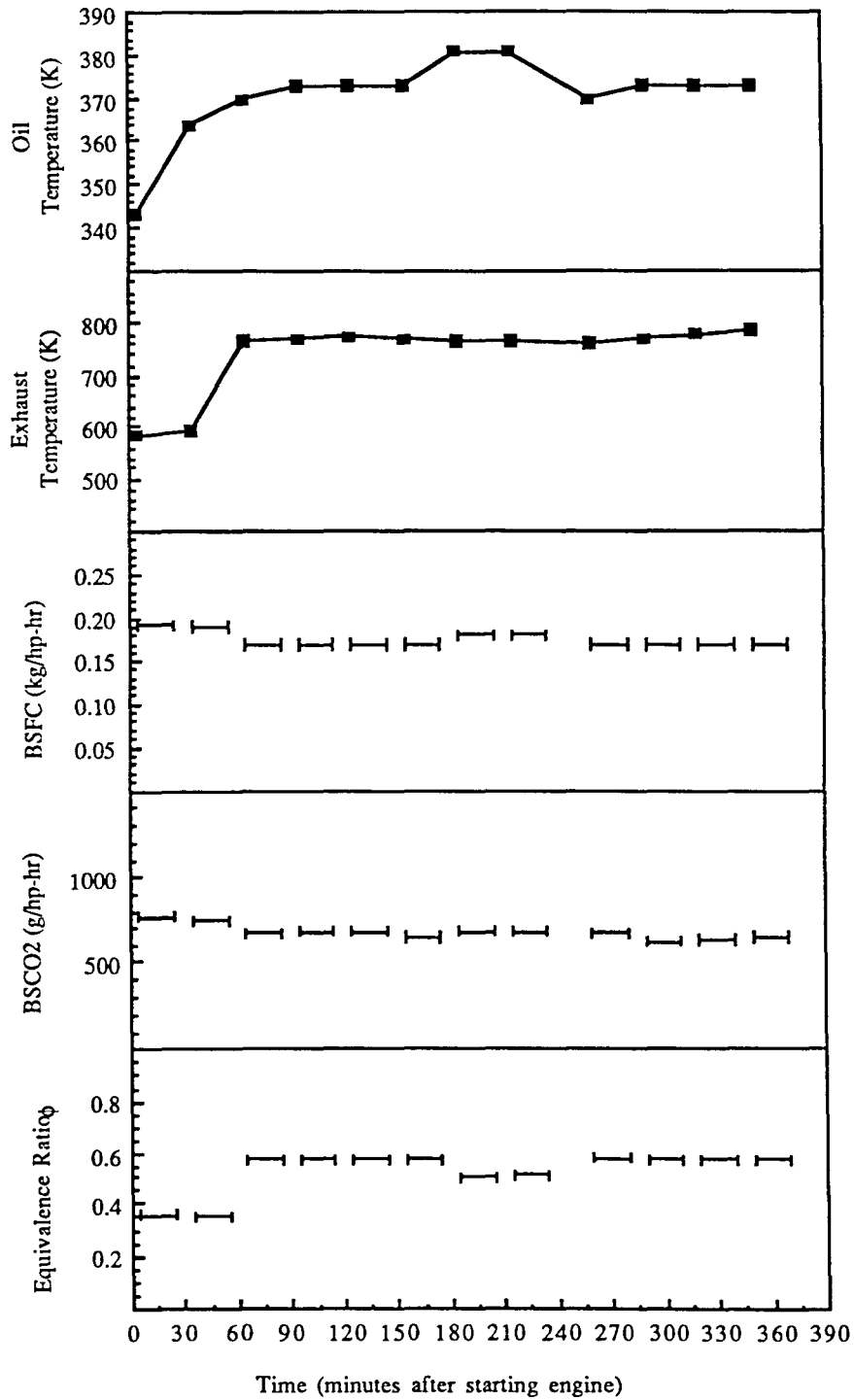
Fig. E8: Engine parameter variations during day 6
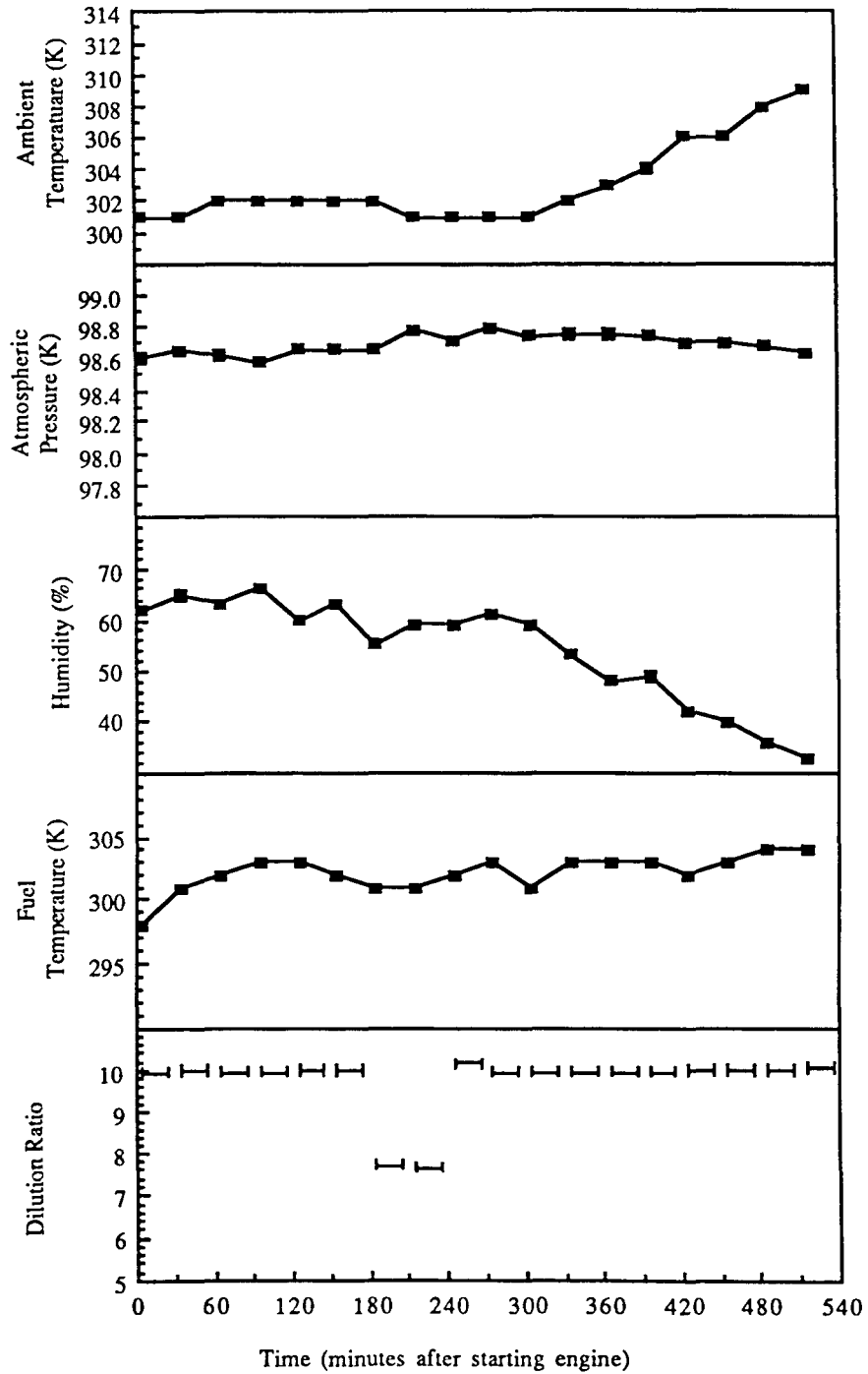
Fig. E9: Ambient conditions, fuel temperature and dilution ratio variations during day 7
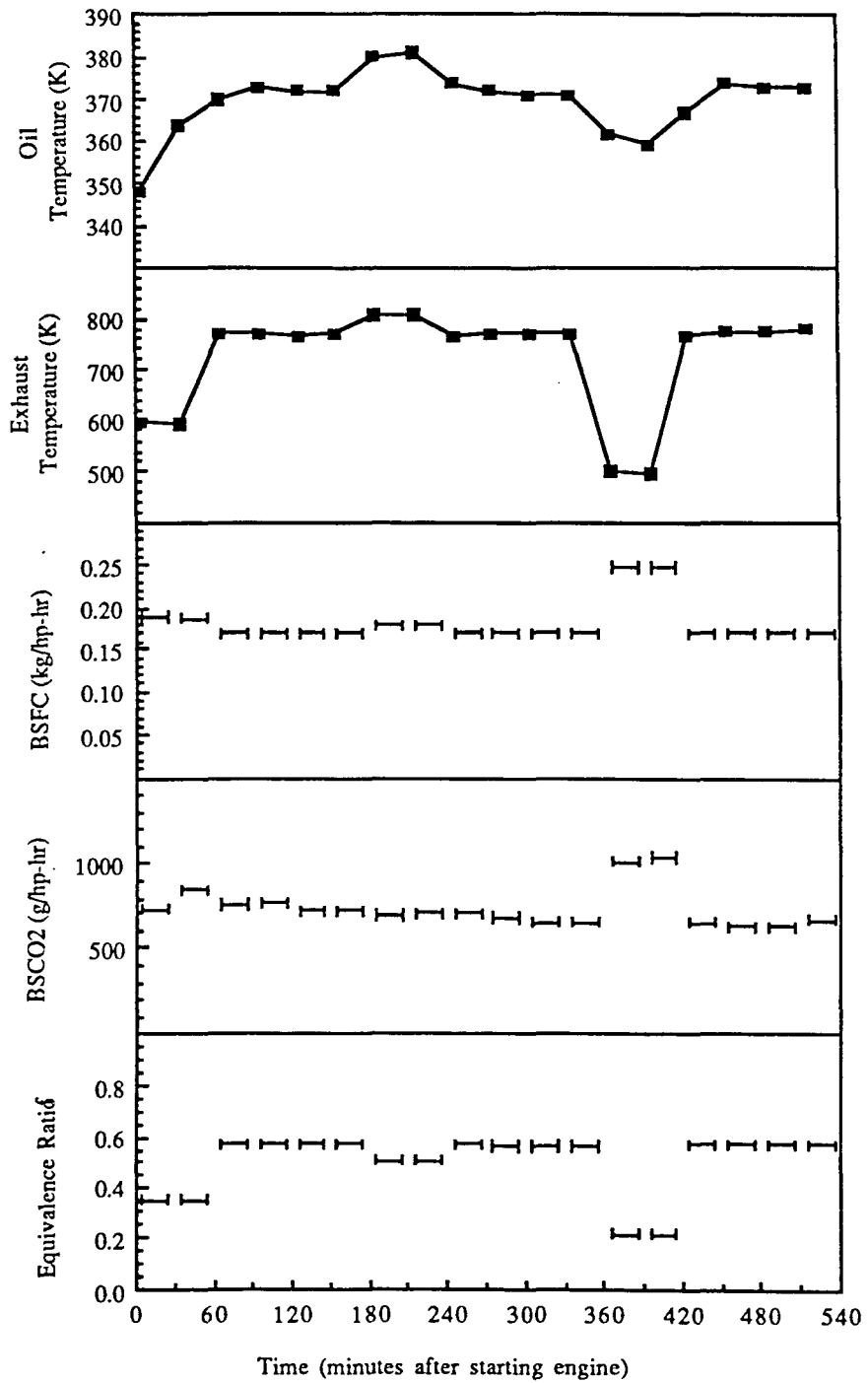
Fig. E10: Engine parameter variations during day 7
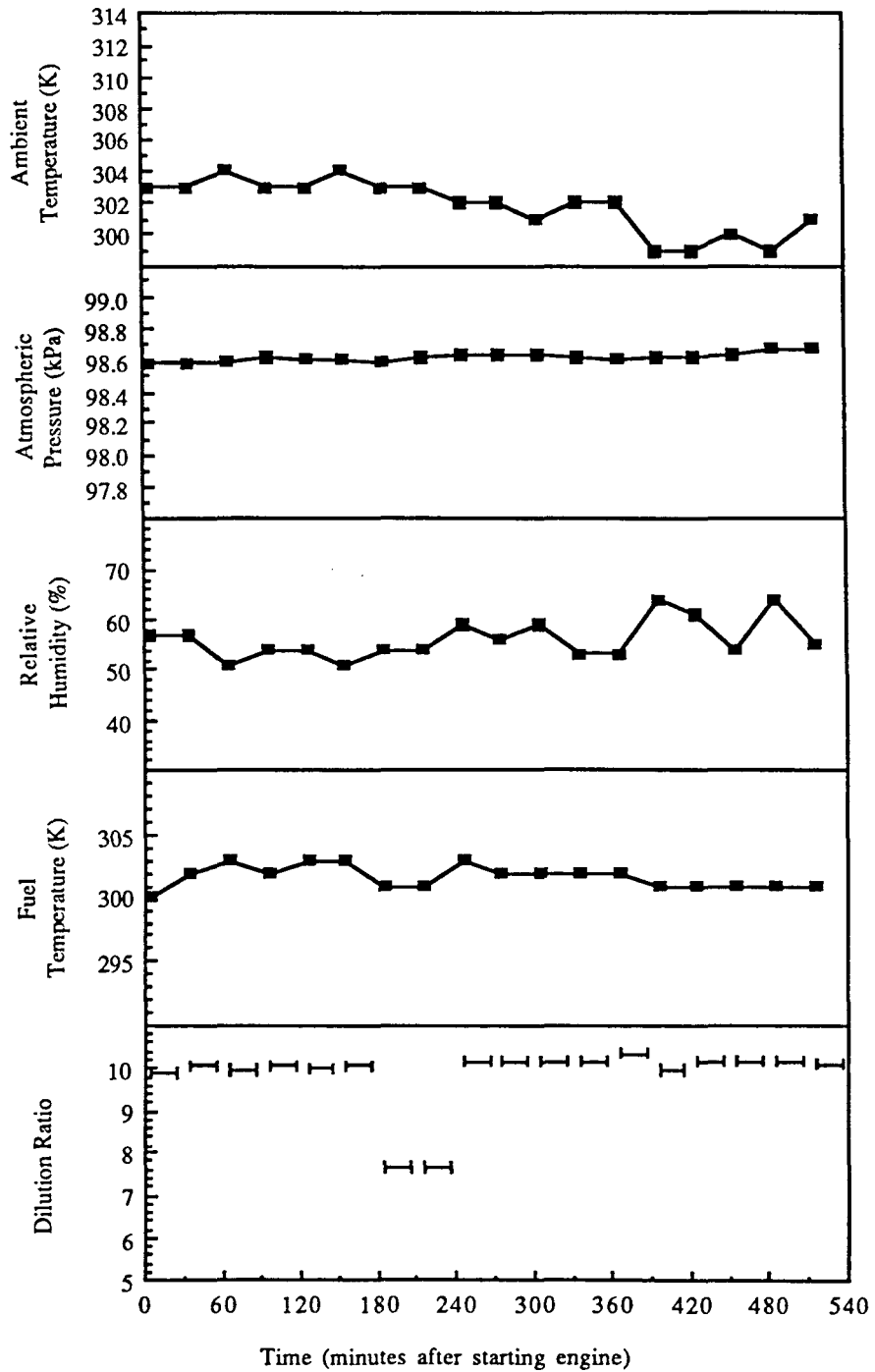
Fig. E11: Ambient conditions, fuel temperature and dilution ratio variations during day 8
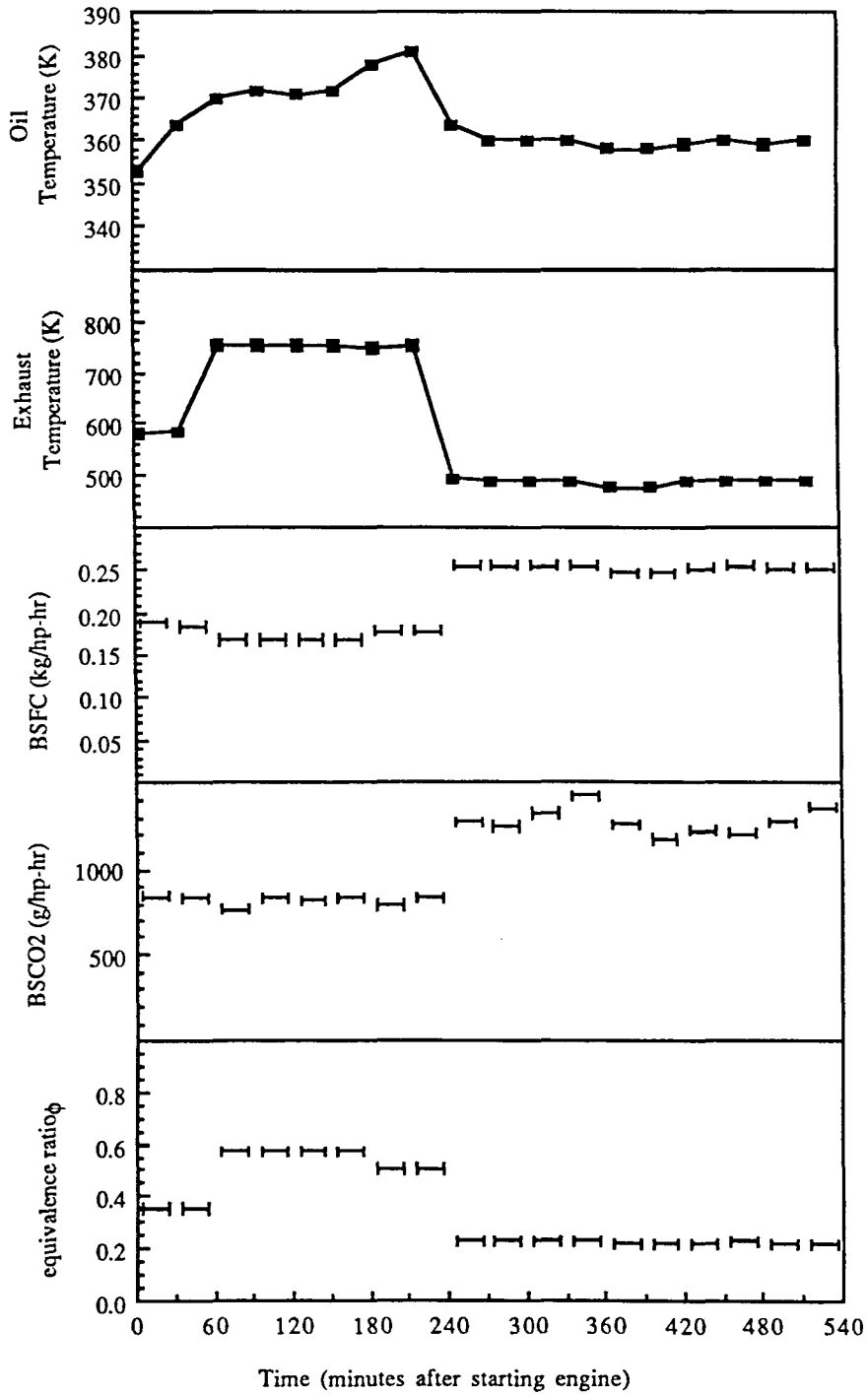
Fig. E12: Engine parameter variations during day 8
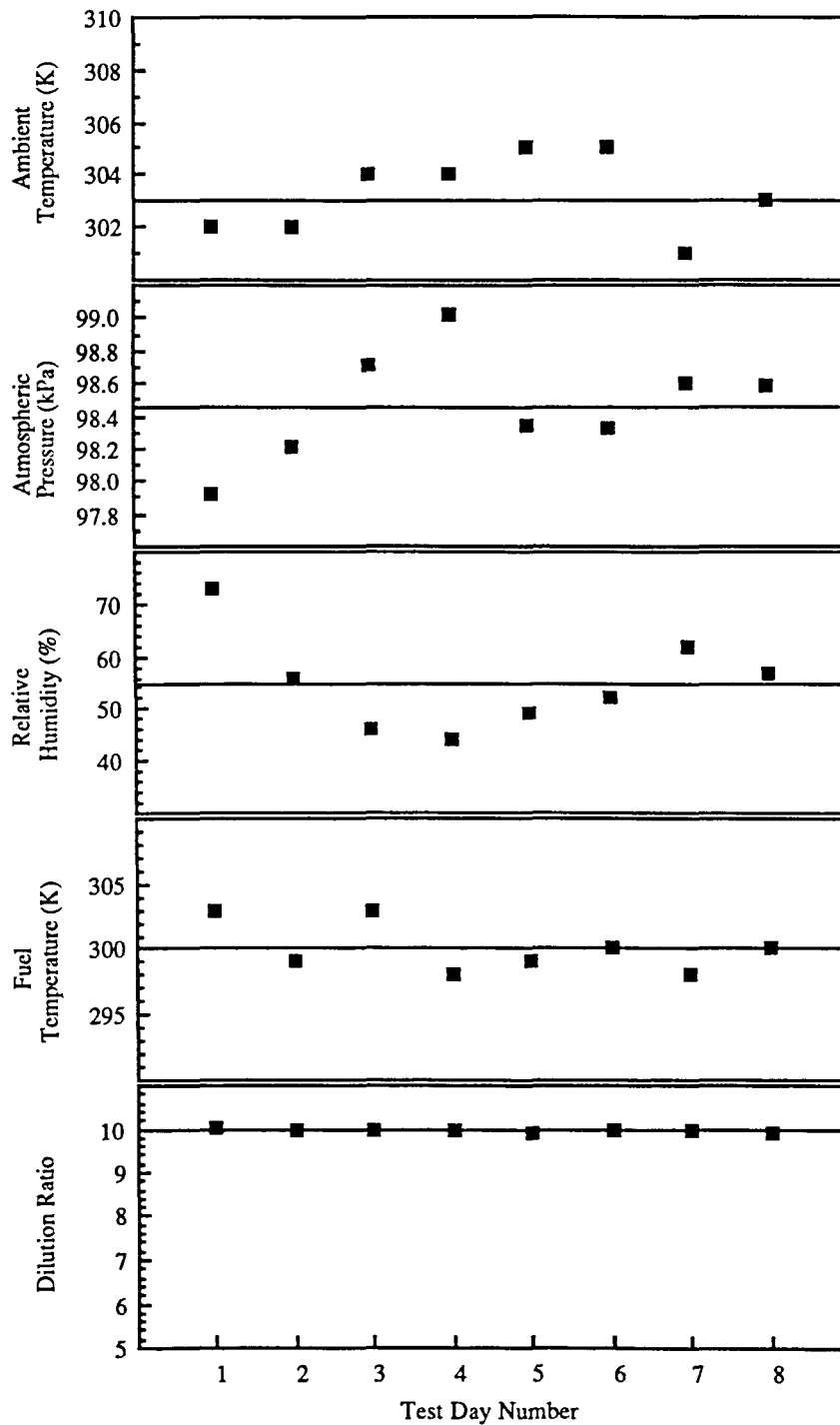
Fig. E13: Ambient conditions, fuel temperature and dilution ratio variations from day to day for measurement 1
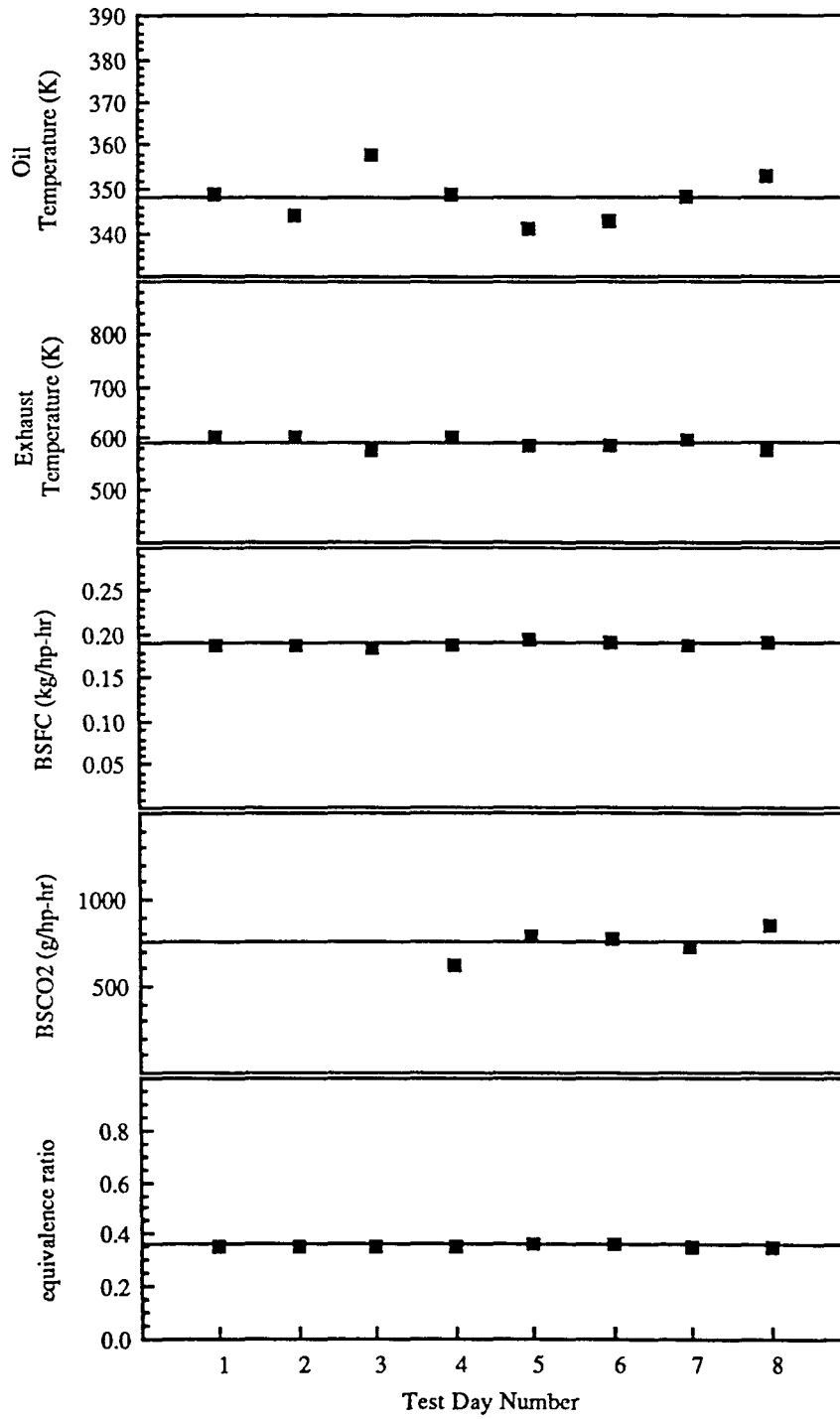
Fig. E14: Engine parameter variations from day to day for measurement 1
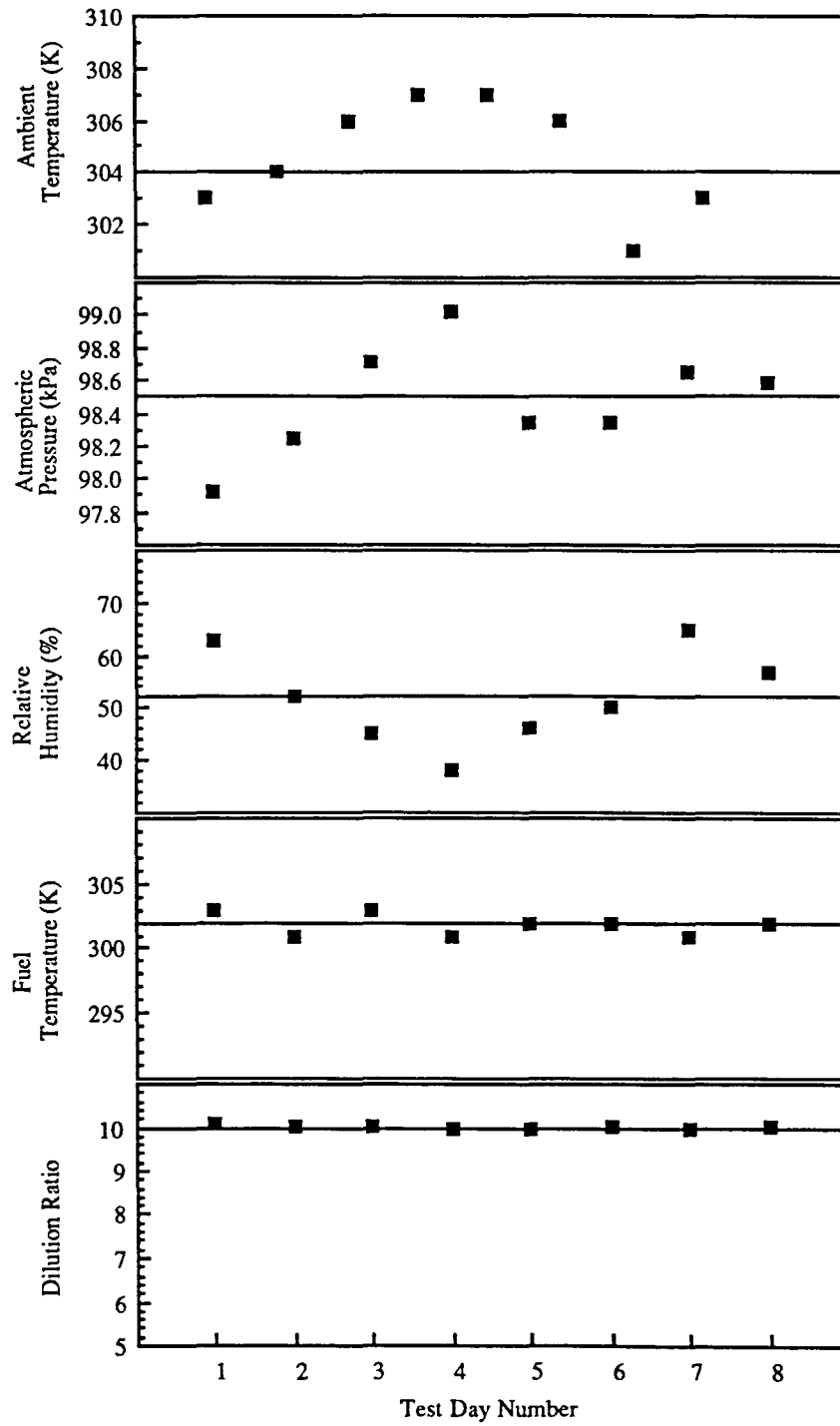
Fig. E15: Ambient conditions, fuel temperature and dilution ratio variations from day to day for measurement 2
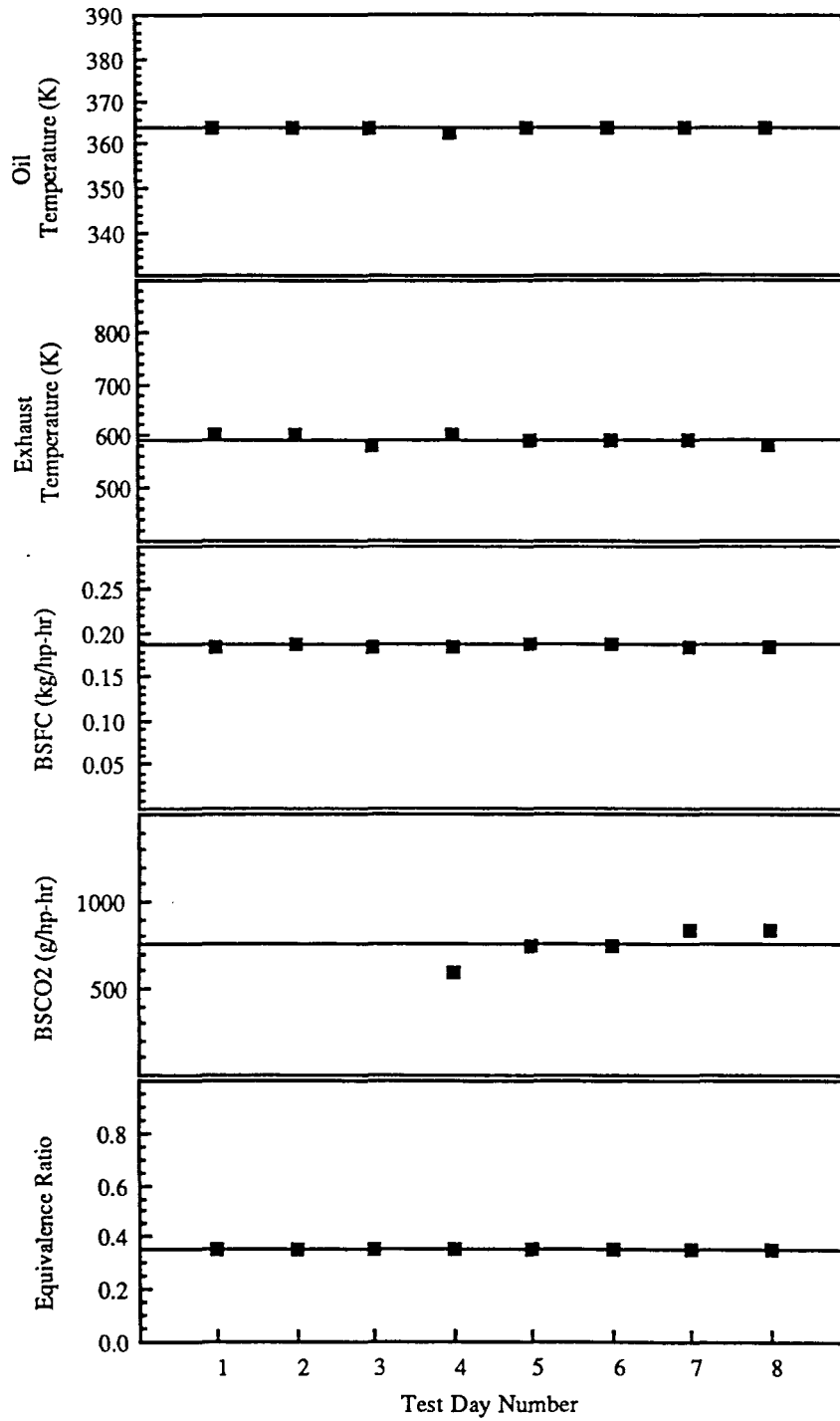
Fig. E16: Engine parameter variations from day to day for measurement 2
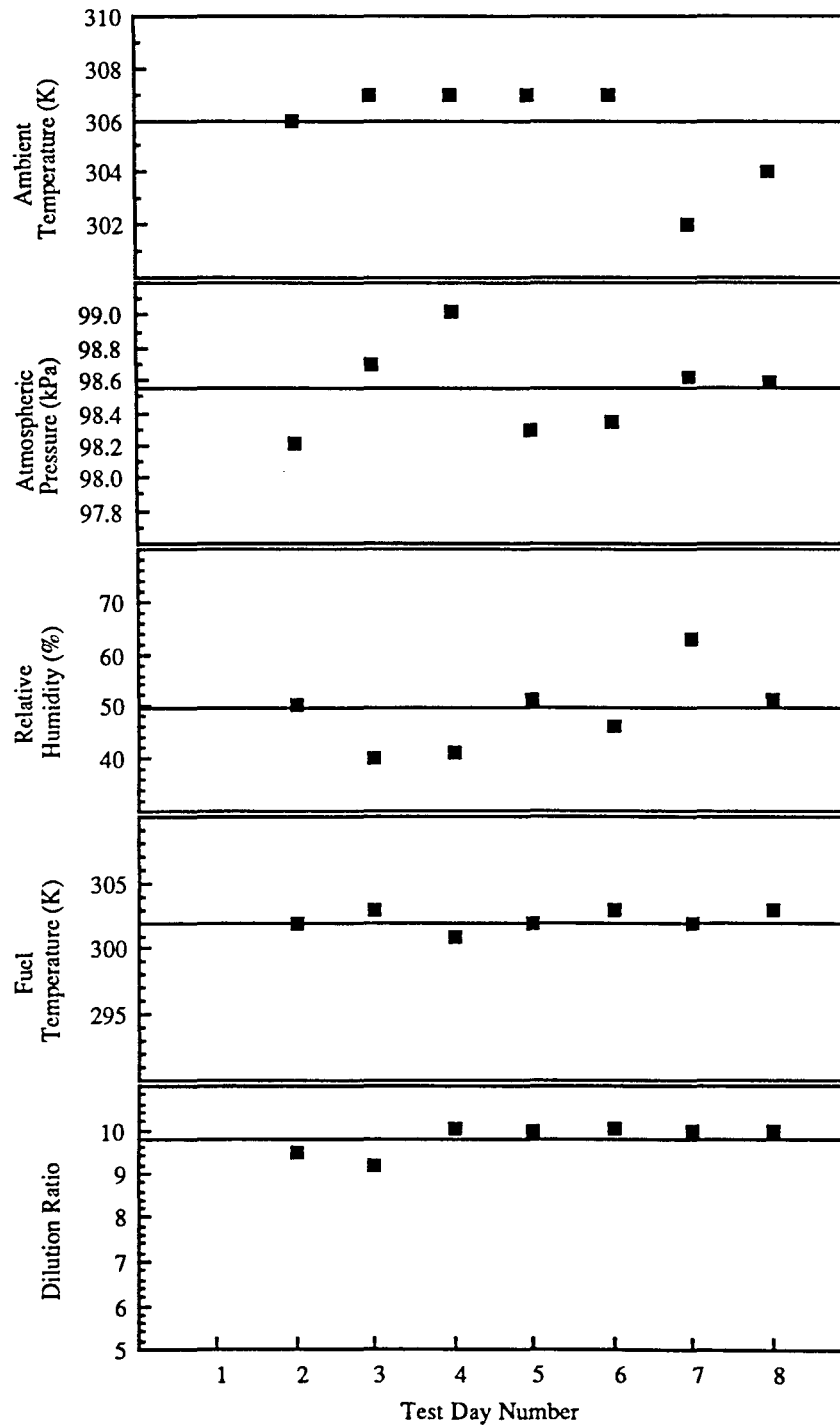
Fig. E17: Ambient conditions, fuel temperature and dilution ratio variations from day to day for measurement 3
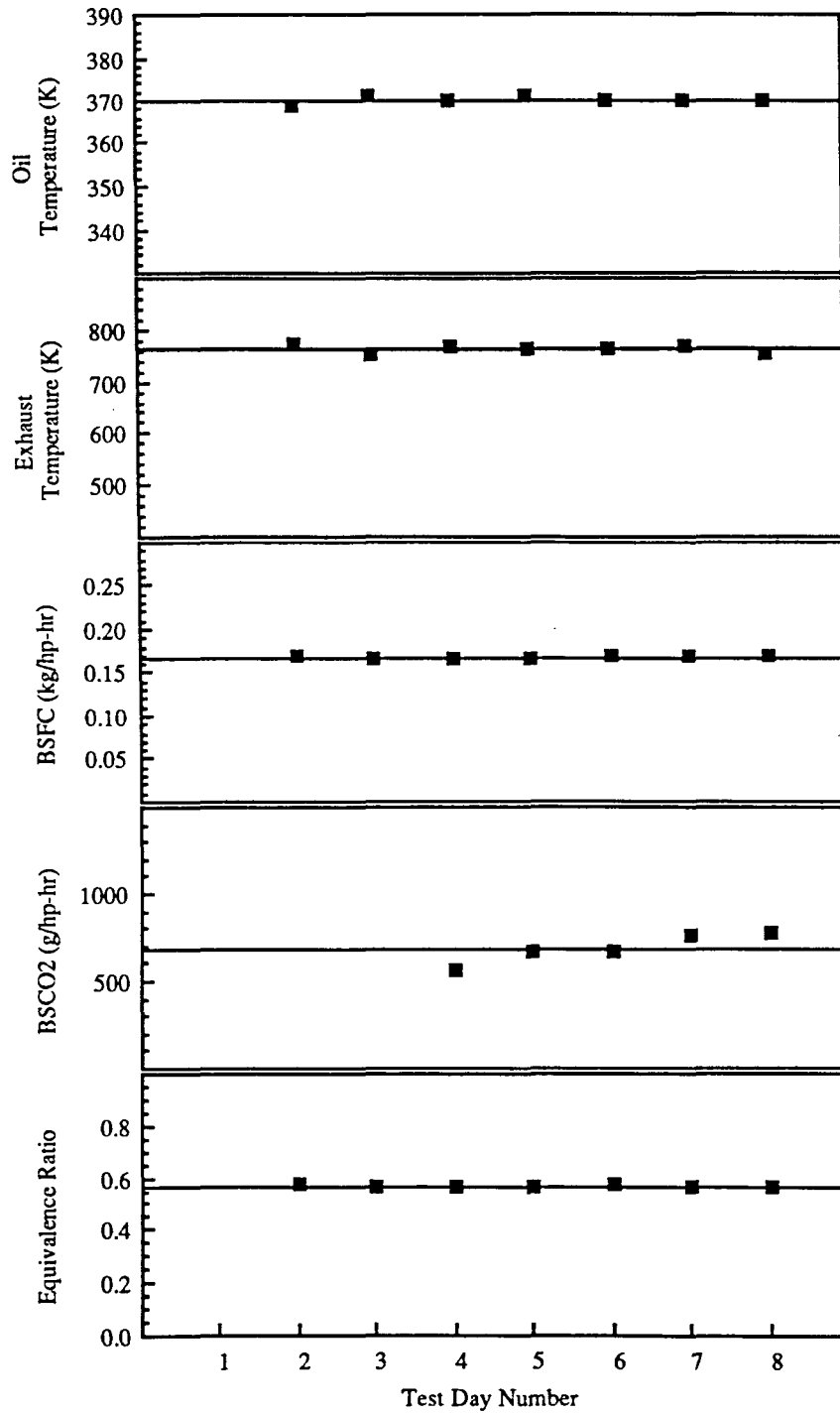
Fig. E18: Engine parameter variations from day to day for measurement 3
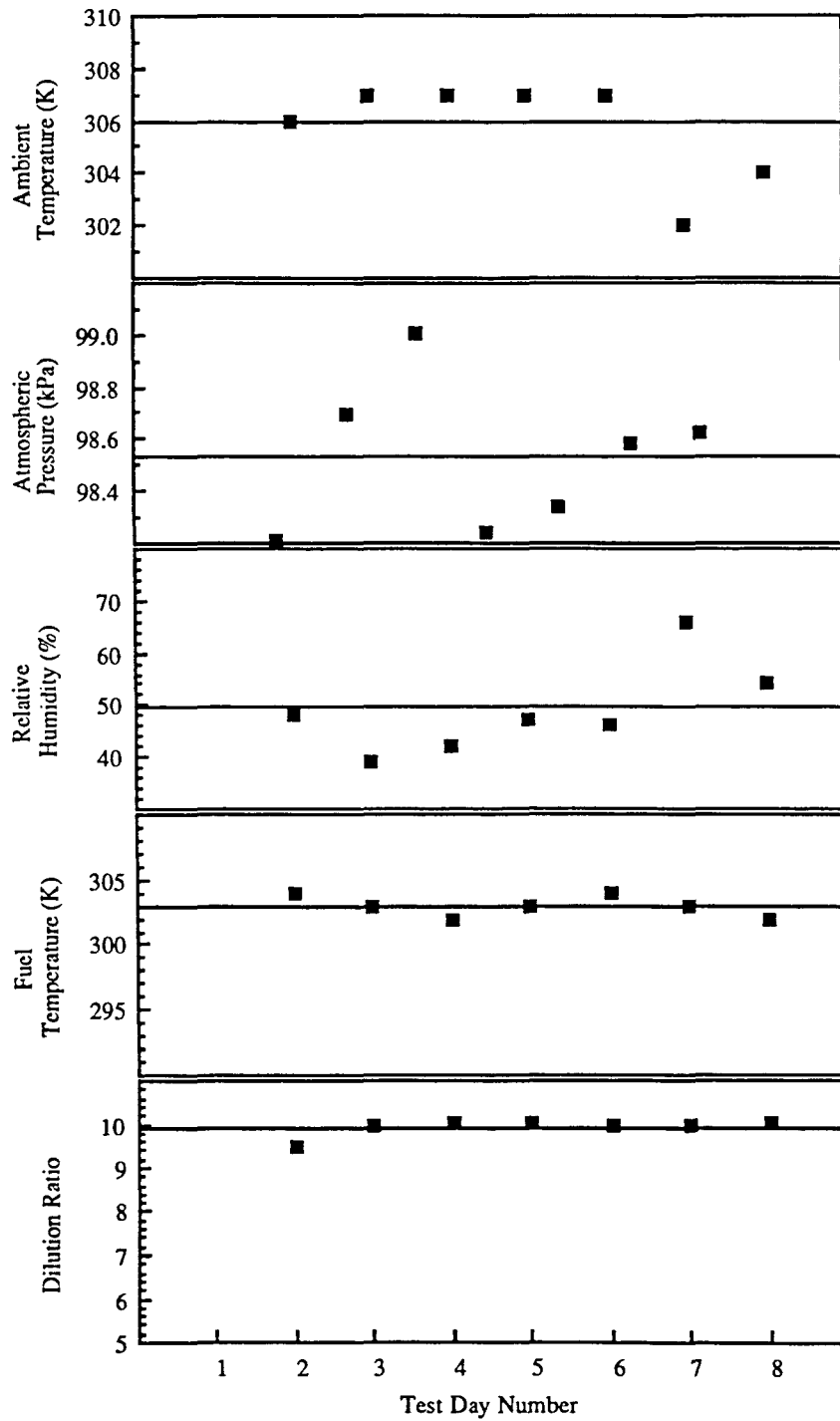
Fig. E19: Ambient conditions, fuel temperature and dilution ratio variations from day to day for measurement 4
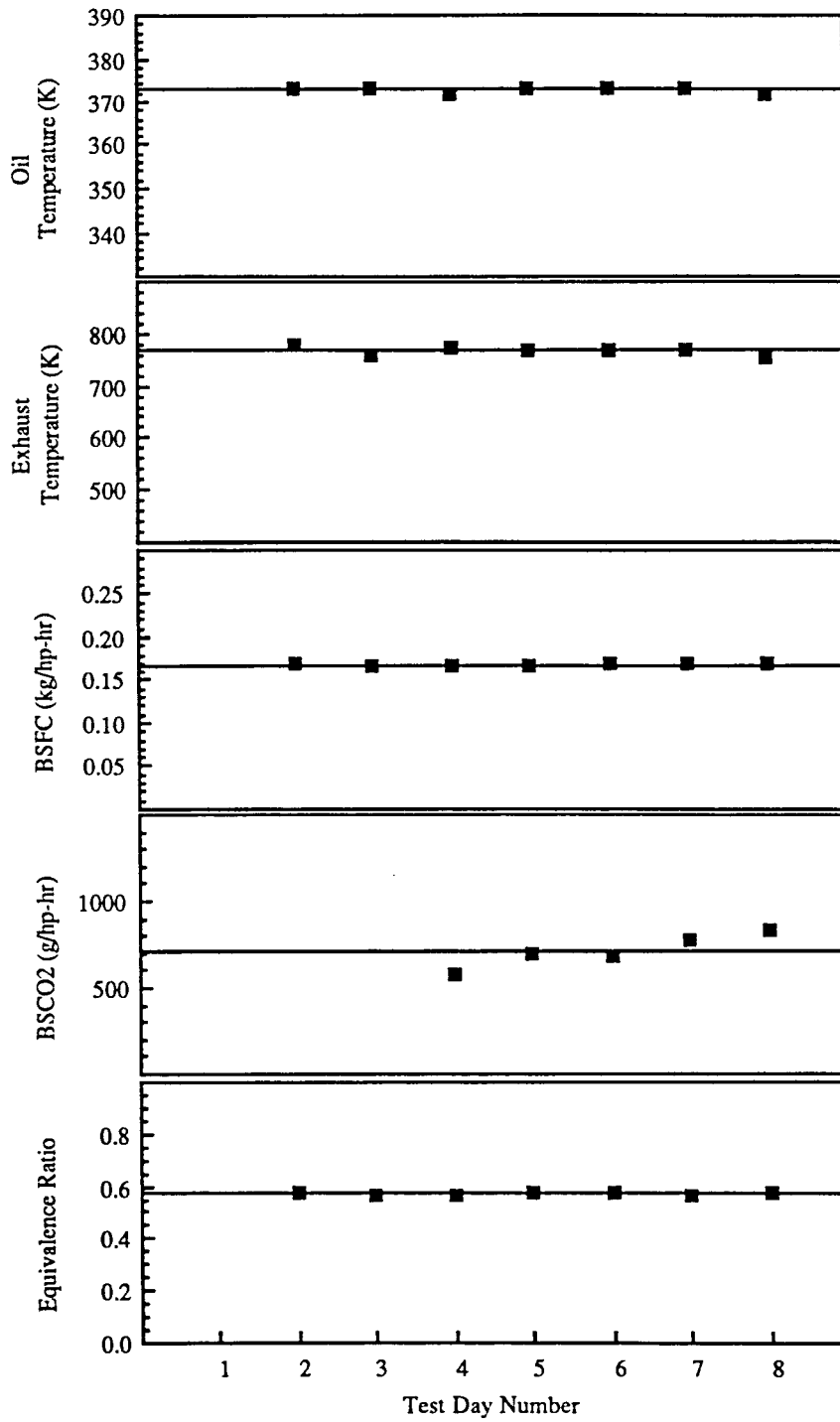
Fig. E20: Engine parameter variations from day to day for measurement 4
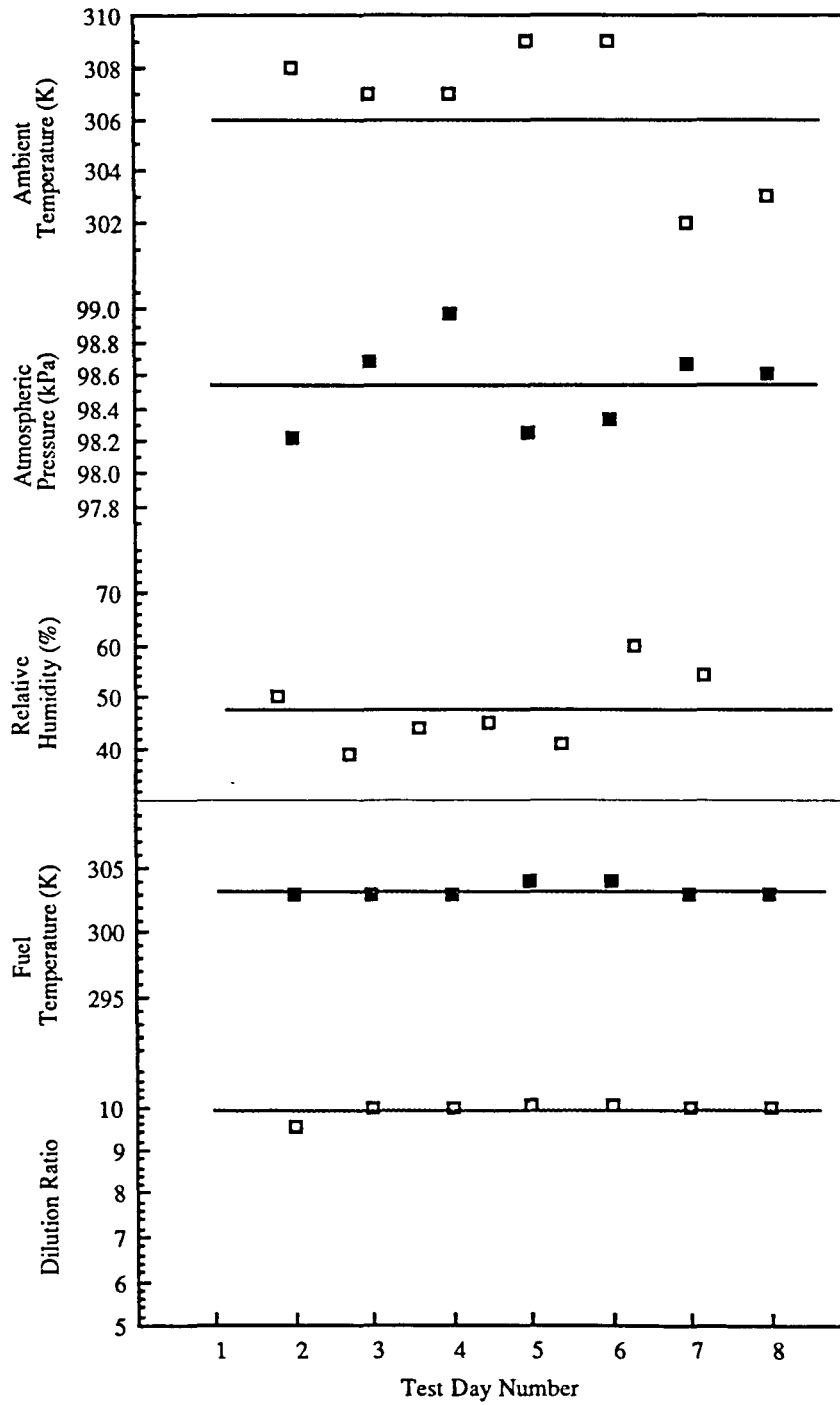
Fig. E21: Ambient conditions, fuel temperature and dilution ratio variations from day to day for measurement 5
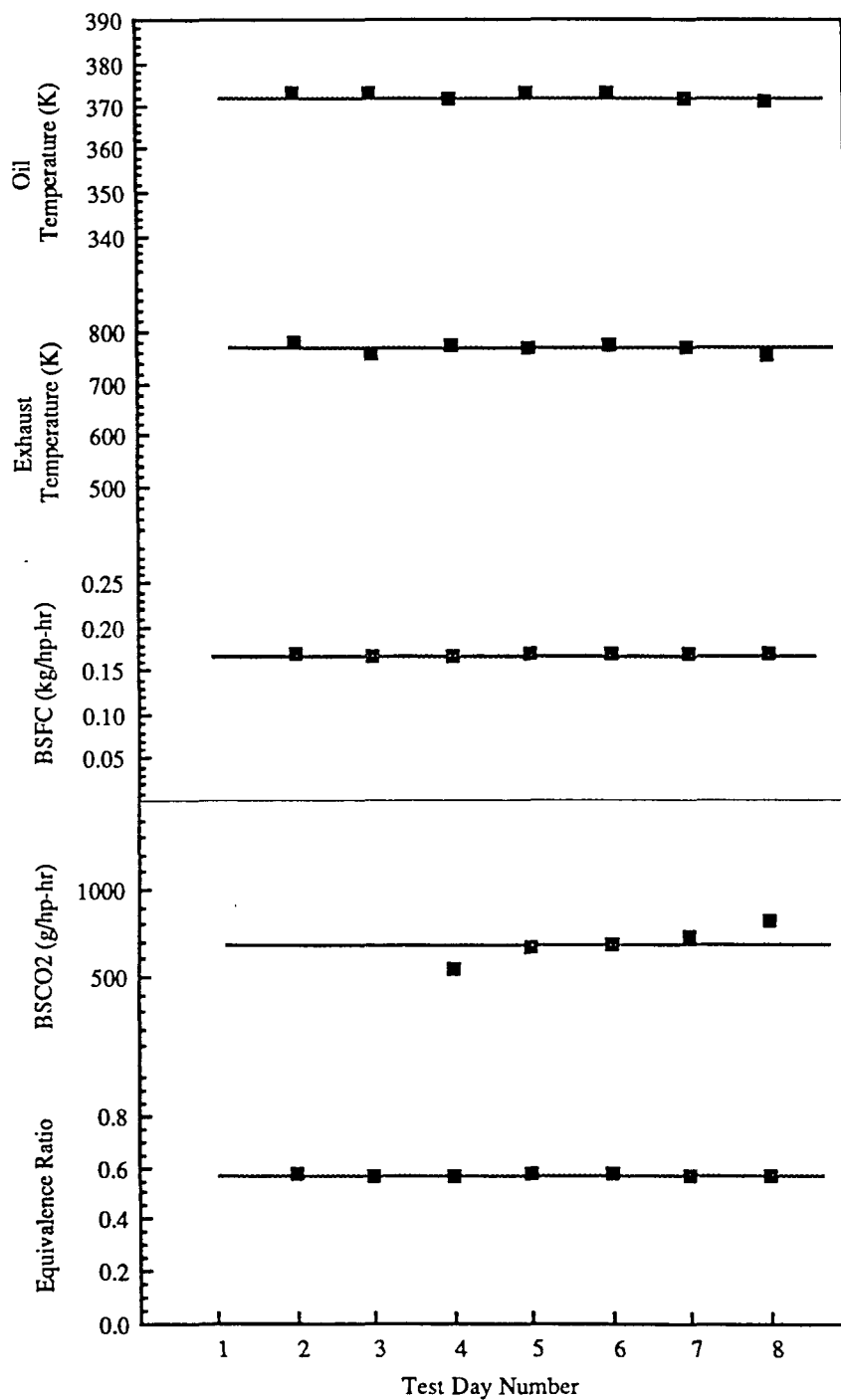
Fig. E22: Engine parameter variations from day to day for measurement 5
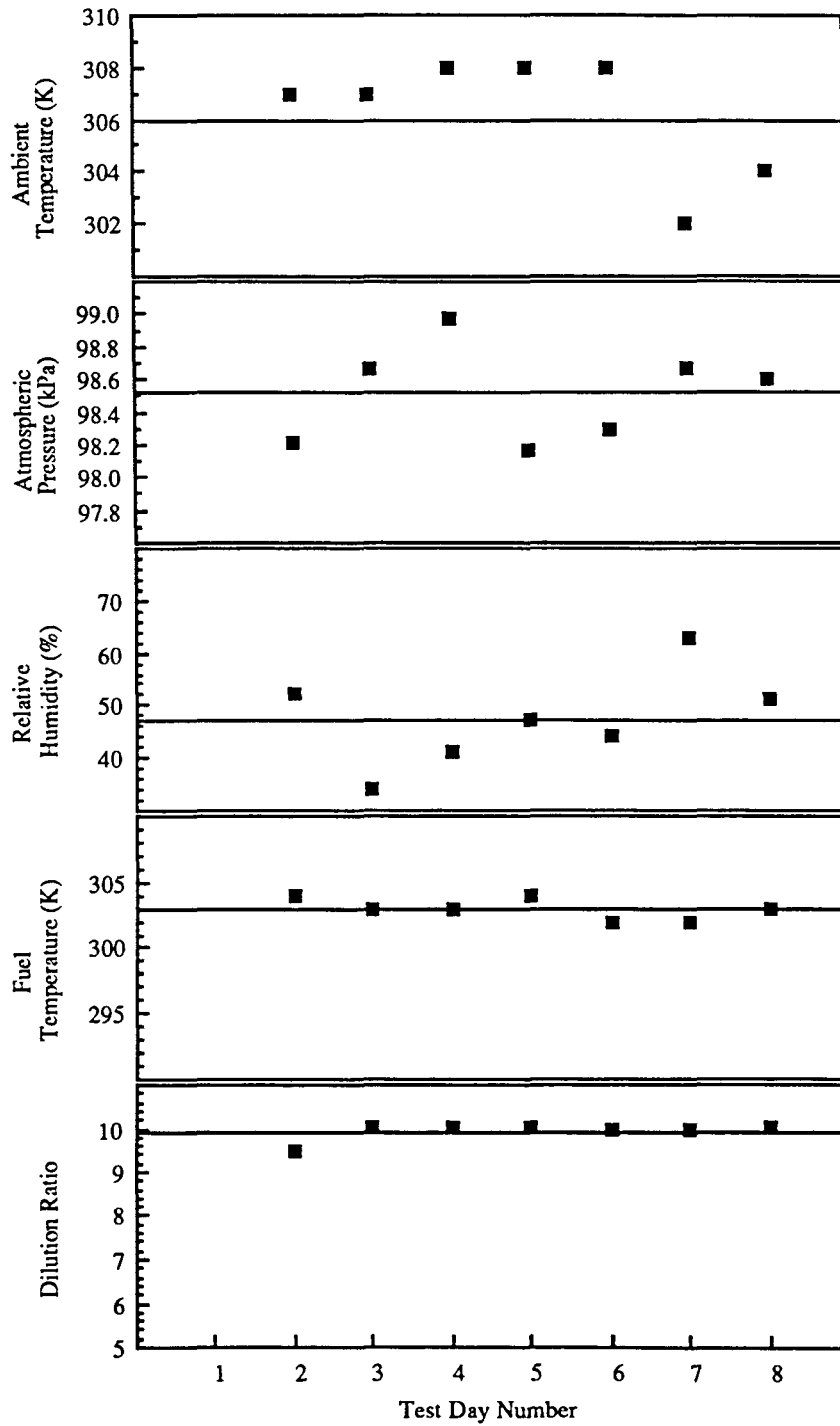
Fig. E23: Ambient conditions, fuel temperature and dilution ratio variations from day to day for measurement 6
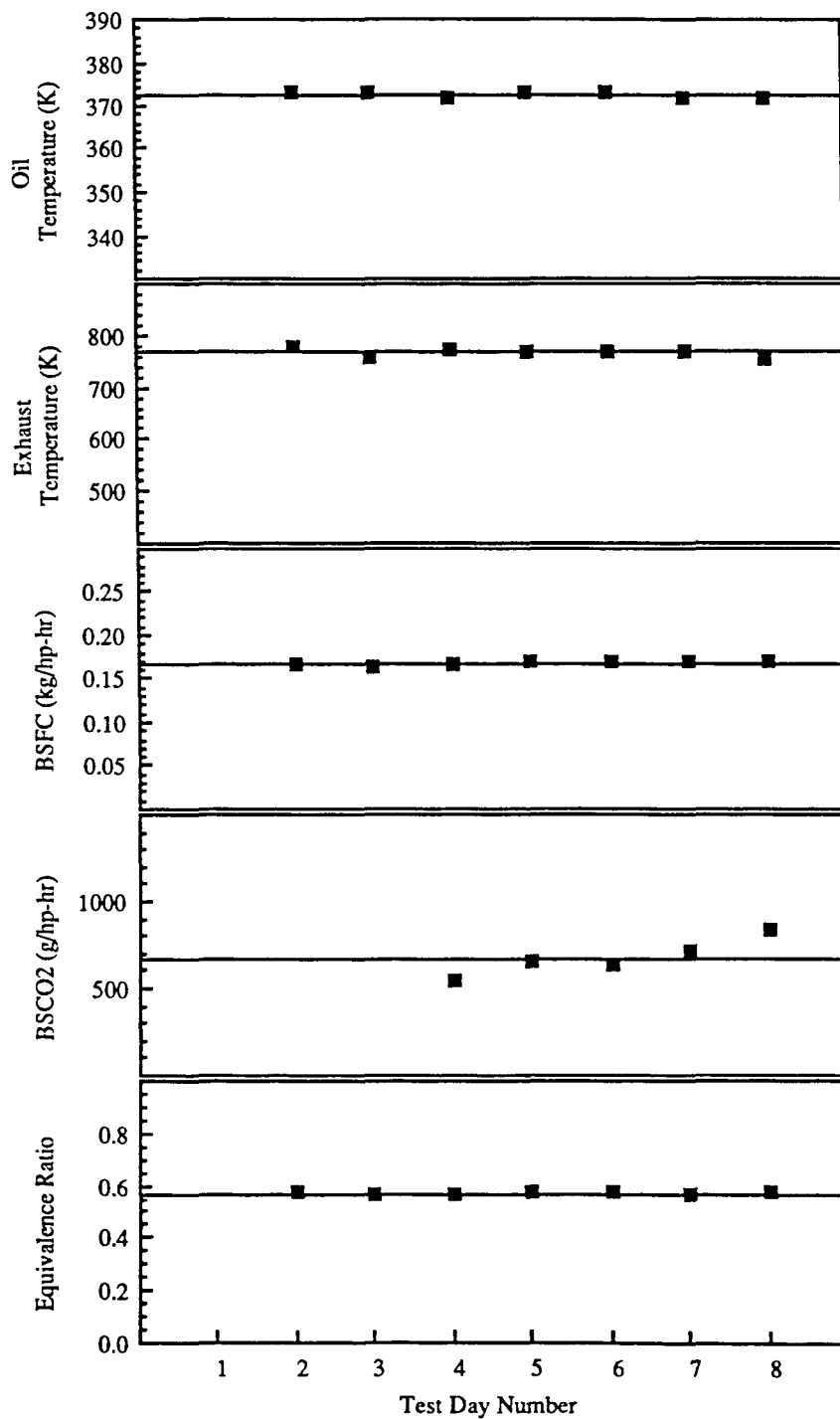
Fig. E24: Engine parameter variations from day to day for measurement 6
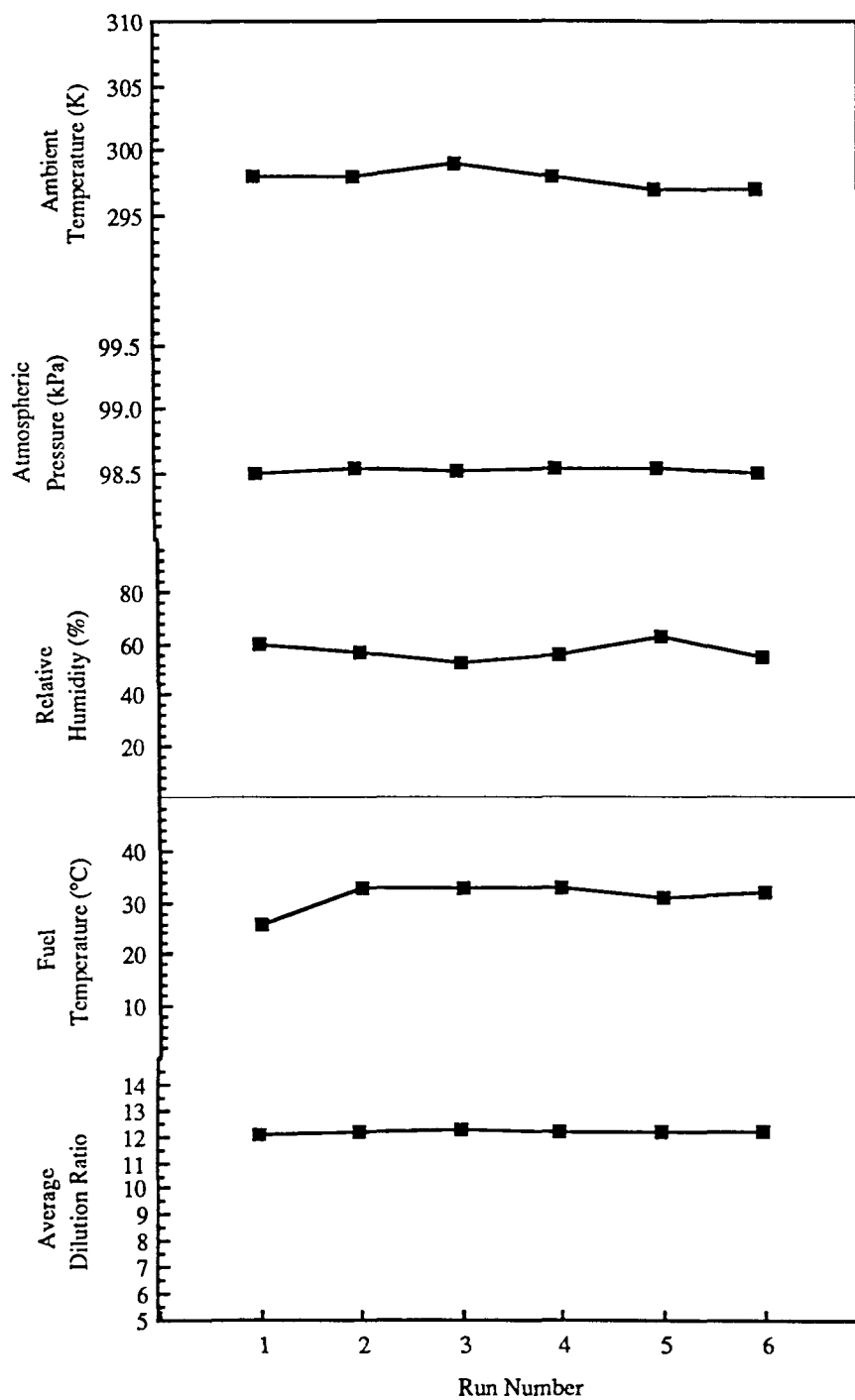
Fig. E25: Ambient conditions, fuel temperature and dilution ratio variations during transient test day 1
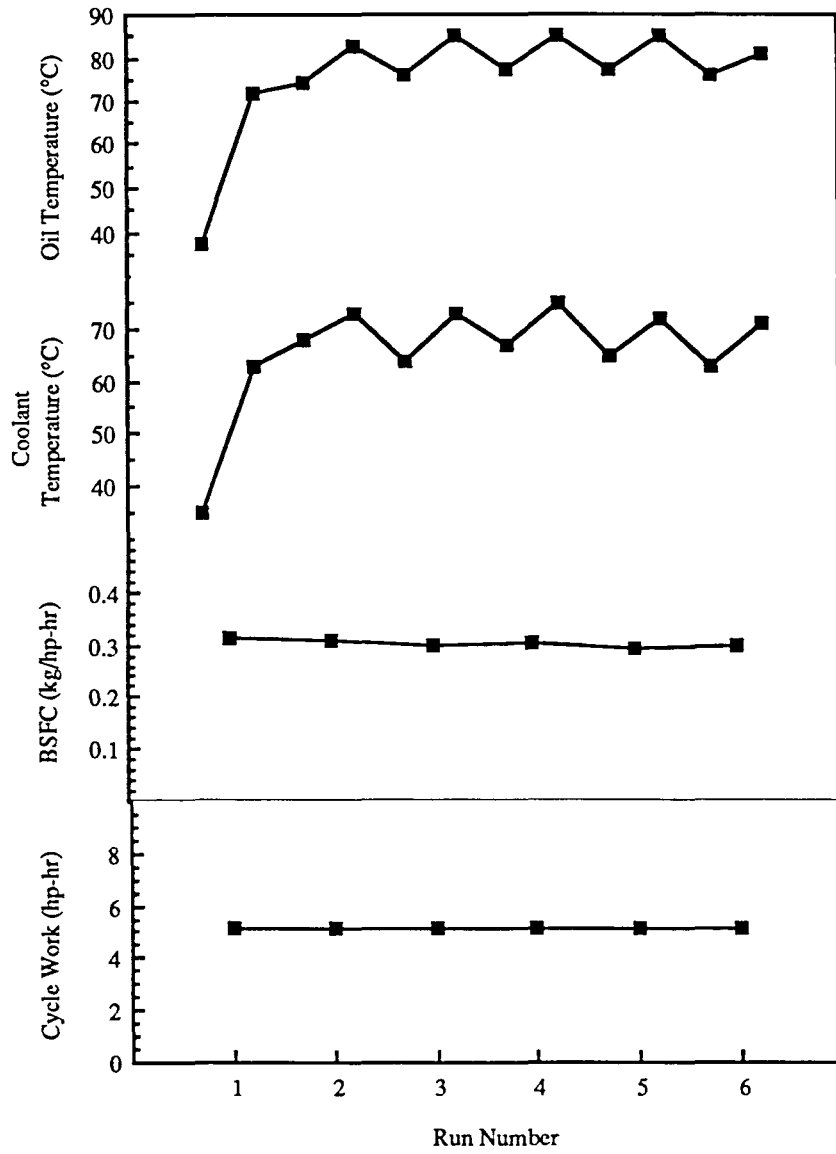
Fig. E26: Engine parameter variations during transient test day 1
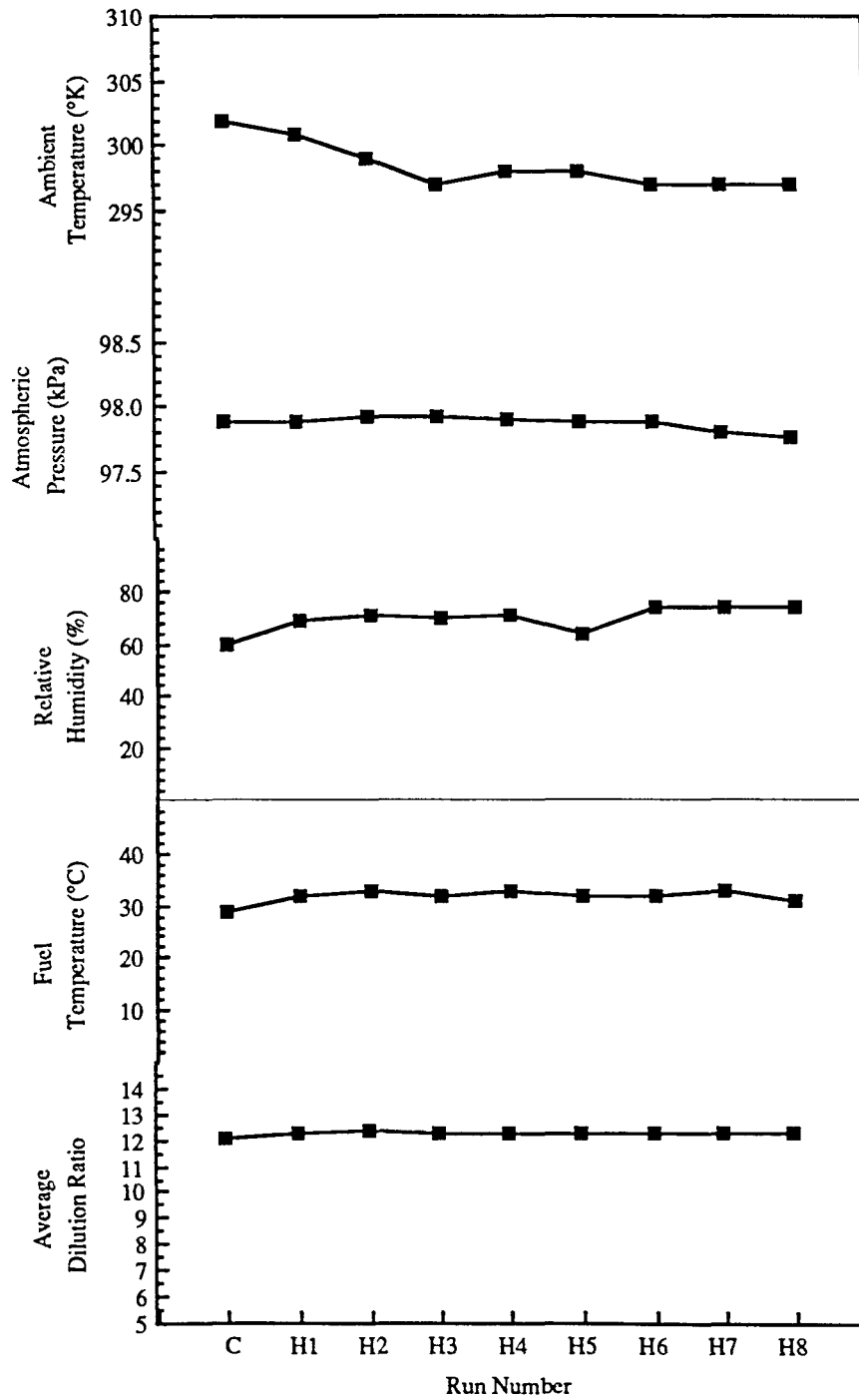
Fig. E27: Ambient conditions, fuel temperature and dilution ratio variations during transient test day 2
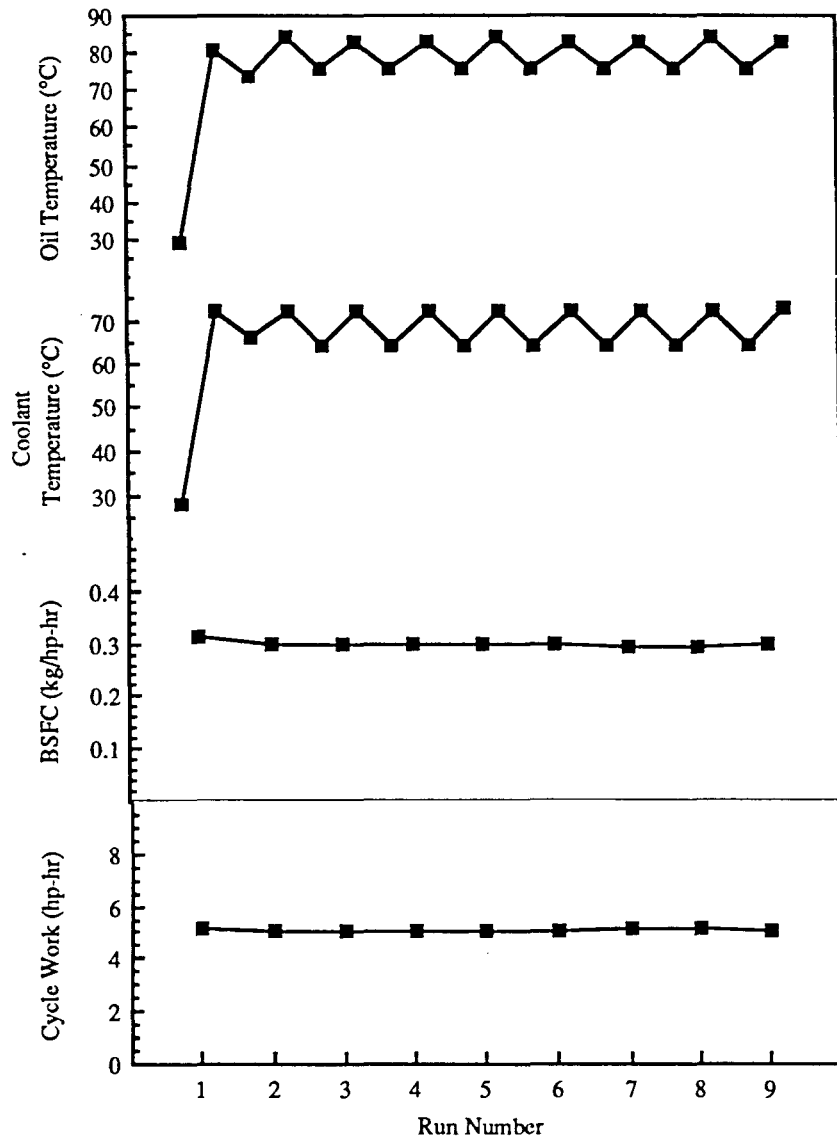
Fig. E28: Engine parameter variations during transient test day 2
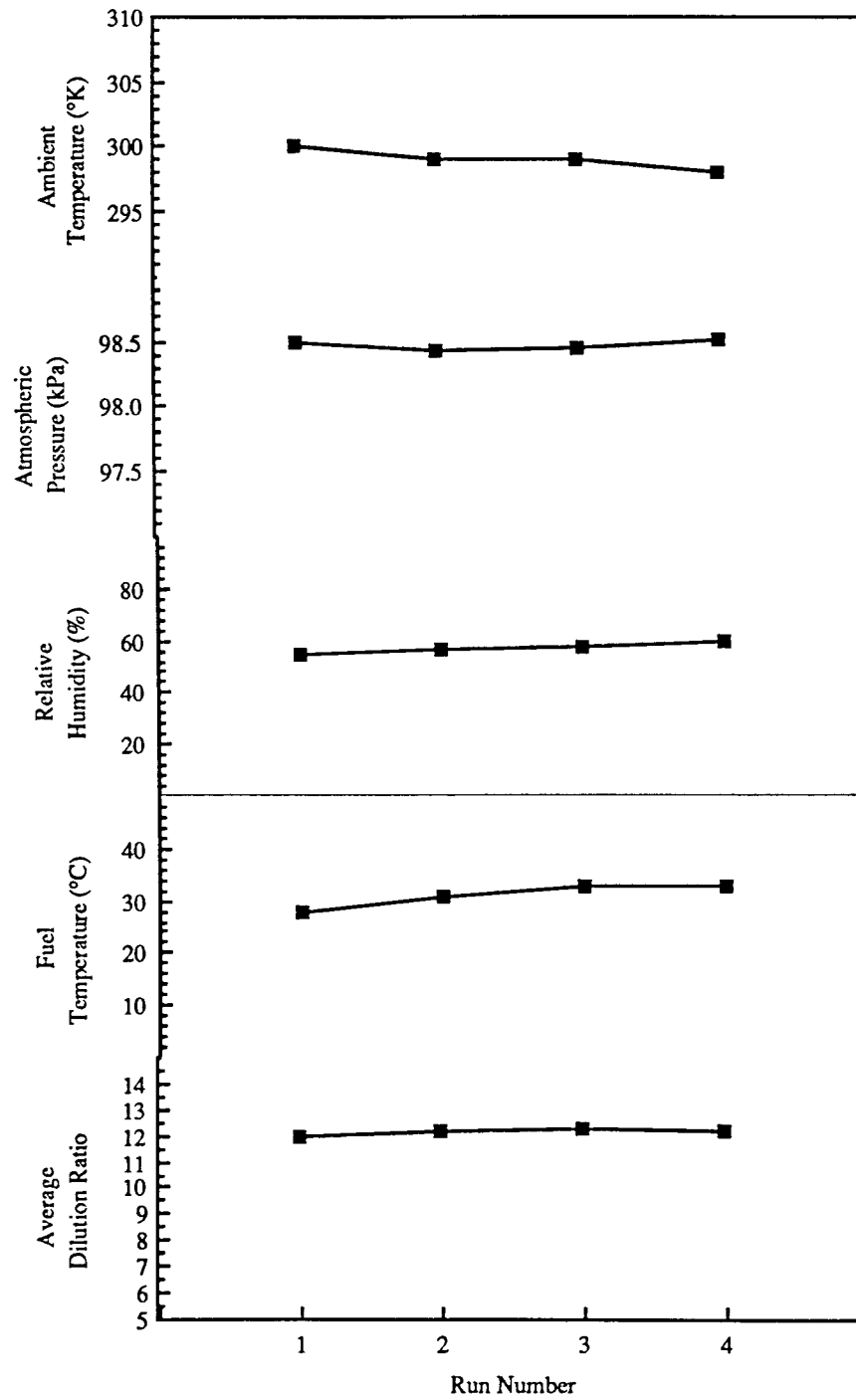
Fig. E29: Ambient conditions, fuel temperature and dilution ratio variations during transient test day 3
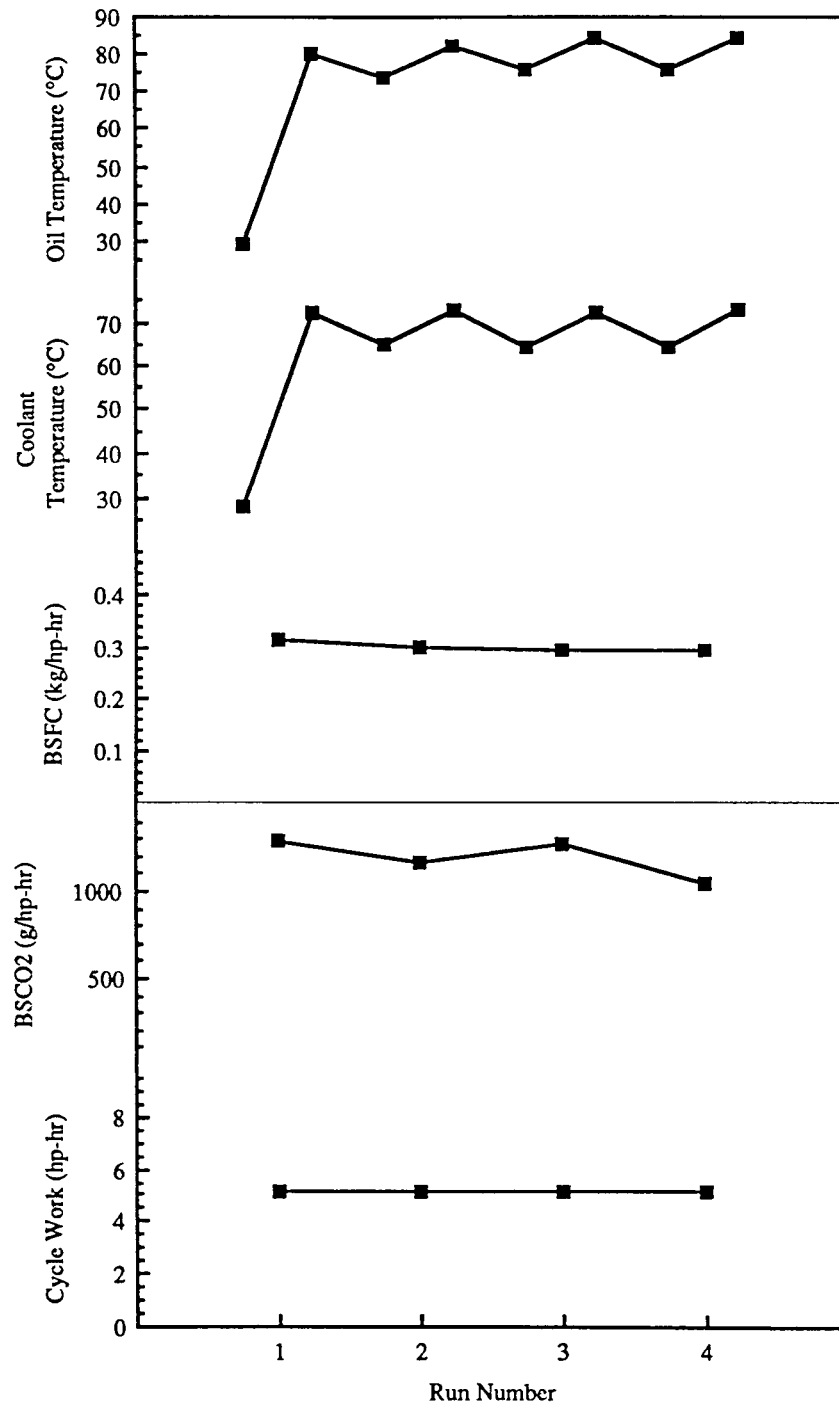
Fig. E30: Engine parameter variations during transient test day 3

APPENDIX F: TEST DATA

This appendix contains the test data and data reduction from the steady-state tests.

110

112